Western Graduate&PostdoctoralStudies

Western University
Scholarship@Western

Electronic Thesis and Dissertation Repository

11-17-2016 12:00 AM

Fate of Benzalkonium Chlorides in Natural Environment and Treatment Processes

Adnan Hossain Khan
The University of Western Ontario

Supervisor
Dr. Madhumita B. Ray
The University of Western Ontario

Graduate Program in Chemical and Biochemical Engineering
A thesis submitted in partial fulfillment of the requirements for the degree in Doctor of Philosophy
© Adnan Hossain Khan 2016

Follow this and additional works at: https://ir.lib.uwo.ca/etd

 Part of the Environmental Engineering Commons

Recommended Citation

Khan, Adnan Hossain, "Fate of Benzalkonium Chlorides in Natural Environment and Treatment Processes" (2016). *Electronic Thesis and Dissertation Repository*. 4249.
https://ir.lib.uwo.ca/etd/4249

This Dissertation/Thesis is brought to you for free and open access by Scholarship@Western. It has been accepted for inclusion in Electronic Thesis and Dissertation Repository by an authorized administrator of Scholarship@Western. For more information, please contact wlswadmin@uwo.ca.

Abstract

Benzalkonium chlorides (BACs) are a type of cationic surfactant and are highly adsorptive to negatively charged surfaces during the wastewater treatment process. They can, therefore, enter the aquatic environment via the suspended organic matter in wastewater effluents, and the terrestrial environment through the application of biosolids as a soil amendment for crop production or by the use of reclaimed wastewater for irrigation. This research investigated the fate of the two most commonly used BACs, benzyl dimethyl dodecyl ammonium chloride (BDDA; C_{12}-alkyl chain) and benzyl dimethyl tetradecyl ammonium chloride (BDTA; C_{14}-alkyl chain), individually and in mixture in various natural and engineered systems.

Under laboratory conditions, the following potential fate processes of these BACs were investigated: bacterial biodegradation, adsorption and leaching in various agricultural soils amended with biosolids, and plant uptake. A pure *Pseudomonas* strain biodegraded BACs, but BDTA was more toxic and inhibited the biodegradation of BDDA. Radiolabelled [U-^{14}C-benzyl] BDDA showed about 85% of the initial concentration mineralized within 300 h. Adsorption studies of BACs to agricultural soils showed, BDTA adsorbed more on soil compared to BDDA. Organic carbon normalized adsorption coefficients (Log K_{oc}, L kg^{-1}) for BACs in the soils were >4, which suggested that BACs tend to retain on the organic fraction of soils. Soil column experiments indicated very low leaching (<1%) of BDDA through 9 cm soil layers. A hydroponic study demonstrated that as about 0.25 mg L^{-1} BACs inhibited plant growth to 50% and BACs were found in the root and shoot tissues of both garden cress (*Lepidium sativum)* and lettuce *(Lactuca sativa)*.

An advanced oxidation process (AOP) based on O_3/H_2O_2 showed that about 1.28 g h^{-1} O_3 and 200 mg L^{-1} of H_2O_2 at pH 11 degraded 90% of the initial BACs within 30 min. The AOP treated water was not toxic to two species of algae (*Chlorella vulgaris* and *Chlamydomonas reinhardtii*); growth rate was about 0.38 d^{-1} for treated and control samples compared to 0.01 d^{-1} for samples contained BACs without AOP. About 25 transformation products were identified in the AOP processes following six different degradation pathways.

Keywords: Benzalkonium chlorides; biodegradation; soil adsorption; soil column leaching; phytotoxicity; plant uptake; advanced oxidation treatment; ozone-hydrogen peroxide

Co-authorship

This thesis is prepared in accordance with the regulations for Integrated-Article (Formerly Manuscript) format thesis stipulated by the School of Graduate and Postdoctoral Studies at the University of Western Ontario. The candidate developed all analytical modelling and the experimental works were carried out at the University of Western Ontario and partly at Agriculture and Agri-Food Canada (AAFC), London, ON, under a close guidance and supervision of Dr. Madhumita B. Ray and Dr. Sheila M. Macfie. The co-authorship of the Chapters 3, 4, 5 and 6 is as follows:

Chapter 3:

"**Biodegradation of Benzalkonium Chlorides Singly and in Mixtures by a *Pseudomonas* sp. Isolated from Returned Activated Sludge**"

The contributions of the co-authors are:

Adnan Hossain Khan	Designed and carried out the experiments, developed and implemented the model, interpreted the experimental results, wrote the draft and the final version of the manuscript
Edward Topp (AAFC)	Assisted in data interpretation, provided laboratory and financial support
Andrew Scott (AAFC)	Assisted in the experimentation
Mark Sumarah (AAFC)	Supported the HPLC-MS analysis
Sheila M. Macfie	Made major revision of the paper
Madhumita B. Ray	Made major revision of the paper and provided financial assistance

Chapter 4:

"Sorption and Leaching of Benzalkonium Chlorides in Agricultural Soils"

The contributions of the co-authors are:

Adnan Hossain Khan	Designed and carried out the experiments, developed and implemented the model, interpreted the experimental results, wrote the draft and the final version of the manuscript
Sheila M. Macfie	Made major revision of the paper
Madhumita B. Ray	Made major revision of the paper, provided laboratory and financial support

Chapter 5:

"Uptake and Phytotoxic Effect of Benzalkonium Chlorides in *Lepidium Sativum* and *Lactuca Sativa* in a Hydroponic System"

The contributions of the co-authors are:

Adnan Hossain Khan	Carried out some experiments (extracted plant parts, analyzed nutrient solutions for BACs, and assisted in the acid digestion for nutrient analysis), did some statistical analysis, interpreted the experimental results, wrote the draft and the final version of the manuscript
Mark Libby	Carried out germination, growth inhibition and acid digestion experiments for *Lepidium sativum*
Daniel Winnick	Carried out germination, growth inhibition and acid digestion experiments for *Lactuca sativa*
John Palmer	Replicated germination, growth inhibition and acid digestion experiments for both plant species
Mark Sumarah (AAFC)	Supported HPLC-MS analysis

Sheila M. Macfie	Assisted in the experimental design, statistical analysis and data interpretation. Made major revision of the paper. Provided laboratory and financial support
Madhumita B. Ray	Made major revision of the paper, provided laboratory and financial support

Chapter 6:

"Toxicity Reduction and Improved Biodegradability of Benzalkonium Chlorides by Ozone/Hydrogen Peroxide Advanced Oxidation Process"

The contributions of the co-authors are:

Adnan Hossain Khan	Designed and carried out the experiments, developed and implemented the model, interpreted the experimental results, wrote the draft and the final version of the manuscript
Junwoo Kim	Assisted in the toxicity test using algae
Mark Sumarah (AAFC)	Supported HPLC-MS analysis
Sheila M. Macfie	Made major revision of the paper
Madhumita B. Ray	Made major revision of the paper, provided laboratory and financial support

Dedicated to my family;

Father: Jalal Uddin Khan (late)

Mother: Jebunnessa Khanum

Wife: Nayeema Siddiqua

Daughter: Athena Adnan

Acknowledgements

My deepest sense of appreciation goes to my academic advisors; Dr. Madhumita B. Ray and Dr. Sheila M. Macfie for their relentless guidance and support during my PhD research. The door of Dr. Ray was always open whenever I ran into a trouble or had a question about my research or writing. I would like to give her exceptional thanks for her patience to understand my situation throughout the time and keep me supported in varied situations. My immense gratitude goes to Dr. Macfie for her guidance on writing my entire thesis and support during my plant uptake experiments. Her advice on "Time Management" helped me to juggle my research and family responsibilities most efficiently, so that I was able to keep my research forwarded to finish on time. My research would be incomplete without the guidance of both of my advisors.

My sincere thankfulness to all of my examiners, Dr. Lars Rehmann, Dr. Clare Robinson, Dr. Amarjeet Bassi and Dr. Niharendu Biswas; for their time to read and examine my thesis to evaluate my doctoral degree.

I would like to thank some of the experts who were involved in my research in various parts. Dr. Edward Topp, allowed me to obtain hands on experience on the biodegradation experiments at Agriculture and Agri-Food Canada, London, ON. Dr. Mark Sumarah, provided me the software "Xcalibur" for mass-spectroscopy analysis and allowed me with their facilities to analyze samples using HPLC-MS. Dr. Mamdouh Abou-Zaid for his discussion about chromatographic analysis during my research.

My countless recognition goes to my family members; my wife, Nayeema Siddiqua, for her patience and motivation in last four years of my PhD research; my daughter, for her inspiring smile; my father (late), and my mother for their honest love and care to me.

I also thank Junwoo Kim (PhD graduate student) for his sharing and discussion of research ideas in last few years. I also thank my research group members for their immense co-operation in the lab. During my PhD research, I received assistance from many researchers; Lyne Sabourin (radiolabel experiments), Yuan-Ching (DNA extraction from *Pseudomonas* sp.), Amanda Barros (soil column experiment), Tim McDowell (HPLC-MS analysis), Dr. Justin Renaud (taught me the software "Xcalibur"), Dr. Charles Wu (nitrogen

content analysis using LECO), Jing Wan (O_3 concentration measurement) and I thank them all. I appreciate all the care and support that I had from the faculty and staff in the department of Chemical and Biochemical Engineering all through my PhD.

This scholarly fulfilment would be impossible without the financial support from the Natural Science and Engineering Council of Canada (NSERCH CREATE program), Western Graduate Research Scholarship and the support from Ontario Graduate Scholarship (OGS), which are gratefully acknowledged.

Table of contents

Abstract ii

Co-authorship iv

Acknowledgements viii

Table of contents x

List of Tables xiv

List of Figures xv

List of Abbreviations xviii

Nomenclature xx

Chapter 1 1

1.1 Introduction 1

1.2 Benzalkonium chlorides 2

1.3 BACs in the natural environment 5

1.4 Toxic effect of BACs in various living organisms 6

1.5 Literature gaps and objectives of this study 7

References 9

Chapter 2 12

Literature Review 12

2.1 Biodegradation of cationic surfactants 12

2.2 Adsorption and leaching of organic pollutants 14

2.3 Plant uptake of organic pollutants in hydroponics 17

2.4 Advanced oxidation processes as pretreatment 19

2.5 Objectives of the research 21

References 22

Chapter 3 29

Biodegradation of Benzalkonium Chlorides Singly and in Mixtures by a *Pseudomonas* sp. Isolated from Returned Activated Sludge 29

3.1 Introduction 29

3.2 Materials and methods 31

3.2.1 Chemicals 31

3.2.2 Maintenance and tentative identification of the bacterium 31
3.2.3 Analytical methods 34
3.2.4 Bacterial growth and kinetics study 36
3.2.5 Determination of kinetic constants 37
3.2.6 Radiolabel experiment 38
3.2.7 Selection of BACs concentrations 39
3.3 Results and discussion 39
3.3.1 Bacterial growth with BACs as the sole source of C and N 39
3.3.2 Biodegradation kinetics 41
3.3.3 Kinetics model 45
3.3.4 Identification of transformation products 47
3.3.5 Mineralization of BDDA 52
3.4 Conclusions 53
References 54
Chapter 4 58
Sorption and Leaching of Benzalkonium Chlorides in Agricultural Soils 58
4.1 Introduction 58
4.2 Materials and methods 60
4.2.1 Chemicals 60
4.2.2 Soil and biosolids 61
4.2.3 Analytical methods 61
4.2.3.1 Soil and biosolids analysis 61
4.2.3.2 BAC extraction from spiked soils and biosolids 62
4.2.3.3 Analysis of benzalkonium chlorides 63
4.2.4 Adsorption kinetics and equilibrium experiments 64
4.2.5 Column experiment 66
4.3 Results and discussion 69
4.3.1 Physical characteristics of soils and biosolids 69
4.3.2 Quantification of BACs using UV-Vis spectrophotometer 70
4.3.3 Adsorption kinetics 71
4.3.4 Adsorption isotherm parameters 73
4.3.5 Extraction efficiency of BDDA from soils and biosolids 78

4.3.6 Leaching of BDDA in the soil column experiment 80
4.4 Conclusions 83
References 83
Chapter 5 88
Uptake and Phytotoxic Effect of Benzalkonium chlorides in *Lepidium Sativum* and *Lactuca Sativa* in a Hydroponic System 88
5.1 Introduction 88
5.2 Materials and methods 90
5.2.1 Germination and emerging seedling experiment 90
5.2.2 Phytotoxicity of BACs to seedlings 91
5.2.2.1 Macro and micronutrient analysis in plant tissues 92
5.2.3 Extraction and detection of BACs from plant tissue 94
5.2.3.1 BACs remaining in solution 95
5.2.4 Statistical analysis 96
5.3 Results and discussion 96
5.3.1 Germination and emerging seedlings 96
5.3.2 Toxic effect on plant growth 99
5.3.3 Nutrient analysis in plants 102
5.3.4 Uptake of BACs by plants 108
5.3.5 Nutrient solution analysis for BACs 111
5.4 Conclusions 115
References 115
Chapter 6 120
Toxicity Reduction and Improved Biodegradability of Benzalkonium Chlorides by Ozone/Hydrogen Peroxide Advanced Oxidation Process 120
6.1 Introduction 120
6.2 Material and methods 123
6.2.1 Chemicals 123
6.2.2 Experimental set-up for AOP 123
6.2.3 Selection of factors and ozone doses for AOP 124
6.2.4 Experimental design for AOP optimization 126
6.2.5 Analytical methods 128

6.2.5.1 Ozone concentration in liquid phase 128
6.2.5.2 Quantification of BACs and their intermediate products 130
6.2.5.3 Toxicity analysis of effluents using algae 131
6.2.5.4 Biodegradability test 132
6.2.5.5 Growth of mixed bacterial culture in AOP treated wastewater 133
6.2.6 Cost estimation 134
6.3 Results and discussions 135
6.3.1 Ozone concentration in liquid phase at different pH 135
6.3.2 Optimization of the AOP 136
6.3.2.1 Regression analysis and ANOVA for CCD 137
6.3.2.2 Contour plots to identify the optimum AOP region for BAC removal 140
6.3.3 AOP kinetics study 140
6.3.4 Formation of intermediates and degradation pathways 144
6.3.5 Toxicity of AOP treated solutions 153
6.3.6 Biodegradability of AOP treated solutions 154
6.3.7 AOP applied in wastewater influent 157
6.3.8 Cost estimation of AOP treatment for BACs containing solutions 158
6.4 Conclusions 159
Supplementary for cost estimation 159
References 163
Chapter 7 169
General Discussion and Recommendations 169
7.1 General discussion and recommendations for future work 169
7.2 Conclusions 173
References 175
Resume 176

List of Tables

		Page No
Table 1.1	Representative QAC groups and their general structure.	4
Table 3.1	The results of a BLASTn search in GenBank for the 16SrRNA sequence of strain C505.	33
Table 3.2	Kinetics constants ($V_{max(spe)}$ and $K_{m(spe)}$) calculated using Hanes-Woolf model.	46
Table 4.1	Properties of the benzalkonium chlorides used in this study.	60
Table 4.2	Selected physical characteristics of the soils.	70
Table 4.3	Langmuir and Freundlich adsorption isotherm parameters for BDDA and BDTA in three different soils.	76
Table 4.4	Solid-liquid distribution coefficient for BDDA and BDTA on different types of soil-water system as adsorbent.	79
Table 4.5	Percentage BDDA extracted from reference samples.	79
Table 5.1	Limit of quantification (LOQ) for analyzed elements using ICP-MS.	93
Table 5.2	BACs taken up by garden cress and lettuce.	113
Table 6.1	Experimental and predicted % removal of BACs using a central composite design (CCD) matrix (runs 1 to 13) for the factors H_2O_2 and pH.	129
Table 6.2	Regression coefficients for the models and *p*-values obtained from CCD for the % removal of BACs.	139
Table 6.3	Analysis of variance of the fitted model for the % removal of BACs.	139
Table 6.4	Identified intermediates (including two parent BACs) due to AOP on BACs.	146
Table 6.S1	General calculation of capital cost for a single AOP reactor.	160
Table 6.S2	Steps of O & M cost.	161

List of Figures

		Page No
Fig 1.1	Typical concentrations of selected 'emerging' organic contaminants in sewage sludge.	2
Fig 1.2	Synthesis routes of alkylbenzyl dimethyl ammonium chloride or BACs.	5
Fig. 1.3	Molecular structure of benzalkonium chlorides.	8
Fig. 3.1	Relationship between optical density at 600 nm (OD_{600}) and bacterial dry mass for the strain C505.	35
Fig. 3.2	Growth of the strain C505 after 7 d, (a) on LB-agar; (b) medium plate spiked with BDDA at 100 mg L^{-1}.	37
Fig.3.3	Growth of strain C505 in a minimal salts medium with various initial concentrations of BDDA and/or BDTA in mg L^{-1} as the sole source of carbon and nitrogen.	41
Fig.3.4	Biodegradation kinetics of BACs.	43
Fig.3.5	Hanes-Woolf models.	46
Fig.3.6	Chromatograms and mass spectra of the parent BACs at time zero for BDDA 150, BDTA 30 and BDDA: BDTA at 50:25 mg L^{-1}; (a) Chromatograms; (b) Mass spectra.	49
Fig.3.7	Liquid chromatography and MS analysis of transformation products formed during biodegradation of 150 mg L^{-1} BDDA.	50
Fig.3.8	Proposed mechanism of BDDA biodegradation by strain C505.	51
Fig.3.9	Mineralization of ^{14}C-labeled BDDA by the strain C505.	53
Fig 4.1	Schematic of soil column leaching experiment.	68
Fig 4.2	Absorption spectrum of BDDA and BDTA.	72
Fig 4.3	Adsorption kinetics of (a) BDDA and (b) BDTA at an initial concentration of 100 mg L^{-1} using three types of soil for 24 h.	73

Fig 4.4	Adsorption isotherms for BDDA and BDTA on three soils.	75
Fig 4.5	Leachate analyzed for BDDA for column packed with Delhi sand and a 300 mL of artificial rain water was poured at 0.2 mL min^{-1}.	82
Fig 5.1	Length of emerging seedlings.	98
Fig 5.2	Dry mass of lettuce (a,b,c) and garden cress (d,e,f) exposed to BDDA and/or BDTA.	101
Fig 5.3	N and Mg content of lettuce and garden cress exposed to BDDA and/or BDTA.	103
Fig 5.4a	Four macronutrients (phosphorus, P; potassium, K; calcium, Ca; and sulfur, S) and 6 micronutrients (boron, B; manganese, Mn; iron, Fe; zinc, Zn; molybdenum, Mo; and copper, Cu) were presented in lettuce shoot exposed to BDDA and/or BDTA.	104
Fig 5.4b	Four macronutrients (phosphorus, P; potassium, K; calcium, Ca; and sulfur, S) and 6 micronutrients (boron, B; manganese, Mn; iron, Fe; zinc, Zn; molybdenum, Mo; and copper, Cu) were presented in lettuce root exposed to BDDA and/or BDTA.	105
Fig 5.4c	Four macronutrients (phosphorus, P; potassium, K; calcium, Ca; and sulfur, S) and 6 micronutrients (boron, B; manganese, Mn; iron, Fe; zinc, Zn; molybdenum, Mo; and copper, Cu) were presented in garden cress shoot exposed to BDDA and/or BDTA.	106
Fig 5.4d	Four macronutrients (phosphorus, P; potassium, K; calcium, Ca; and sulfur, S) and 6 micronutrients (boron, B; manganese, Mn; iron, Fe; zinc, Zn; molybdenum, Mo; and copper, Cu) were presented in garden cress root exposed to BDDA and/or BDTA.	107
Fig 5.5	Total ion chromatograms of plant tissues (lettuce and garden cress) treated with BACs.	110
Fig 5.6	Mass balance for BDDA in hydroponic treatments after harvest (12 d).	114

Fig.6.1	Relationship between gas and liquid phase ozone concentration at steady-state and pH 7, 9 and 11 in Milli-Q water.	136
Fig.6.2	Predicted values plotted against experimental values for the % removal of BACs.	140
Fig.6.3	Contour plots of the combined effect of pH and H_2O_2 for the % removal of BACs using CCD.	141
Fig.6.4	Kinetics of BACs degradation in two different AOP conditions and their first order degradation models.	143
Fig.6.5	Relative quantification of intermediates for T-1 and T-2 with respect to the peak areas of parent BACs.	147/148
Fig.6.6	Proposed degradation pathways during AOP using O_3/H_2O_2.	151
Fig.6.7	Kendrick mass defect vs Kendrick mass for visual interpretation for P-4, 5, 6 and 6a.	153
Fig.6.8	Toxicity test of AOP treated solutions using (a) *Chlorella vulgaris* and (b) *Chlamydomonas reinhardtii* in duplicate.	155
Fig.6.9	Effect of AOP on the biodegradability of solutions containing BACs and the contribution of H_2O_2 during T-1 of the AOP in duplicate samples.	156
Fig.6.10	Growth of mixed bacterial cultures in presence of BDDA:BDTA at 50:25 mg L^{-1} with wastewater on LB-agar plates after 24 h incubation at 37°C.	158
Schematic 7.1	Simplified model to present the fate of BACs in natural and engineered systems.	174

List of Abbreviations

ANOVA	Analysis of variance
AOP	Advanced oxidation process
ARW	Artificial rain water
ASTM	American Society for Testing and Materials
bw	Body weight
BACs	Benzalkonium chlorides
BAH	Benzaldehyde
BDDA	Benzyl dimethyl dodecyl ammonium chloride
BDHA	Benzyl dimethyl hexadecyl ammonium chloride
BDMA	Benzyl dimethyl amine
BDTA	Benzyl dimethyl tetradecyl ammonium chloride
BOD	Biological oxygen demand
CCD	Central composite design
CEC	Cationic exchange capacity
COD	Chemical oxygen demand
DO	Dissolve oxygen
dpm	Disintegrations per minute
DS	Delhi Sand
F-test	Fisher's statistical test
GR	Growth rate
HB	Holiday Beach Clay
HPV	High production volume
HPLC-MS	High performance liquid chromatography-mass spectroscopy
HPLC-UV	High performance liquid chromatography-ultra violet
IWW	Influent wastewater
LOD	Limit of detection
LOQ	Limit of quantification
LL	London Loam

LSC	Liquid scintillation counting
NTU	Nephelometric turbidity unit
OECD	Organization for Economic Co-operation and Development
OM	Organic matter
PCR	Polymerase chain reaction
PRM	Parallel reaction monitoring
p-values	Probability values
QACs	Quaternary ammonium compounds
RAS	Returned activated sludge
RCF	Root concentration factor
RM-ANOVA	Repeated measures analysis of variance
RSM	Response surface methodology
SCF	Shoot concentration factor
SPM	Suspended particulate matter
TOC	Total organic carbon
UV	Ultra-violet
USEPA	United State Environmental Protection Agency
VSS	Volatile suspended solids
WWTP	Wastewater treatment plants

Nomenclature

A	The absorbance measured by the UV-Vis spectrophotometer
α	The star point used in CCD
BOD_5 (mg L^{-1})	Biological oxygen demand measured after 5 d of incubation
b (cm)	Path length
b (L mg^{-1})	Langmuir constant related to the affinity of the binding sites
C (mg L^{-1})	the concentration of the compound in mole L^{-1} or mg L^{-1}
C_0 (mg L^{-1})	Initial concentration
C_t (mg L^{-1})	Concentration at different time (t)
C_e (mg L^{-1})	Equilibrium concentration
ds (mg L^{-1})	Change of substrate concentration
dt	Change of time
$ddMS^2$	Data-dependent tandem mass spectroscopy
$\mathcal{E}$ (L mol^{-1} cm^{-1})	Molar absorptivity
EC_{50}	Effective concentration to inhibit the growth to 50%
K_d (L kg^{-1})	Distribution coefficients
K_m (mg L^{-1})	Michaelis constant
$K_{m(spe)}$ (mg L^{-1})	Specific Michaelis constant
K (mg^{-1} h^{-1})	Rate constant
K_{spe} (mg^{-1} h^{-1})	Specific rate constant
K_f (mg/g (L/mg) $^{1/n}$)	The Freundlich constants
k	The number of factors for CCD
LC_{50}	Concentration lethal to 50% of the test subjects

Log K_{oc} (L kg^{-1})	Carbon normalized adsorption coefficients
Log K_{ow}	Octanol-water partitioning coefficient
m/z	Mass to charge ratio
N	The number of experiments for CCD
N_0	The number of central points for CCD
μ (hours^{-1})	The specific growth rates of bacterium
μCi	Microcurie (unit of radioactive material)
OD_{600}	Optical density measured at 600 nm
OD_0	Optical density at time zero
OD_t	Optical density over time
ρ_{bulk} (g cm^{-3})	Bulk density
$\rho_{particle}$ (g cm^{-3})	Particle density
q_e (mg g^{-1})	Concentration of compound adsorbed on per unit adsorbent
q_{max} (mg g^{-1})	Maximum concentration of compound adsorbed on per unit adsorbent
V (liter)	Volume of water
V (mg L^{-1} h^{-1})	The rate of biodegradation
V_{max} (mg L^{-1} h^{-1})	Maximum forward velocity
$V_{max(spe)}$ (mg L^{-1} h^{-1})	Specific forward velocity
x	Coded form of the variables for CCD
X_H	High values of the selected variables in their uncoded form for CCD
X_L	Low values of the selected variables in their uncoded form for CCD

Chapter 1

Introduction

1.1 Introduction

Environmental pollution due to anthropogenic activities started in the early 20th century after the industrial revolution. Numerous inventions and the production of synthetic and semi-synthetic compounds (e.g., pharmaceuticals, pesticides and personal care products) brought prosperity and well-being of the people. However, the revolutionary pesticide/insecticide DDT (dichloro diphenyl trichloro ethane), which saved many lives from malaria by killing mosquitos, was found to bioaccumulate in fat cells of animals through their food chain, and to increase the risk of breast cancer among exposed women (Cohn et al., 2007).

The release of large amounts of emerging contaminants in the natural environment is a concern to many environmental scientists. In North America, about 26 metric tons of pharmaceutical waste is disposed annually down the drain, and another 26 tons are disposed annually with municipal solid waste in landfills (Gualtero, 2005). Xenobiotic compounds in the environment are drawing significant public, scientific, and regulatory concern because of their potential toxicity, mutagenicity, carcinogenicity, and genotoxicity (Randhawa and Kullar, 2011). Due to their recalcitrant nature, many of these compounds find their way into the soil environment either through the disposal of municipal wastewater, application of biosolids to agricultural fields, use of reclaimed wastewater for irrigation, industrial effluent, accidental spill, seepage of landfill leachate to ground water and as a manufacturing waste disposed in the landfill. As a result, many pollutants, such as pharmaceuticals and personal care products, have the potential to find their way into the food chain through plant uptake. A recent review by Miller et al. (2016) listed the uptake of a variety of micropollutants such as carbamazepine, sulfamethazine, antibiotics etc. in several food crops such as cucumber, cabbage and lettuce. The authors mentioned that there are not sufficient experimental data to facilitate quantitative predictions of uptake of various pollutants by different plant groups, indicating the need for sustained research in this area.

1.2 Benzalkonium chlorides

Benzalkonium chlorides (BACs) are organic cationic surfactants and a sub-group of quaternary ammonium compounds (QACs). Quaternary ammonium compounds (QACs) belong to the priority list of potential organic contaminants (Clarke and Smith, 2011). Figure 1.1 shows the broad range of concentrations of organic contaminants in sewage sludge. According to figure 1.1, QACs have the third highest concentration among the organic contaminants found in sewage sludge (around 100 mg kg^{-1} dw).

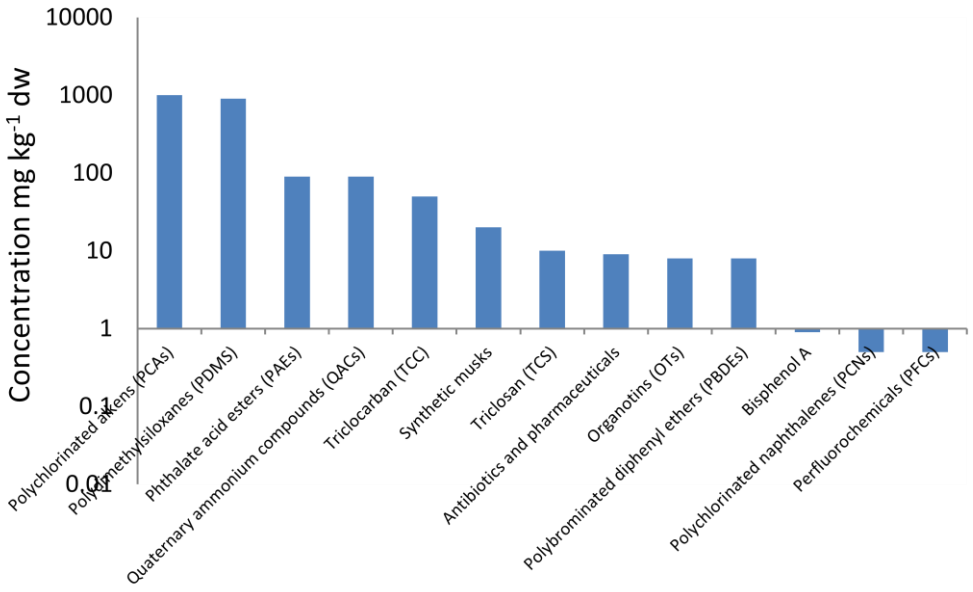

Fig 1.1 Typical concentrations of selected 'emerging' organic contaminants in sewage sludge (mgkg^{-1} dw) (Redrawn from Clarke and Smith, 2011).

Benzalkonium chlorides (BACs) contain four functional groups attached to a central nitrogen atom (R_4N^+). In a BAC molecule, these functional groups include at least one long alkyl chain (C_8 to C_{18}) and one benzyl group with methyl groups as the remaining functional

groups. The commercial use of non-ionic, anionic, cationic and amphoteric surfactants was 12 million tonnes in 2010, with a projected increase of 4.5% per year until 2018 to generate revenues of approximately US$41 billion (Brycki et al., 2014). QACs accounted for approximately 15% of the total consumption of surfactants and are classified into three major subgroups by United State Environmental Protection Agency (USEPA), as presented in Table 1.1.

Commercial synthesis of BACs was described by Dery (2001) as presented in Fig 1.2. BACs are produced by the quaternization of tertiary amines. First, a nucleophilic substitution reaction occurred between the fatty alcohol or alpha-olefin to produce alkyl halide or benzyl halide, which further reacts to produce the tertiary amine.

Cationic surfactants such as BACs have disinfectant properties, and have been applied to many targeted microbes, such as slime-forming bacteria, Gram-negative and Gram-positive bacteria, envelope and non-envelope viruses, mold/mildew, and algae (USEPA 2006). According to the USEPA, BACs can also be used for surface sanitization in industrial processes; to sanitize water systems, swimming pools, aquatic areas and wood; and sanitation of equipment in agricultural, public, commercial, and medical premises.

Table 1.1 Representative QAC groups and their general structure (X is a halide counter ion; redrawn from USEPA, 2006)

QAC group	**Molecular structure**	***LogK_{ow}**
Monoalkonium halides	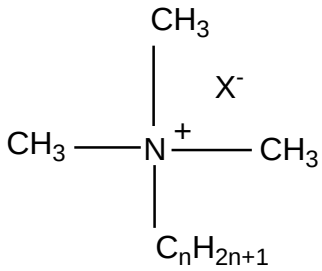	0.36 to 1.5 (n=12 to 16)
Dialkonium halides	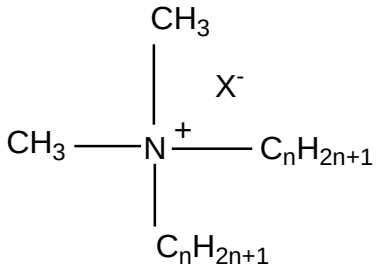	0.28 to 2.56 (n=8 to 10)
Benzalkonium halides	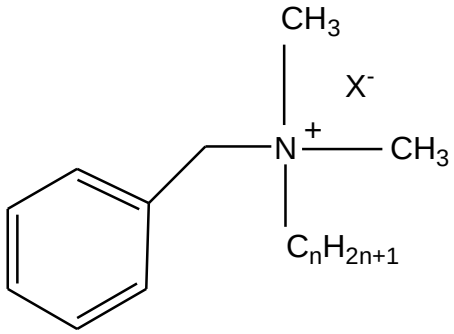	0.59 to 2.97 (n=12 to 16)

* Tezel (2009)

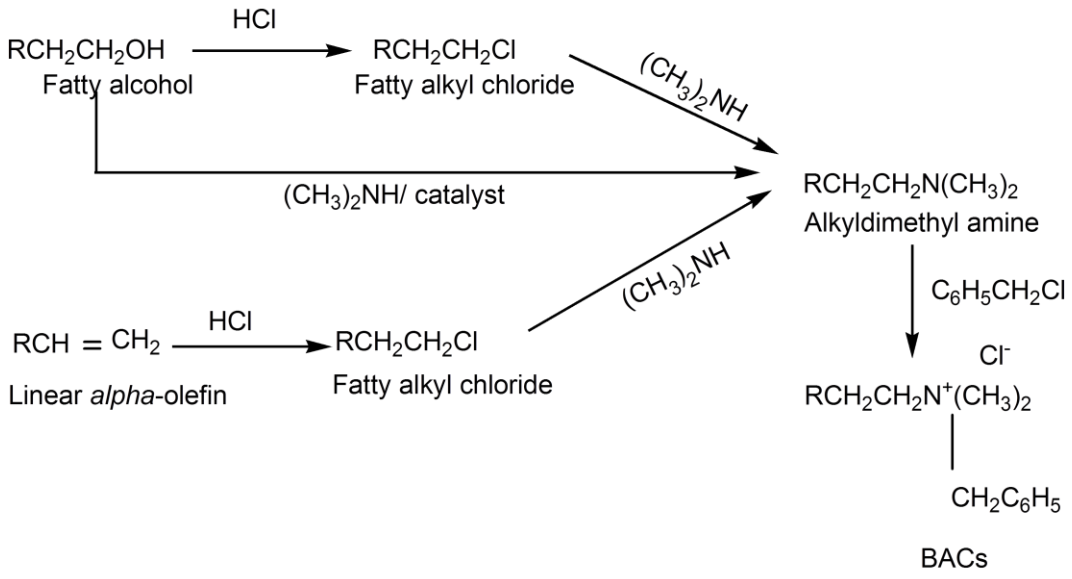

Fig 1.2 Synthesis routes for alkylbenzyl dimethyl ammonium chloride or BACs (redrawn from, Dery, 2001)

1.3 BACs in the natural environment

About 75% of the QACs, including BACs, used annually are released into wastewater treatment plants, whereas the rest is directly discharged into the environment, resulting in a significant presence of BACs in sewage systems (Ismail et al., 2010).

BACs are biodegradable in aerobic conditions (Ying, 2006; Bassey and Grigson, 2011). The positive charge of BACs makes them highly adsorptive onto negatively charged biomass, sediments, clays, and different minerals such as halides, sulphides, sulphates, and oxides. As a result, the BACs are partitioned onto the sludge during biological wastewater treatment and subsequently transferred along with the sludge to anaerobic digester where their biodegradability is retarded (Garcia et al., 1999). Consequently, the terrestrial environment can be contaminated with BACs through the application of municipal biosolids to agricultural land. Additionally, BACs can enter the aquatic environment via the suspended organic matter in wastewater effluent (Li et al., 2014) and eventually reach agricultural land through the application of reclaimed wastewater for irrigation. Therefore, there is a possibility of BACs

being transferred to the food chain due to uptake by plants grown on soils amended with biosolids or irrigated by wastewater laden with BACs.

The concentration of BACs in the natural environment varies widely. For example, the concentration of BACs was very high, up to 6.03 mg L^{-1}, in hospital effluents in many European countries (Kümmerer et al., 1997). A survey conducted in western Austria on nine different wastewater treatment plants, and 0.31 mg L^{-1} BACs was measured in the influent with a sharp reduction in the effluents of 0.002 mg L^{-1} of total BACs (Clara et al., 2007). The reduced amount was either biodegraded or adsorbed on the sludge in the wastewater treatment plant. About 9.0 mg kg^{-1} of BACs measured in sewage sludge (dry weight) in Austria (Martínez-Carballo et al., 2007) suggested that a significant portion of BACs was adsorbed on sludge. The fraction of BACs released into the effluents accumulated and was found in river sediments, up to 1.1 mg kg^{-1} in China (Li et al., 2014). In another study, BACs were also found in river sediments close to wastewater treatment plant or urban areas in the range of 0.022 to 0.21 mg kg^{-1} in USA (Ferrer and Furlong, 2002). Relatively higher amount of BACs were found in river sediments even after 99% removal of BACs in biological treatment plants (Clara et al., 2007), probably because BACs accumulated on sediments over time or BACs were exposed to river water from undertreated or untreated effluents containing BACs.

In a recent study, about 0.005 to 28.5 mg kg^{-1} of total BACs was measured in various soils in Korea (Kang and Shin, 2016). A very high concentration of BACs (5 to 30 mg L^{-1}) was measured in a roof runoff in France (Gromaire et al., 2015). Due to the abundance of BACs in various environments, it is very important to determine their ultimate fate in natural and engineered systems.

1.4 Toxic effect of BACs in various living organisms

A toxic effect of BACs was found in many aquatic organisms at environmentally relevant concentrations. An interview of Patricia Hunt (faculty at the Washington State University) published in Nature news reported that, n-alkyl dimethyl benzyl ammonium chloride and didecyl dimethyl ammonium chloride, which are common cage-disinfection chemicals, caused a decline in mouse fertility (Hunt, 2008). Ferk et al. (2007) demonstrated

that QACs induced moderate but significant genotoxic effects in eukaryotic cells at concentrations found in wastewaters (0.3 to 10 mg L^{-1}) and QACs released into the environment may cause genetic damage in exposed organisms. Grabińska-Sota (2011) found potential genotoxicity in *Bacillus subtilis* for a dosage of 10 mg L^{-1} of a type of BAC. Microalgae are more sensitive to the toxic effect of BACs. The EC_{50} (effective concentration to inhibit the growth to 50%) for a natural assemblage of algae in sea water was 36.4 µg L^{-1} in 24 h and 63.9 µg L^{-1} in 72 h (Pérez et al., 2009). According to the USEPA (2006), the LC_{50} (concentration lethal to 50% of the test subjects) of BACs to aquatic invertebrates was 5.9 µg L^{-1}. The USEPA (2006) also defined BACs as moderately toxic to birds (LC_{50} = 136 mg kg^{-1} bw^{-1}) and slightly toxic to mammals (LC_{50} = 430 mg kg^{-1} bw^{-1}). Given the sensitivity of aquatic organisms to BACs and their widespread use, it is important to understand their fate in the natural environment, including attenuation due to natural biodegradation, chemical processes and distribution in the soil environment, and the consequences when BACs come in contact with vegetation.

1.5 Literature gaps and objectives of this study

Agriculture accounts for 86% of total water consumption; integration of municipal and agricultural water management systems using reclaimed wastewater for irrigation can reduce water demand in water-stressed regions (Miller et al., 2016). Similarly, application of biosolids, a significant source of nutrients, to agricultural land is an efficient resource recovery process. For example, a total of 2.39 x 10^6 dw tons of biosolids (37% of total biosolids produced) per year are land-applied in several European countries (Kinney et al., 2006). In Ontario, Canada, 120 thousand dw tonnes of sewage biosolids are applied per year to agricultural fields as fertilizer (Sabourin et al., 2012). However, the fate of various micropollutants in agro-ecosystems and the risks of chronic exposure to these compounds through consumption of contaminated crops are of considerable research interest. In the present work, research is focused on two benzalkonium chlorides, which are commonly used in commercial products and are the most abundant in nature (Li et al., 2014). The selected

BACs are benzyl dimethyl dodecyl ammonium chloride (BDDA; 12-carbon alkyl chain) and benzyl dimethyl tetradecyl ammonium chloride (BDTA; 14-carbon alkyl chain) (Fig 1.3).

The fates (biodegradation, sorption, leaching and plant uptake) of these two BACs in the natural environment have not yet been studied. Initially, biodegradability of the two BACs was studied, followed by a study on sorption and leaching from agricultural soils amended with biosolids; and finally the possibility of plant uptake of BACs was investigated. An advanced oxidation of BACs was also developed for their removal before they are released into the natural environment.

The importance of this research lies in understanding the fate of BACs in a natural or engineered system for better understanding of the environmental risks associated with these compounds.

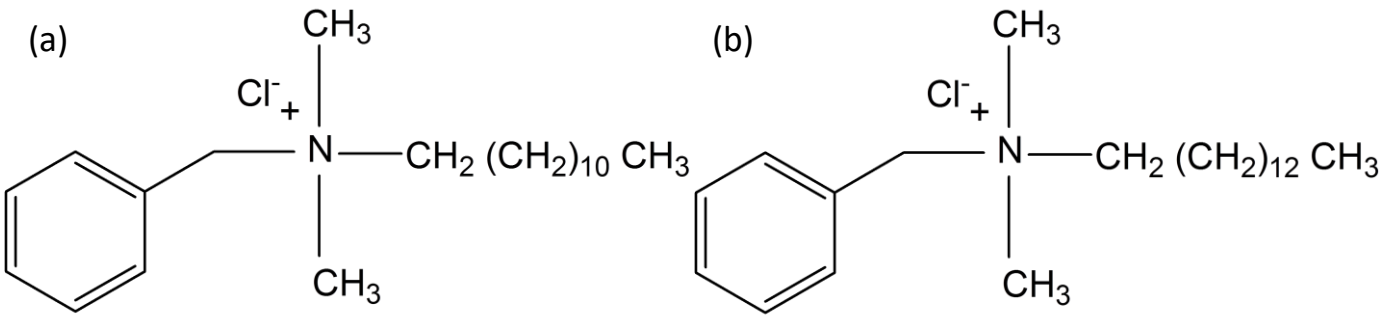

Fig. 1.3 Molecular structure of two common benzalkonium chlorides; (a) BDDA and (b) BDTA.

References

Bassey D.E., Grigson S.J.W., 2011. Degradation of benzyldimethyl hexadecylammonium chloride by *Bacillus niabensis* and *Thalassospira* sp. isolated from marine sediments. Toxicological and Environmental Chemistry 93, 44-56.

Brycki, B., Waligórska, M., Szulc, A., 2014. The biodegradation of monomeric and dimeric alkylammonium surfactants. Journal of Hazardous Materials 280, 797–815.

Clara M., Scharf S., Scheffknecht C., Gans O., 2007. Occurrence of selected surfactants in untreated and treated sewage. Water Research 41, 4339–4348.

Clarke B.O., Smith S.R., 2011. Review of 'emerging' organic contaminants in biosolids and assessment of international research priorities for the agricultural use of biosolids. Environment International 37, 226–247.

Cohn B.A., Wolff M.S., Cirillo P.M., Sholtz R.I., 2007. DDT and breast cancer in young women: new data on the significance of age at exposure. Environmental Health Perspective 115, 1406-1414.

Dery M., 2001. Cationic Surfactants: The synthesis and manufacture of cationic surfactants. *In* K. Holmberg (ed.), Handbook of Applied Surface and Colloid Chemistry, vol. 1. John Wiley & Sons, Ltd, West Sussex, England.

Ferrer I., Furlong E.T., 2002. Accelerated solvent extraction followed by on-line solid-phase extraction coupled to ion trap LC/MS/MS for analysis of benzalkonium chlorides in sediment samples. Analytical Chemistry 74, 1275-1280.

Ferk F., Misık M., Hoelzl C., Uhl M., Fuerhacker M., Grillitsch B., Parzefall W., Nersesyan A., Micieta K., Grummt T., Ehrlich V., Knasmuller S., 2007. Benzalkonium chloride (BAC) and dimethyldioctadecyl-ammonium bromide (DDAB), two common quaternary ammonium compounds, cause genotoxic effects in mammalian and plant cells at environmentally relevant concentrations. Mutagenesis 22, 363–370.

Garcia M.T., Campos E., Sanchez-Leal J., Ribosa I., 1999. Effect of the alkyl chain length on the anaerobic biodegradability and toxicity of quaternary ammonium based surfactants. Chemosphere 38, 3443-3483.

Grabińska-Sota E., 2011. Genotoxicity and biodegradation of quaternary ammonium salts in aquatic environments. Journal of Hazardous Materials 195, 182-187.

Gromaire M.C., Van de Voorde A., Lorgeoux C., Chebbo G., 2015. Benzalkonium runoff from roofs treated with biocide products–In situ pilot-scale study. Water Research 81, 279–287.

Gualtero S.M., 2005. Pollution prevention measures for unwanted pharmaceuticals. Industrial Ecology. (http://citeseerx.ist.psu.edu/viewdoc/summary?doi=10.1.1.571.9100; accessed September, 2016)

Hunt P., 2008. Lab disinfectant harms mouse fertility. Patricia Hunt interviewed by Brendan Maher. Nature 453 (7198), 964. (http://www.nature.com/news/2008/080618/full/453964a.html; accessed September, 2016)

Ismail Z.Z., Tezel U., Pavlostathis S.G., 2010. Sorption of quaternary ammonium compounds to municipal sludge. Water Research 44, 2303-2313.

Kang H.I., Shin H.S., 2016. Rapid and sensitive determination of benzalkonium chloride biocide residues in soil using liquid chromatography–tandem mass spectrometry after ultrasonically assisted extraction. Bulletin of the Korean Chemical Society 37, 1219–1227.

Kinney C., Furlong E.T., Zaugg S.D., Burkhardt M. R., Werner S.L., Cahill J.D., Jorgensen G.R., 2006. Survey of organic wastewater contaminants in biosolids destined for land application. Environmental Science and Technology 40, 7207-7215.

Kümmerer K., Eitel A., Braun U., Hubner P., Daschner F., Mascart G., Milandri M., Reinthaler F., Verhoef J., 1997. Analysis of benzalkonium chloride in the effluent from European hospitals by solid-phase extraction and high-performance liquid chromatography with post-column ion-pairing and fluorescence detection. Journal of Chromatography A 774, 281–286.

Li X., Luo X., Mai B., Liu J., Chen L., Lin S., 2014. Occurrence of quaternary ammonium compounds (QACs) and their application as a tracer for sewage derived pollution in urban estuarine sediments. Environmental Pollution 185, 127-133.

Martínez-Carballo E., González-Barreiro C., Sitka A., Kreuzinger N., Scharf S., Gans O., 2007. Determination of selected quaternary ammonium compounds by liquid chromatography with mass spectrometry. Part II. Application to sediment and sludge samples in Austria. Environmental Pollution 146, 543-547.

Miller E.L., Nason S.L., Karthikeyan K.G., Pedersen J.A., 2016. Root uptake of pharmaceuticals and personal care product ingredients. Environmental Science and Technology 50, 525–541.

Pérez P., Fernández E., Beiras R., 2009. Toxicity of benzalkonium chloride on monoalgal cultures and natural assemblages of marine phytoplankton. Water Air Soil Pollution 201, 319–330.

Randhawa G.K., Kullar J.S., 2011. Bioremediation of pharmaceuticals, pesticides and petrochemiclas with gomeya/cow dung. International Scholarly Research Network ISRN Pharmacology 2011, 1–7.
(http://www.ncbi.nlm.nih.gov/pmc/articles/PMC3197002/; accessed September, 2016)

Sabourin L., Duenk P., Bonte-Gelok S., Payne M., Lapen D.R., Topp E., 2012. Uptake of pharmaceuticals, hormones and parabens into vegetables grown in soil fertilized with municipal biosolids. Science of the Total Environment 431, 233–236.

United States Environmental Protection Agency (EPA739-R-06-009), August 2006. Reregistration eligibility decision for alkyl dimethyl benzyl ammonium chloride (ADBAC).
(https://archive.epa.gov/pesticides/reregistration/web/html/index-9.html; accessed September, 2016)

Ying G.G., 2006. Fate, behavior and effects of surfactants and their degradation products in the environment. Environment International 32, 417- 431.

Chapter 2

Literature Review

Development of sophisticated equipment and analytical chemistry, increasing numbers of compounds and their metabolites are being found in the environment. Most of these contaminants, mainly recalcitrant organic compounds, are released into the natural environment in many ways, such as, by the disposal of secondary effluents (directly or indirectly) from wastewater plants (Gros et al., 2010), by the application of wastewater for irrigation and/or by the land application of biosolids (treated sludge from wastewater treatment plants) as fertilizer (Walters et al., 2010), seepage of leachates into ground water from age old landfill (Bashir et al., 2009), runoff of pesticides from agricultural land to surface streams (Berenzen et al., 2005).

At present, there is no regulation in Ontario and many other provinces in Canada regarding the application of sewage sludge into agricultural land as fertilizer, which might contain recalcitrant organic pollutants (Canadian Council of Ministers of the Environment, 2010). In this research, two commonly used cationic surfactants (BDDA and/or BDTA) were selected as model pollutants to study their fate and degradation in natural and engineered systems. A brief literature review on these compounds is presented below.

2.1 Biodegradation of cationic surfactants

Biodegradation is a natural process and relies principally on bacteria, fungi and plants to transform contaminants to relatively less toxic compounds as a part of their regular life functions. Metabolic processes of these organisms are capable of utilizing some chemical contaminants as an energy source and eventually transform them into harmless products such as carbon dioxide and water.

Quaternary ammonium compounds enhance the bactericidal properties of commercial products and these compounds are resistant to microbial biodegradation at higher concentrations (Patrauchan and Oriel, 2003). However, biodegradation is the dominant process for degradation of low concentrations of QACs in the environment and several studies concerning the biodegradation of QACs have been published. One of the earliest

studies of bacterial degradation of QACs was conducted by Dean-Raymond and Alexander (1977). The authors isolated bacteria from soil and sludge and characterized the biodegradation of ten QACs, determining the biological oxygen demand of the samples instead of monitoring individual QACs. A few other reports on the biodegradation of QACs are also available (Sullivan, 1983; Kroon et al., 1994; Nishiyama et al. 1995; Nishihara et al., 2000; Nishiyama and Nishihara, 2002; Takenaka et al., 2007; Liffourrena et al., 2008) and the QACs investigated in these studies were mostly mono or dialkonium salts and degradation was assessed using various strains of *Pseudomonas* sp. The very first study on the biodegradation of benzalkonium chloride (QAC with a benzyl group) in the concentration range of 30–300 mg L^{-1} was carried out using *Aeromonas hydrophila* ssp. K., isolated from a polluted soil (Patrauchan and Oriel, 2003). The metabolic pathway of the bacterium *Aeromonas hydrophila* ssp. K. involves the cleavage of C_{alkyl}-N bond as the initiation step of BAC catabolism. Their study also indicated that BACs were toxic at higher concentration and inhibited bacterial growth at 100, 200, and 300 mg L^{-1} of BAC. As a result of transformation, benzylamine, benzaldehyde (BAH), and benzoic acid were formed; BAH, as the only growth substrate, was utilized very rapidly and completely converted to benzoic acid, which accumulated in the medium. Benzylamine was converted to BAH as a result of oxidative deamination reaction by amine oxidase. In addition, the co-product of deamination reaction is an ammonium ion that may serve as a nitrogen source. *Aeromonas hydrophila* ssp. K. was able to utilize benzoic acid as sole carbon source, although no other intermediates were analyzed.

In another study, two bacteria isolated from marine sediments (*Bacillus niabensis* and *Thalassospira* sp.) were tested for the biodegradation of benzyl dimethyl hexadecyl ammonium chloride (BDHA with C_{16} alkyl chain length) (Bassey and Grigson, 2011). These authors also indicated cleavage of the C_{alkyl}-N bond as the initial step for the breakdown of BDHA by the bacteria. Both strains were capable of degrading BDHA when it was present at concentrations in the range 2–4 mg mL^{-1}. The presence of N,N-dimethylbenzylamine as a metabolite suggests the cleavage of the C-$_{alkyl}$-N bond. Biotransformation of BDTA (benzyl dimethyl tetradecyl ammonium chloride) to BDMA (benzyl dimethyl amine) occurred using a

mixed community of *Pseudomonas* sp., which reduced the toxic effect of BDTA by about 500 times as measured by EC_{50} (Tezel et al., 2012).

The above studies indicate that QACs such as BACs are biodegradable in aerobic conditions. It has also been found that various bacteria, such as *Pseudomonas* sp., *Aeromonas hydrophila* ssp. K., *Bacillus niabensis* and *Thalassospira* sp. were efficient in biodegradation and/or biotransformation of the QACs.

Being bactericidal, biodegradation of QACs depends on the initial concentration of the compounds as well as the presence of strains capable of degrading the compounds. Regardless of their biodegradability, QACs/BACs can be found in many environmental samples such as municipal sludge, soil and river sediments close to urban or industrial locations (Martínez-Carballo et al., 2007; Li et al., 2014). Typically, BACs in commercial products are a mixture of BACs with various alkyl chain lengths (Takeoka G.R., 2005); as a result, it is more likely that they will be found as a mixture in environmental samples. Although substantial research has been conducted on the biodegradation of QACs as single compounds, studies related to biodegradation of a mixture of QACs and their inhibitory or synergistic effect on biodegradation are not available in published literature. In addition to that, biodegradation kinetics of such compounds are unavailable in the published reports, information which is very important for any engineered system that aims to scale-up QACs/BACs degradation using microorganisms. Therefore, one of the objectives of this research is to investigate the biodegradation of two commonly used BACs, individually and in mixture, and to extract kinetic data.

2.2 Adsorption and leaching of organic pollutants

The use of reclaimed wastewater for irrigation or the application of biosolids as fertilizer for soil amendment has the potential to transfer organic pollutants (such as BACs) into the soil environment. The fate of pollutants in the natural environment includes transport processes such as convection, diffusion and dispersion, adsorption and leaching, and persistence (biodegradation and chemical oxidation). Adsorption plays an important role in the behaviour of chemical compounds in soils and influences degradation, and leaching.

There is not much literature on the adsorption of BACs on sludge or soil; so far, only three studies report the adsorption of BACs on different types of sludge during the wastewater treatment process. García et al. (2006) studied the adsorption of BACs on sludge collected from a thickening tank, while Ismail et al. (2010) determined the adsorption of QACs (two different monoalkonium and benzalkonium halides) on four different sludges, primary, waste-activated, mesophilic and thermophilic digested sludge. The adsorption capacity of sludge was higher for benzalkonium halides compared to monoalkonium halides (Ismail et al., 2010). However, in both studies, the authors have indicated that the adsorption of BACs on sludge increases with the increasing carbon chain length in the BAC molecules. The sorption process is governed by both electrostatics as well as hydrophobic interactions between the surfactant molecules and the negatively charged sludge particles. Ren et al. (2011) studied the adsorption of tetradecyl benzyl dimethyl ammonium chloride (BDTA) on activated sludge at different pH, ionic strength and temperature. Adsorption equilibrium was achieved within 2 h of contact time, and the adsorption capacity increased with increasing solution pH up to pH 9.

Sarkar et al. (2010) were the first to report the sorption of different QACs (monoalkonium halides) on agricultural soils. They investigated the effect of three commonly used QACs, namely hexadecyl trimethyl ammonium bromide, octadecyl trimethyl ammonium bromide and Arquad, on dehydrogenase and potential nitrification activities in three different soils. The QACs inhibited the dehydrogenase activity and nitrification of the soils, and the toxic effect of QACs on soil microbial activities was influenced by the relative release of adsorbed QACs in soils. As a result, it is important to monitor the adsorption and leaching of these compounds to determine their bioavailability and the fate in soil environment, which are the key factors for the risk assessment of a micropollutant in soil. Therefore, reliable methods for the determination of leaching behaviour of contaminants are required.

Several different approaches have been used to determine desorption and leaching of organic compounds from contaminated soil. For example, stirred aqueous batch tests, introduction of a third phase as an adsorbent to the soil/water system, and column leaching tests are commonly adopted methods for leaching and desorption studies of organic

compounds from soil (Enell et al., 2004; García Frutos et al., 2011). Stirred aqueous batch tests have been applied by many authors to study the sorption and desorption of organic compounds in soil (Ismail et al., 2010); however, the effect of grinding of soils may overestimate the desorption rate of compounds when using this method (Enell et al., 2004). Column leaching methods are considered to be more realistic in determining the leaching and desorption of organic compounds occurring in the field (García Frutos et al., 2011).

The leaching of organic contaminants in soils depends on the adsorption equilibrium between the compounds in soil solution and adsorbed amount to the solid constituents of the soil, which in turn depends on available binding sites on the soil, mostly due to hydroxyl and carboxylic acid functionalities. The van der Waals attractions are important with soils with higher amount of clays as the compounds migrate between sheets in the clay structure or in binding sites on the edges of those sheets. The soils containing both higher clay and organic matter content have more potential binding sites for retention of the compounds consequently reducing the extent of leaching. The only study related to desorption/leaching of a BAC (hexadecyl benzyl dimethyl ammonium chloride with 16 carbon alkyl chain) from sewage sludge reported that about 5% of the BAC was desorbed in 24 h (Ismail et al., 2010). In another study, two different monoalkonium chlorides were found to desorb by 10 to 60%, depending on their molecular structure, from soil samples (Sarkar et al., 2010).

It is unavoidable to release organic pollutants (such as BACs) in the natural environment and it can happen in many ways, such as by the land application of biosolids, use of reclaimed wastewater for irrigation or by direct discharge of pollutants or due to soil erosion into sediments if BACs are present in agricultural land due to soil amendment with biosolids. The first two possibilities can be mitigated by redesigning/improving the conventional wastewater treatment technologies, which of course will take many years with the potential involvement of money. As a result, understanding on the sorption and leaching behaviour of BACs would be beneficial to characterize the risk associated to these compounds. For example, uptake of BACs from soil by plants is only possible if they are desorbed and become mobile in the rooting zone of soil environment.

To date, no study has been performed to determine the adsorption parameters of BACs on various types of agricultural soils and the leaching possibilities of BACs from biosolids or when soils are amended with biosolids. As a result, understanding the adsorption and leaching behaviour of BACs from soils amended with biosolids would be beneficial to characterize the risk associated with them.

2.3 Plant uptake of organic pollutants in hydroponics

The eco-toxicological effects of a large group of organic contaminants, such as pharmaceuticals, personal care products, plasticizers, surfactants, and herbicides, are relatively unknown (Murray et al., 2010; Calderon-Preciado et al., 2011). The potential presence of thousands of organic contaminants in wastewater effluents and in biosolids (Clarke and Smith, 2011) has engaged scientists to revisit the possible routes of exposure of these organic contaminants to livestock and humans. Information on the uptake of organic contaminants by plants and subsequent transfer to the food chain has been reported for many pollutants. The potential for uptake of organic pollutants by crop plants largely depends on plant physiology, soil characteristics, and also on the physical properties of contaminants such as polarity, solubility, hydrophobicity and molecular size.

In a greenhouse experiment, Wu et al. (2010) studied the uptake of three pharmaceuticals (carbamazepine, diphenhydramine, and fluoxetine) and two personal care products (triclosan and triclocarban) by soybean (*Glycine max* (L.) Merr.). Two types of treatments simulating biosolids application and wastewater irrigation were investigated. The plant tissues and soils were analyzed for target compounds after growing periods of 60 and 110 d. Carbamazepine, triclosan, and triclocarban were concentrated in root tissues and translocated into aboveground parts including beans, whereas accumulation and translocation for diphenhydramine and fluoxetine was limited. A higher concentration in plants was seen for biosolids application than wastewater irrigation due to a higher loading of compounds in biosolids. However, compounds introduced by irrigation appeared to be more available for uptake and translocation. The same authors detected carbamazepine, diphenhydramine, and triclocarban in five different crop plants that were grown in an

agricultural field treated with biosolids (Wu et al., 2012). At the time of harvest, three compounds were detected in all plants grown in biosolids-treated soils. Calculated root concentration factor and shoot concentration factor (ratio of pollutants concentration in plant tissue to the concentration in solution at harvest) were highest for carbamazepine followed by triclocarban and diphenhydramine, and the root concentration factor was positively correlated with root lipid content for carbamazepine but not for diphenhydramine and triclocarban. The authors also indicated that the difference in uptake behaviour between plant species could not solely be attributed to the root lipid content. In contrast, Sabourin et al. (2012) reported the presence of only 8 micropollutants from a total of 141 compounds with concentration ranging from 0.33 to 6.25 ng g^{-1} dry weights in tomatoes, carrots, potatoes and sweet corn that were harvested one year after the application of biosolids in a field experiment. Overall, this study suggests that the potential for micropollutant uptake into crops under normal farming conditions is not significant.

Plant uptake studies conducted under hydroponic conditions are useful to evaluate the interaction between the physicochemical properties of organic pollutants and the plant by avoiding several complicated factors related to a soil system, such as sorption to soil components and transformations of pollutants mediated by soil microbes and particles. Hydroponic conditions relatively assure maximum availability of organic compounds to plant roots compared to soil matrices but they do not always result in more uptake than that for soil exposure (Miller et al., 2016). Several advantages of hydroponic systems compared to traditional farming methods exist. Hydroponics utilize reused nutrient-laden water, does not require natural precipitation, fertile land, and pesticides. It also uses less water and space than a traditional agricultural system. An anticipated projection of global hydroponic market is estimated from $19.95 billion in 2015 to $27.33 billion in 2020 (http://www.researchandmarkets.com/research/4ksm75/global, accessed September 2016). Therefore, plant uptake studies using a hydroponics system will generate useful information, especially for plants grown on recycled water.

Many studies in hydroponics have demonstrated that organic pollutants from various sources can be taken up by plant roots and translocated to the aboveground parts of the

plant. An antidiabetic medicine, metformin, with molecular weight 129 g mol^{-1} was taken up by *Typha latifolia* (cattail) roots and translocated into leaves (Cui and Schröder, 2016). The presence of metabolites of metformin in the plant indicates that phytoremediation of metformin can occur using *Typha latifolia*. Bisphenol A and nonylphenol are the two most common compounds among many endocrine disrupting compounds found to be taken up by *Lactuca sativa* (lettuce) and *Lycopersicon esculentum* (tomato) and the compounds were found in both plants including the tissue of tomato fruit (Lu et al., 2015). Eleven diverse crop plants namely cucumber (*Cucumis sativus*), tomato (*Solanum lycopersicum*), cabbage (*Brassica oleracea*), okra (*Abelmoschus esculentus*), pepper (*Capsicum annuum*), potato (*Solanum tuberosum*), beet (*Beta vulgaris*), onion (*Allium cepa*), broccoli (*Brassica oleracea*), celery (*Apium graveolens*), and asparagus (*Asparagus officianalis*), were tested hydroponically for the uptake of triclocarban and triclosan (commonly used antimicrobial compounds) by Mathews et al. (2014). Both compounds in the concentration range of 86 to 1350 mg kg^{-1} and 0.3 to 5 mg kg^{-1} were determined in roots and shoots, respectively, of all plants.

There are three main pathways by which chemical compounds can enter plants (Ryan et al., 1988). These are:

- Root uptake followed by translocation in the plant's transpiration stream.
- Vegetative uptake of vapour from the air surrounding the plant.
- Uptake by external contamination of shoots by soil and dust, followed by retention in the cuticle or penetration through it.

To date, no peer-reviewed study on the uptake of BACs or any QACs by crop plants either from soil or hydroponic system has been published, which is one of the objectives of this research.

2.4 Advanced oxidation processes as pretreatment

With growing concern over the presence of micropollutants in wastewater, tertiary treatment of wastewater using various combinations of membrane processes, activated carbon adsorption, and advanced oxidation are being performed with stringent water quality

requirements. Advanced oxidation processes (AOPs) that produce hydroxyl radicals in-situ are widely used for the removal of trace amounts of recalcitrant organics from various streams (Munter, 2001). Unlike phase-transfer processes such as air stripping and adsorption, AOPs are destructive processes and can cause complete mineralization of organic compounds. Fast and non-selective radical reactions (i.e. AOPs) have found widespread interest among scientists and engineers for the removal of recalcitrant pollutants from municipal and industrial wastewater (Vogelpohl, 2007).

In the future, AOPs may lead the water treatment technologies to remove highly stable and low or non-biodegradable organic pollutants, which are not treatable by conventional biological wastewater treatment processes (Malato et al., 2007). Any combination of AOPs, such as photochemical (ultra-violet/ozone (UV/O_3); UV/H_2O_2), photo-catalysis (TiO_2/UV, photo-Fenton), and chemical oxidation (O_3, O_3/H_2O_2, H_2O_2/Fe^{2+}), produce $OH^{\bullet}$ and superoxide radicals, which are very reactive towards most organic molecules and the process is very fast and non-selective (Skoumal et al., 2006).

Despite many advantages, the relatively high cost of AOPs limits its implementation at the industrial scale for wastewater treatment (Sarria et al., 2003). However, AOPs can be a viable pretreatment when transformation products formed from recalcitrant compounds are readily biodegradable in a downstream biological treatment (Sarria et al., 2003). As a result, AOPs combined with biological treatment could be a cost viable approach for future wastewater treatment processes (Cañizares et al., 2009).

For the application of AOPs combining biological degradation, Scott and Ollis (1995) have divided wastewater effluents into four different categories: (i) presence of bio-recalcitrant large macromolecules (i.e. soluble polymers), (ii) large concentration of biodegradable compounds with small concentration of recalcitrant organic pollutants, (iii) toxic or growth-inhibiting compounds for microbial cultures, and (iv) inert metabolites that might accumulate in the medium.

Several published studies report the use of AOPs to remove cationic surfactants from wastewater or drinking water. The earliest study was conducted to evaluate the effect of ozone on compounds containing saturated and unsaturated chemical bonds. Di- and

trimethyl alkyl ammonium chlorides (QACs) with a mixture of saturated and unsaturated bonds were tested, and the unsaturated QACs were degraded but the degradation of saturated QACs was negligible (Corless et al., 1989). A few other research groups used various AOPs namely ferret (iron VI) (Eng et al., 2006; Yang et al., 2013), photo Fenton (ultra-violet (UV) in presence of Fe^{+2} with H_2O_2; Ono et al., 2012), and UV/H_2O_2 (Olmez-Hanci et al., 2011) to promote QAC oxidation. Only six studies of AOPs for BACs were found; three of the studies used photocatalytic oxidation (Hidaka et al., 1992; Zhao et al., 1993; Loveira et al., 2012), one used UV/H_2O_2 (Adams and Kuzhikannil, 2000), and two recent studies used ozone with NiO and TiO_2 nano-particles (Suchithra et al., 2015; Carbajo et al., 2016). Only two studies dealt with pretreatment of QACs to improve their biodegradability Adams and Kuzhikannil, (2000) and Carbajo et al. (2016).

Among the various AOPs, photocatalytic processes are not efficient in wastewater even at low turbidity (< 2 NTU; Cantwell and Hofmann, 2011) due to poor penetration of UV light; and the use of nanoparticles are toxic to microorganisms and would inhibit the biological treatment processes (Garner and Keller, 2014), if AOP is used as a pretreatment process. As a result, chemical oxidation using ozone or ferret (iron VI) is the most promising alternative; however, oxidation using ferret is highly pH-dependent (Eng et al., 2006). Based on this literature review, the following objectives of this research are derived.

2.5 Objectives of the research

QACs (BAC is a sub group of QAC) have been listed as high production volume (HPV) chemicals by the USEPA and the Organization for Economic Co-operation and Development. In addition to the toxicological effect of BACs, due to their benzyl group, BACs are UV detectable and hold an extra advantage over other cationic surfactants from experimental perspective. Therefore, BACs have been selected as model compounds to represent the large group of cationic surfactants.

Although, the presence of QACs such as BAC in aquatic environments, wastewater effluent, sludge and soil has been established in the literature, there is no systematic information on the environmental fate of the two most widely used BACs, BDDA and BDTA,

such as, biodegradation, adsorption, leaching and plant uptake. The objective of this research is to understand the fate of BDDA and BDTA in the natural environment with the following specific objectives which constitute the respective chapters of this thesis. The specific objectives are:

I. Investigate the biodegradation of BDDA and BDTA individually and in mixture (Chapter 3)
II. Determine the sorption isotherms of BDDA and BDTA in various agricultural soils and evaluate their leaching possibility from the soils amended with biosolids (Chapter 4)
III. Determine the uptake of BDDA and BDTA in vegetable plants in a hydroponic system (Chapter 5)
IV. Develop an advanced oxidation process for BDDA and BDTA to reduce their bio-toxicity (Chapter 6)

References

Adams C.D., Kuzhikannil J.J., 2000. Effects of UV/H_2O_2 peroxidation on the aerobic biodegradability of quaternary amine surfactants. Water Research 34, 668–672.

Bashir M.J.K., Isa M.H., Kutty S.R.M., Awang Z.B., Aziz H.A., Mohajeri S., Farooqi I.H., 2009. Landfill leachate treatment by electrochemical oxidation. Waste Management 29, 2534–2541.

Bassey D.E., Grigson S.J.W., 2011. Degradation of benzyldimethyl hexadecylammonium chloride by *Bacillus niabensis* and *Thalassospira* sp. isolated from marine sediments. Toxicological and Environmental Chemistry 93, 44-56.

Berenzen N., Lentzen-Godding A., Probst M., Schulz H., Schulz R., Liess M., 2005. A comparison of predicted and measured levels of runoff-related pesticide concentrations in small lowland streams on a landscape level. Chemosphere 58, 683–691.

Brycki, B., Waligórska, M., Szulc, A., 2014. The biodegradation of monomeric and dimeric alkylammonium surfactants. Journal of Hazardous Materials 280, 797–815.

Calderon-Preciado D., Matamoros V., Bayona J.M., 2011. Occurrence and potential crop uptake of emerging contaminants and related compounds in an agricultural irrigation network. Science of the Total Environment 412-413, 14-19.

Canadian Council of Ministers of the Environment, 2010. A review of the current Canadian legislative framework for wastewater biosolids, pp-48 (accessed September, 2016)

Cañizares P., Paz R., Saez C., Rodrigo M.A., 2009. Costs of the electrochemical oxidation of wastewaters: a comparison with ozonation and Fenton oxidation processes. Journal of Environmental Management 90, 410–420.

Cantwell R.E., Hofmann R., 2011. Ultraviolet absorption properties of suspended particulate matter in untreated surface waters. Water Research 45, 1322–1328.

Carbajo J.B., Petre A.L., Rosal R., Berná A., Letón P., García-Calvo E., Perdigón-Melón J.A., 2016. Ozonation as pretreatment of activated sludge process of a wastewater containing benzalkonium chloride and NiO nanoparticles. Chemical Engineering Journal 283, 740–749.

Clarke B.O., Smith S.R., 2011. Review of 'emerging' organic contaminants in biosolids and assessment of international research priorities for the agricultural use of biosolids. Environment International 37, 226–247.

Corless C., Reynolds G., Graham N., Perry R., Gibson T.M., Haley J., 1989. Aqueous ozonation of a quaternary ammonium surfactant. Water Research 23, 1367–1371.

Cui H., Schröder P., 2016. Uptake, translocation and possible biodegradation of the antidiabetic agent metformin by hydroponically grown *Typha latifolia*. Journal of Hazardous Materials 308, 355–361.

Dean-Raymond D., Alexander M., 1977. Bacterial metabolism of quaternary ammonium compounds. Applied and Environmental Microbiology 33, 1037-1041.

Enell A., Reichenberg F., Warfvinge P., Ewald G., 2004. A column method for determination of leaching of polycyclic aromatic hydrocarbons from aged contaminated soil. Chemosphere 54, 707–715.

Eng Y.Y., Sharma V.K., Ray A. K., 2006. Ferrate (VI): Green chemistry oxidant for degradation of cationic surfactant. Chemosphere 63, 1785–1790.

García Frutos F.J., Escolano O., García S., Ivey G.A., 2011. Mobilization assessment and possibility of increased availability of PAHs in contaminated soil using column tests. Soil and Sediment Contamination 20, 581-591.

García M.T., Campos E., Sánchez-Leal J., Comelles F., 2006. Sorption of alkyl benzyl dimethyl ammonium compounds by activated sludge. Journal of Dispersion Science and Technology 27, 739–744.

Garner K.L., Keller A.A., 2014. Emerging patterns for engineered nanomaterials in the environment: a review of fate and toxicity studies. Journal of Nanoparticle Research 16, 2502–2530.

Gros M., Petrovic M., Ginebreda A., BarcelÓ D., 2010. Removal of pharmaceuticals during wastewater treatment and environmental risk assessment using hazard indexes. Environmental International 36, 15–26.

Hidaka H., Zhao J., Peiizzetti E., Serpone N., 1992. Photodegradation of surfactants. 8. Comparison of photocatalytic processes between anionic sodium dodecylbenzenesulfonate and cationic benzyldodecyldlmethylammonlum chloride on the TiO_2 surface. Journal of Physical Chemistry 96, 2226–2230.

Ismail Z.Z., Tezel U., Pavlostathis S.G., 2010. Sorption of quaternary ammonium compounds to municipal sludge. Water research 44, 2303-2313.

Kang H.I., Shin H.S., 2016. Rapid and sensitive determination of benzalkonium chloride biocide residues in soil using liquid chromatography–tandem mass spectrometry after ultrasonically assisted extraction. Bulletin of the Korean Chemical Society 37, 1219–1227.

Kroon A.G.M., Pomper M.A., van Ginkel C.G., 1994. Metabolism of dodecyl dimethyl amine by *Pseudomonas* MA3. Applied Microbiology Biotechnology 42, 134-139.

Liffourrena A.S., Lopez F.G., Salvano M.A., Domenech C.E., Lucchesi G.I., 2008. Degradation of tetradecyl trimethyl ammonium by *Pseudomonas putida* A ATCC 12633 restricted by accumulation of trimethyl amine is alleviated by addition of Al^{3+} ions. Journal of Applied Microbiology 104, 396−402.

Li X., Luo X., Mai B., Liu J., Chen L., Lin S., 2014. Occurrence of quaternary ammonium compounds (QACs) and their application as a tracer for sewage derived pollution in urban estuarine sediments. Environmental Pollution 185, 127-133.

Loveira E.L., Fiol P.S., Senn A., Curutchet G., Candal R., Litter M.I., 2012. TiO_2-photocatalytic treatment coupled with biological systems for the elimination of benzalkonium chloride in water. Separation and Purification Technology 91, 108–116.

Lu J., Wu J., Stoffella P.J., Wilson P.C., 2015. Uptake and distribution of bisphenol A and nonylphenol in vegetable crops irrigated with reclaimed water. Journal of Hazardous Materials 283, 865–870.

Malato S., Blanco J., Maldonado M.I., Oller I., Gernjak W., Pérez-Estrada L., 2007. Coupling solar photo-Fenton and biotreatment at industrial scale: Main results of a demonstration plant. Journal of Hazardous Materials 146, 440–446.

Martínez-Carballo E., González-Barreiro C., Sitka A., Kreuzinger N., Scharf S., Gans O., 2007. Determination of selected quaternary ammonium compounds by liquid chromatography with mass spectrometry. Part II. Application to sediment and sludge samples in Austria. Environmental Pollution 146, 543-547.

Mathews S., Henderson S., Reinhold D., 2014. Uptake and accumulation of antimicrobials, triclocarban and triclosan, by food crops in a hydroponic system. Environmental Science and Pollution Research 21, 6025–6033.

Miller E.L., Nason S.L., Karthikeyan K.G., Pedersen J.A., 2016. Root uptake of pharmaceuticals and personal care product ingredients. Environmental Science and Technology 50, 525–541.

Munter R., 2001. Advanced oxidation processes current status and prospects. Proceedings of the Estonian Academy of Sciences. 50, 59–80.

Murray K.E., Thomas S.M., Bodour A.A., 2010. Prioritizing research for trace pollutants and emerging contaminants in the freshwater environment. Environmental Pollution 158, 3462-3471.

Nishiyama N., Toshima Y., Ikeda Y., 1995. Biodegradation of alkyltrimethylammonium salts in activated sludge. Chemosphere 30, 593-603.

Nishihara T., Okamoto T., Nishiyama N., 2000. Biodegradation of didecyldimethylammonium chloride by *Pseudomonas fluorescens* TN4 isolated from activated sludge. Journal of Applied Microbiology 88, 641-647.

Nishiyama N., Nishihara T., 2002. Biodegradation of dedecyltrimethylammonium bromide by *Pseudomonas fluorescens* F7 and F2 isolated from activated sludge. Microbes and Environment 17, 164–169.

Olmez-Hanci T., Arslan-Alaton I., Basar G., 2011. Multivariate analysis of anionic, cationic and nonionic textile surfactant degradation with the H_2O_2/UV-C process by using the capabilities of response surface methodology. Journal of Hazardous Materials 185, 193–203.

Ono E., Tokumura M., Kawase Y., 2012. Photo-Fenton degradation of non-ionic surfactant and its mixture with cationic or anionic surfactants. Journal of Environmental Science and Health, Part A 47, 1087–1095.

Patrauchan M.A., Oriel P.J., 2003. Degradation of benzyldimethylalkylammonium chloride by *Aeromonas hydrophila* sp. *K.* Journal of Applied Microbiology 94, 266-272.

Ren R., Liu D., Li K., Sun J., Zhang C., 2011. Adsorption of quaternary ammonium compounds onto activated sludge. Journal of Water Research and Protection 3, 105–113.

Ryan J.A., Bell R.M., Davidson J.M., O'Connor G.A., 1988. Plant uptake of non-ionic organic chemicals from soils. Chemosphere 17, 2299-2323.

Sabourin L., Duenk P., Bonte-Gelok S., Payne M., Lapen D.R., Topp E., 2012. Uptake of pharmaceuticals, hormones and parabens into vegetables grown in soil fertilized with municipal biosolids. Science of the Total Environment 431, 233–236.

Sarkar B., Megharaj M., Xi Y., Krishnamurti G.S.R., Naidu R., 2010. Sorption of quaternary ammonium compounds in soils: Implications to the soil microbial activities. Journal of Hazardous Materials 184, 448–456.

Sarria V., Kenfack S., Guillod O., Pulgarin C., 2003. An innovative coupled solar-biological system at field pilot scale for the treatment of biorecalcitrant pollutants. Journal of Photochemistry and Photobiology A: Chemistry 159, 89–99.

Scott J.P., Ollis D.F., 1995. Integration of chemical and biological oxidation processes for water treatment: review and recommendations. Environmental Progress and Sustainable Energy 14, 88-103.

Skoumal M., Cabot P.L., Centellas F., Arias C., Rodríguez R.M., Garrido J.A., Brillas E., 2006. Mineralization of paracetamol by ozonation catalyzed with Fe^{2+}, Cu^{2+} and UVA light. Applied Catalysis B: Environmental 66, 228–240.

Suchithra P.S., Carleer R., Ananthakumar S., Yperman J., 2015. A hybridization approach to efficient TiO_2 photodegradation of aqueous benzalkonium chloride. Journal of Hazardous Materials 293, 122–130.

Sullivan D.E., 1983. Biodegradation of a cationic surfactant in activated sludge. Water Research 17, 1145-1151.

Takenaka S., Tonoki T., Taira K., Murakami S., Aoki K., 2007. Adaptation of *Pseudomonas* sp. Stain 7-6 to quaternary ammonium compounds and their degradation via dual pathways. Applied and Environmental Microbiology 73, 1797-1802.

Takeoka G.R., Dao L.T., Wong R.Y., Harden L.A., 2005. Identification of benzalkonium chloride in commercial grapefruit seed extracts. Journal of Agricultural and Food Chemistry 53, 7630–7636.

Tezel U., Tandukar M., Martinez R.J., Sobecky P.A., Pavlostathis S.G., 2012. Aerobic biotransformation of n-tetradecyl benzyl dimethyl ammonium chloride by an enriched *Pseudomonas spp.* community. Environmental Science and Technology 46, 8714−8722.

United States Environmental Protection Agency (EPA739-R-06-009), August 2006. Reregistration eligibility decision for alkyl dimethyl benzyl ammonium chloride (ADBAC).
(https://archive.epa.gov/pesticides/reregistration/web/html/index-9.html; accessed September, 2016)

Vogelpohl A., 2007. Applications of AOPs in wastewater treatment. Water Science and Technology 55, 207–211.

Walters E., McClellan K., Halden R.U., 2010. Occurrence and loss over three years of 72 pharmaceuticals and personal care products from biosolids–soil mixtures in outdoor mesocosms. Water Research 44, 6011–6020.

Wu C., Spongberg A.L., Witter J.D., Fang M., Czajkowski K.P., 2010. Uptake of pharmaceutical and personal care products by soybean plants from soils applied with biosolids and irrigated with contaminated water. Environmental Science and Technology 44, 6157-6161.

Wu C., Spongberg A.L., Witter J.D., Sridhar B.B. M., 2012. Transfer of wastewater associated pharmaceuticals and personal care products to crop plants from biosolids treated soil. Ecotoxicology and Environmental Safety 85, 104-109.

Yang W., Lin X., Wang H., Yang W., 2013. Ferrate (VI): a novel oxidant for degradation of cationic surfactant–cetylpyridinium bromide. Water Science and Technology 67, 2184–2189.

Zhao J., Hidaka H., 1993. Photodegradation of surfactants. 11. ζ-potential measurements in the photocatalytic oxidation of surfactants in aqueous TiO_2 dispersions. Langmuir 9, 1646–1650.

Chapter 3

Biodegradation of Benzalkonium Chlorides Singly and in Mixtures by a *Pseudomonas* sp. Isolated from Returned Activated Sludge

[A revised version of this chapter is published; Khan et al., 2015. Journal of Hazardous Materials 299, 595–602.]

3.1 Introduction

Quaternary ammonium compounds (QACs) with long, hydrophobic alkyl chains attached to a positively charged nitrogen atom, are widely used in domestic, agricultural, healthcare, and industrial applications as surfactants, emulsifiers, fabric softeners, disinfectants, personal care products, and corrosion inhibitors (Gerba, 2015). The cationic character of QACs makes them highly adsorptive to the negatively charged surfaces of sediments, minerals, and organic matter during the wastewater treatment process (Tezel and Pavlostathis, 2009; Garcia et al., 1999). QACs can therefore enter the aquatic environment via the suspended organic matter in wastewater effluent (Li et al., 2014), and the terrestrial environment through the application of biosolids as a soil amendment for crop production (Ismail et al, 2010). The total concentration of QACs from 22 to 167 mg kg^{-1} has been measured in biosolids (Martínez-Carballo et al., 2007; Li et al., 2014). Due to their extensive use, concentrations up to 3.8 μg L^{-1} of QACs have been found in surface water (Grabińska-Sota, 2011).

Benzalkonium chloride (BAC) compounds are a subset of QACs consisting of alkyl benzyl dimethyl ammonium chlorides with C_8 to C_{18} alkyl groups (Zhang et al., 2011). The most widely used BACs have a carbon chain length of C_{12} or C_{14} and are found in concentrations up to 9 mg kg^{-1} dry weight in sewage sludge (Martínez-Carballo et al., 2007). Grabińska-Sota (2011) found potential genotoxicity in *Bacillus subtilis* in response to about 10 mg L^{-1} of a type of BAC. However, BACs were found to be genotoxic in eukaryotic cells even at a low concentration of 1.0 mg L^{-1} and their release into the environment may cause

genetic damage in exposed organisms (Ferk et al., 2007). There is a concern that development of bacterial resistance to QACs will be accompanied by resistance to clinically relevant antibiotics (Buffet-Battailon et al., 2012). Genetic elements that are associated with horizontal gene transfer of antibiotic resistance genes are enriched in QAC-polluted environments, and there is therefore a concern that exposure to QAC will accelerate the dissemination of antibiotic resistance within populations of environmental bacteria (Gaze et al., 2005; Gillings et al. 2009). It should be noted however, that environmental surveys have to date failed to establish a link between the use of QACs and the abundance of antibiotic resistant bacteria (Gerba, 2015).

Biodegradation is the dominant process for BAC dissipation in the environment and therefore a crucial mechanism for reducing exposure and impacts on sensitive species (Brycki et al., 2014). Several studies concerning the biodegradation of QACs have been published (Tezel et al., 2012; Bassey and Grigson, 2011; Takenaka et al., 2007; Patrauchan and Oriel, 2003; Nishihara et al., 2000; Nishiyama et al., 1995; Kroon et al., 1994; Sullivan, 1983; Dean-Raymond and Alexander, 1977). Microorganisms capable of degrading QACs mostly belong to the genus *Pseudomonas* (Tezel et al., 2012; Liffourrena et al., 2008; Takenaka et al., 2007; Nishiyama and Nishihara, 2002; Nishihara et al., 2000; Kroon et al., 1994; van Ginkel et al., 1992; Geftic et al., 1979; Dean-Raymond and Alexander, 1977). Some other species can also degrade QACs, including *Xanthomonas* sp. (Dean-Raymond and Alexander, 1977), *Bacillus niabensis*, *Thalassospira* sp. (Bassey and Grigson, 2011) and *Aeromonas* sp. (Patrauchan and Oriel, 2003). However, while BACs are often found as mixtures in natural environments, the ability of microbes such as *Pseudomonas* to degrade mixtures of BACs and the synergistic or inhibitory effects of such mixtures on aerobic biodegradation is not reported yet.

In the present study, a *Pseudomonas* sp., designated strain C505, was isolated from returned activated sludge (RAS) on the basis of using benzyl dimethyl dodecyl ammonium chloride (BDDA) as the sole source of carbon. The kinetics of biodegradation of BDDA and benzyl dimethyl tetradecyl ammonium chloride (BDTA) were established with each QAC provided alone or in a mixture. Some of the biodegradation intermediates and the extent of mineralization were also determined.

3.2 Materials and methods

3.2.1 Chemicals

Benzyl dimethyl dodecyl ammonium chloride (BDDA) and benzyl dimethyl tetradecyl ammonium chloride (BDTA) were purchased from Sigma-Aldrich (St. Louis, MO, USA); each had purity ≥ 99.0% and were used as certified reference materials. Radiolabeled BDDA (MC 2369), [benzyl-^{14}C; radioactive purity 98%, specific activity 50 µCi mL $^{-1}$ in ethanol or 52 mCi mmol^{-1}] was purchased from Moravek Biochemicals, USA and stored at –20°C until use. Milli-Q water was obtained from an ultrapure water purification system (Millex-GV, 0.22 µm, Millipore, Toronto, ON). High performance liquid chromatography (HPLC) grade acetonitrile (purity ≥ 99.9%) was purchased from Fisher Scientific (Fair Lawn, NJ, USA). All other chemicals used were of analytical reagent grade.

3.2.2 Maintenance and tentative identification of the bacterium

Strain C505 was isolated from return activated sludge (RAS), collected from the Adelaide Pollution Control Plant in London, ON, Canada. The C505 strain was enriched and isolated in a mineral salts medium with BDDA provided as the sole carbon and nitrogen source.

The mineral salts medium (Topp et al., 2000) consisted of the following (per liter): 1.6 g K_2HPO_4, 0.4 g KH_2PO_4, 0.2 g $MgSO_4 \cdot 7H_2O$, 0.1 g NaCl, 0.025 g $CaCl_2 \cdot 2H_2O$, and 1 ml of a trace metal solution consisting of the following per liter: 10 mg $ZnSO_4.7H_2O$, 3 mg $MnCl_2.4H_2O$, 30 mg H_3BO_3, 20 mg $CoCl_2.6H_2O$, 1 mg $CuCl_2.2H_2O$, 2 mg $NiCl_2.H_2O$, 3 mg $NaMoO_4.2H_2O$. The pH of the medium was measured to 6.8±0.2. The mineral salts medium was autoclaved at 120°C for 20 min and after that supplemented with BDDA at 100 mg L^{-1} and 1 mL of freshly prepared 5 mg L^{-1} $FeSO_4.7H_2O$. The fresh $FeSO_4.7H_2O$ solution was sterilized using a 0.22 µm pore size cellulose acetate filter (SteriCup, Millipore, Mississauga, ON) (Topp et al., 2013). Liquid stock cultures of the isolated strain C505 were stored at 4°C in mineral salts medium supplemented with 100 mg L^{-1} of BDDA. Before use, the strain was streaked on solid mineral

salts medium containing 100 mg L^{-1} BDDA and agar (16 g L^{-1}) and incubated for one week at 30°C.

Strain C505 was presumptively identified as a *Pseudomonas* sp. on the basis of 16S rDNA sequence. Genomic DNA was extracted from pelleted cells using the Promega Wizard kit (Thermo Fisher Scientific, Ottawa, ON) following the manufacturer's instructions. A partial 16S rDNA gene product was generated by PCR (polymerase chain reaction) using primers that amplified a portion of the 16S rDNA gene GM5F (5'-CCTACGGGAGGCAGCAG-3') (Muyzer et al., 1993) and 907R (5'-CCGTCAATTCCTTTGAGTTT-3') (Lane et al., 1985). The full length 16S rDNA product was generated using the primers FD1 (5'-AGAGTTTGATCMTGGCTCAG-3') and 1492R (5'- TACGGHTACCTTGTTACGACTT-3') (Weisburg et al., 1991).

The PCR conditions were 94°C for 10 min, followed by 30 cycles of 94°C for 20 sec, 55°C for 30 sec and 72°C for 45 sec, with a final elongation step at 72°C for 5 min. Polymerase chain reaction products were visualized on 1.5% agarose gel stained with GelRed to check for the expected sizes of 600 and 1500 base pairs using Molecular Imager, Gel Doc™XR+, with Image Lab™ software. Polymerase chain reaction products were purified using the QIAquick Gel extraction kit from Qiagen, Mississauga, ON, Canada (Topp et al., 2013). Sequencing was carried out at the Robart's Institute DNA Sequencing Facility at the University of Western Ontario, London, ON, Canada, by using a 3130xl Genetic Analyzer. The 16S PCR sequences were analyzed using BioEdit software; forward and reverse sequences were aligned to obtain the whole sequence and compared with nucleotide sequences in the GenBank database using BLASTn (NCBI, 2014). The sequence was within 99% similarity of several *Pseudomonas* species, most closely *Ps. putida* with 99.43% identity. On this basis and without further information the strain is designated as *Pseudomonas* sp. strain C505 (Table 3.1).

Table 3.1 The results of a BLASTn search in GenBank (http://www.ncbi.nlm.nih.gov/) for the 16SrRNA sequence of strain C505.

Query ID	Subject ID	% Identity	Alignment Length	Mismatches	Gap opens	Q. Start	Q. End	S. Start	S. End	E Value	Bit Score	Database	Accession ID	Identification
11635	gi|359805136|dbj|AB681703.1|	99.43	1409	4	4	1	1407	29	1435	0	2562	dbj	AB681703.1	*Pseudomonas* putida gene for 16S rRNA, partial

3.2.3 Analytical methods

Growth of the strain C505 was determined by measuring the optical density of the culture at 600 nm (OD_{600}) (Nishihara et al., 2000) using an Eppendorf Biophotometer (VWR International, Mississauga, ON). Ultraviolet absorbance spectra of the culture supernatants were determined using a PowerWave XS microplate reader and Gen5 microplate reader software (Biotek, Winooski, VT, USA). The relationship between OD_{600} and dry biomass was established for the strain C505 and is presented in Fig 3.1. The OD_{600} was measured for each experimental sample, and the kinetic data were normalized by dry biomass to calculate the specific BACs degradation rate values (Zhang et al., 2011).

Quantification of BACs was carried out using a high performance liquid chromatography (HPLC) coupled with a diode array UV-visible detector (Agilent Technologies, 1260 infinity, Mississauga, ON), equipped with a Luna CN column (C-18, 3µm pore, 100 mm length x 4.6 mm internal diameter) with security guard CN columns (Phenomenex, Canada) and the absorbance was measured at 210 nm in accordance with existing literature (Tezel and Pavlostathis, 2009). The mobile phase consisted of acetonitrile and 40 mM ammonium acetate (adjusted to pH 5.0 using 1 M H_3PO_4) at a ratio of 60:40. The solvent gradient utilized was acetonitrile and 40 mM ammonium acetate for 0 to 20 min; 100% acetonitrile between 20 to 24 min; and acetonitrile: 40 mM ammonium acetate between 24 to 25 min, with a flow rate of 0.8 mL min^{-1} and an injection volume of 50 µL.

The retention times for BDDA and BDTA were 11.9±0.2 min and 13.1±0.2 min, respectively. Standard curves for HPLC-UV analysis were obtained using BAC concentrations of 6.25. 12.5, 25, 50, and 100 mg L^{-1}, and had r^2 values of 0.988 and 0.989 for BDDA and BDTA, respectively. A reagent blank (solution without BDDA or BDTA) was tested and no absorbance was measured. The lower limit of detection under the operating conditions for both the compounds by HPLC-UV analysis was 3 mg L^{-1}.

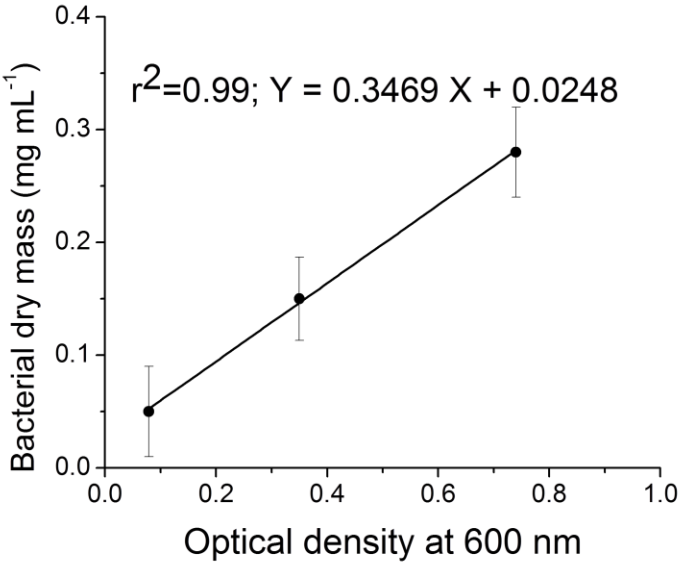

Fig. 3.1 Relationship between optical density at 600 nm (OD_{600}) and bacterial dry mass for the strain C505. The regression equation was used to convert the OD_{600} value of each experimental sample to bacterial dry mass in order to normalize the data.

Biodegradation intermediates were identified using a HPLC-MS (mass spectrometry) with a Q-Exactive Orbitrap (Thermo Scientific), using an Agilent Eclipse plus C-18 RRHD column (1.8 µm pore, 50 mm length x 2.1 mm internal diameter) at a flow rate of 0.3 mL min^{-1} and an injection volume of 2 µL. The solvent gradient used was 100% H_2O for 0 to 0.5 min; 100% acetonitrile between 0.5 to 4.5 min, and 100% H_2O between 4.5 to 6.0 min. A top 5 $ddMS^2$ analysis was performed in positive mode. The full MS scans were performed at a resolution of 70,000 and AGC target of 1e5. The MS^2 scans were performed at a resolution of 17,500 and AGC target of 1e5. The spray voltage was held at 3.6 kV, the S-lens at 65 V and

the sheath and auxiliary gas were set to 20 mL min^{-1}, and 9 mL min^{-1} respectively. The data were analyzed with Xcalibur™ and MZmine.

The rate of mineralization of the parent BDDA was determined by measuring the production of $^{14}CO_2$. Radioactivity captured in NaOH as $^{14}CO_2$ or remaining in pure medium as total radioactive carbon was determined by liquid scintillation counting (LSC) using a Model LA 6500 instrument (Beckman Coulter, Irvine, CA). Each sample was added to 10 mL UniverSol scintillation cocktail (ICN, Costa Mesa, CA) in a plastic scintillation vial, the vial was allowed to stand for 24 hours before being measured by LSC (Al-Rajab et al., 2010).

Three independent replicates were analyzed in each of the experiments described above. The lowest detection limit for HPLC-UV analysis was determined from signal to noise ratio (S/N) when it was 3 or less using Equation 3.1 (Skoog et al., 2007). In all cases, one control (without bacterium added) sample was tested.

$$\frac{S}{N} = \frac{Mean\ of\ peak\ area}{Standard\ Deviation} = \frac{1}{Relative\ Standard\ Deviation} \quad \text{---------- (3.1)}$$

3.2.4 Bacterial growth and kinetics study

The strain C505 grown on BDDA was further grown in LB-agar broth (to obtain sufficient mass of strain C505) and was harvested during the mid-logarithmic phase of growth, usually between 8 to 10 h for the biodegradation kinetics study. The bacterium C505 was grown on LB-agar plate (Fig 3.2a) and the same bacterium was observed to metabolize BDDA as a sole source of carbon and nitrogen (Fig 3.2b). In both cases, the observation was conducted after 7 d of incubation at 30°C in static condition. After harvesting, the strain was washed and re-suspended in minimal salts medium to avoid the possible transfer of LB broth. The biodegradation kinetics experiments were performed in 15 mL Falcon tubes. Each tube contained 5 mL of medium consisting one or both BACs; after inoculation with strain C505 (initial optical density 0.1-0.14), the tubes were sealed and incubated at 30°C in static condition.

At each sampling time (0, 20 30 42, 54, 70, 90, 114, 138, 162 and 210 h), 400 µL of solution was collected in 1.5 mL micro-tubes; of which about 100 µL was used to measure

OD_{600} for cell growth, and the remaining 300 µL was centrifuged at 13000 g for 5 min to pellet cells. After centrifugation, the 100 µL was used to monitor degradation using the plate reader and the remaining 200 µL of the supernatant was preserved in an HPLC 1.5 mL glass vials at –20°C for HPLC-UV analysis. Degradation of BAC over time was analysed using two-way repeated measures analysis of variance (RM-ANOVA) followed by Holm-Sidak pairwise multiple comparisons using software Sigma Plot version 12.5, Systat Software Inc.

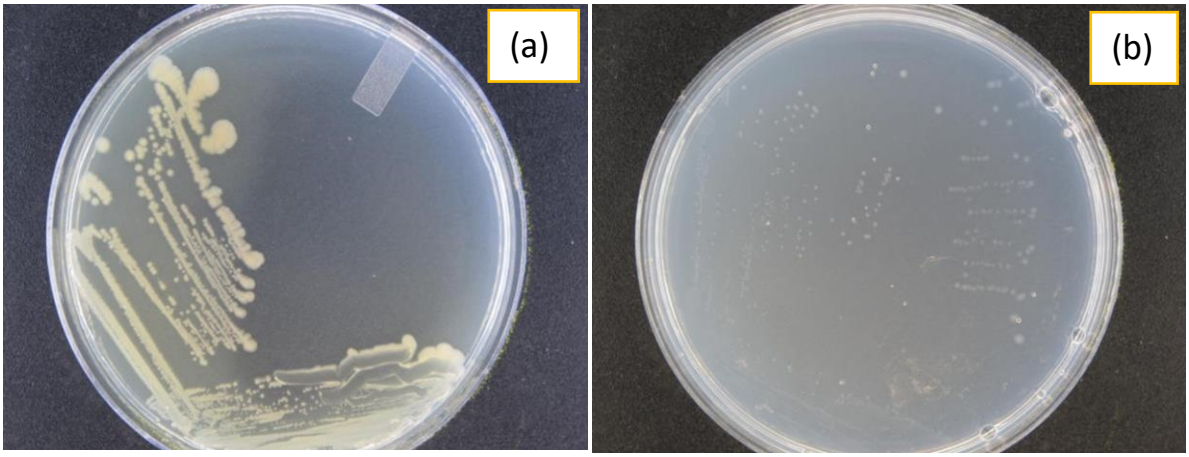

Fig. 3.2 Growth of the strain C505 after 7 d, (a) on LB-agar; (b) medium plate spiked with BDDA at 100 mg L^{-1}.

3.2.5 Determination of kinetic constants

The kinetic constants of BDDA and BDTA biodegradation by the strain C505 were determined using Hanes-Woolf linearization (Equation 3.2) of the Michaelis-Menten equation where, V (mg L^{-1} h^{-1}) is the rate of biodegradation and was calculated from the

change of substrate concentration with time (ds/dt). Substrate (BDDA or BDTA) concentration is denoted by [S] in mg L^{-1}, V_{max} (mg L^{-1} h^{-1}) is the maximum forward velocity of the reaction and K_m (mg L^{-1}) is the half saturation or Michaelis constant, which is when the rate of reaction, V, is half of V_{max} and numerically K_m is equal to [S]. The instantaneous rate values were normalized by dry biomass at each data point to find the specific rate (V_{spe} = L^{-1} h^{-1}). Due to the normalized rate values, other constants (i.e. V_{max} and K_m) of Hanes-Woolf model (Equation 3.2) were termed as $V_{max(spe)}$ and $K_{m(spe)}$.

The advantages of Hanes-Woolf linearization compared to other (Lineweaver burk or Eadie-Hofstee plots) methods are a good distribution of data points, and the velocities of reaction are not biased at low substrate concentrations (Ritchie and Prvan, 1996).

$$\frac{[S]}{V} = \frac{1}{V_{max}} * [S] + \frac{K_m}{V_{max}} \quad \text{----------(3.2)}$$

3.2.6 Radiolabel experiment

The radiolabel experiment was also conducted in 15 mL Falcon tubes, which were inoculated and incubated in the same way as described above for the radiolabel kinetics study. Each tube contained 5 mL of medium with 100 mg L^{-1} of cold (unlabeled) BDDA and 50,000 dpm of hot ^{14}C-BDDA and was placed inside a sealable 1 L Mason jar. A scintillation vial containing 5 mL of 1 M NaOH solution for trapping $^{14}CO_2$ was also placed inside each Mason jar (Al-Rajab et al., 2009).

At each sampling time (0, 20, 42, 54, 70, 90, 114, 186, 258 and 300 h), 300 µL of solution was collected in 1.5 mL micro-tubes and centrifuged at 13000 g for 5 min to pellet cells. Of 300 µL supernatant, 100 µL was placed in a scintillation vial with the addition of 100 µL 1N HCl and allowed to stand for 5 min to liberate $^{14}CO_2$ gas, then 10 mL UniverSol scintillation cocktail was added and the total ^{14}C was measured by LSC after 24 hours (Al-Rajab et al., 2010).

Another 100 µL of radiolabeled supernatant was added to the same amount of UniverSol scintillation cocktail in a scintillation vial and measured after 24 hours by LSC; the difference in these two measurements was the $^{14}CO_2$ dissolved in the medium. The

remaining 100 µL of the solution was preserved at –20°C. Due to the removal of 300 µL solution at each sampling time, a certain amount of total ^{14}C was removed from the incubation and did not play a role in the $^{14}CO_2$ production. The removal of solution was taken into account during the calculation of the percentage mineralization. At each time point, the radioactivity of $^{14}CO_2$ in the entire NaOH solution was determined using LSC and the vial inside the Mason jar was replaced each time with fresh 5 mL of 1M NaOH solution.

3.2.7 Selection of BACs concentrations

The two BACs (BDDA, BDTA) were tested for biodegradation individually and in a mixture. A preliminary biodegradation experiment was conducted to find suitable concentrations for BDDA, BDTA and their mixture. BDDA or BDTA were not degraded after 14 d of incubation in pure medium when present at concentrations of 175 mg L^{-1} or 40 mg L^{-1} or added as a mixture of 100 mg L^{-1} BDDA and 25 mg L^{-1} BDTA. As a result, 150 mg L^{-1} of BDDA and 30 mg L^{-1} of BDTA were considered the upper limits for the biodegradation experiment. To determine biodegradation kinetics of the BACs mixture, a 100:10 mg L^{-1} of BDDA: BDTA mixture was selected and compared with 100 mg L^{-1} of pure BDDA.

Another ratio of BDDA: BDTA in the mixture was chosen based on the study of Li et al. (2014) who determined BDDA: BDTA in sewage sludge and river sediment to be approximately 2:1. Therefore, a mixture containing 50:25 mg L^{-1} of BDDA: BDTA was chosen to conduct the biodegradation of BACs in mixture by the strain C505. While the individual concentration of BACs in sewage sludge or sediment samples is typically less than 10 mg kg^{-1} (Martínez-Carballo et al., 2007), the total concentration of QACs can be up to 15 times higher (Li et al., 2014).

3.3 Results and discussion

3.3.1 Bacterial growth with BACs as the sole source of C and N

In cases where strain C505 grew, maximum optical density was seen at around 50 hours (Fig 3.3a), which is similar to the 48 hour peak found for an *Aeromonas* sp. grown on BACs (Patrauchan and Oriel, 2003). Strain C5O5 grew on BDDA provided at concentrations of

up to 150 mg L^{-1}. It was unable to tolerate BDTA at concentrations of 30 mg L^{-1} or more. Inhibition of bacterial growth was also observed when BDDA and BDTA were mixed (at both 100:10 and 50:25 mg L^{-1}). Apparently, the longer chained BDTA was more toxic to the strain C505 compared to the shorter chained BDDA. Hegstad et al. (2010) suggested that the antimicrobial activity of QACs is a function of the compounds' *N*-alkyl chain length and the optimal activity is achieved with chain lengths of n=14-16 for gram-negative bacteria (including *Pseudomonas*). Similar enhanced antimicrobial activity has also been measured for alkyl trimethyl ammonium salts with longer alkyl chain lengths (Nishiyama et al., 1995).

The specific growth rates ($\mu=h^{-1}$) calculated between 0 to 54 hours (Fig 3.3b) of the bacterial cultures can also be used to compare the relative abilities of strain C505 to utilize BDDA and BDTA as sources of C and N. Strain C505 grew fastest when given 100 mg L^{-1} BDDA, indicating an initial inhibitory effect of 150 mg L^{-1} BDDA (Fig 3.3b), but the bacterial densities from 96 to 210 hours were higher for strain C505 grown at the higher concentration of BDDA (Fig 3.3a), indicating that the bacteria can continue to access C and N from this BAC despite the initial apparent toxicity.

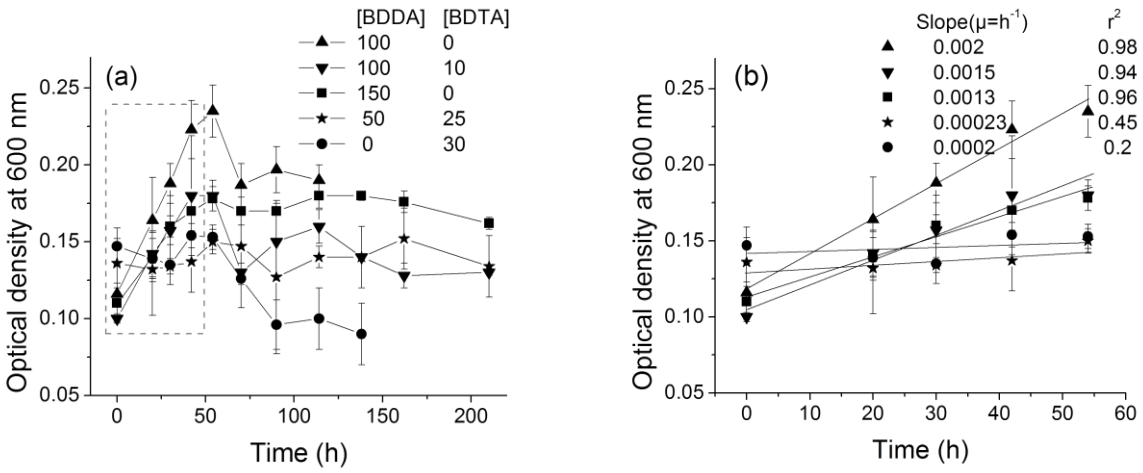

Fig.3.3 Growth of strain C505 in a minimal salts medium with various initial concentrations of BDDA and/or BDTA in mg L^{-1} as the sole source of carbon and nitrogen. Growth was measured as optical density at 600 nm; (a) Growth over the 10-d experimental period; (b) Growth over the first 54 h. Data are presented as the mean and standard deviation of three replicates.

3.3.2 Biodegradation kinetics

The biodegradation of varying concentrations of BDDA (Fig 3.4a) and BDTA (Fig 3.4b) is shown for pure and mixed solutions. The un-inoculated control samples showed an average 10% reduction in concentration, with a maximum reduction of 20%, for the entire duration of the kinetic experiments; this could be due to measurement errors and/or some adsorption of the cationic BACs to the culture vials. Similar reduction of BDDA was also observed in the un-inoculated samples during mineralization experiments using radiolabelled (^{14}C-BDDA) technique (described later).

Adsorption equilibrium of BACs on the mixed biomass cultures occurs quickly, typically within 0.5 to 3 h compared to biodegradation (Ismail et al., 2010). In this work, adsorption of

BACs on biomass was negligible due to the small amount of biomass used. The variation of biomass growth from 70 h onward was ≤ 0.03 OD for all combinations of BACs (Fig. 3.3a). The use of a small amount of inoculum with low growth allowed assessment of the relative inhibitory effects of BACs biodegradation in the liquid phase (Zhang et al., 2011).

Strain C505 degraded BDDA in the presence or absence of BDTA, with the percentage of BDDA declining over time over the experimental period (p ≤0.001 for all BDDA:BDTA combinations). Among the BACs plus bacteria treatments, the rate of degradation of BDDA was slower when it was mixed with BDTA. It took 100 hours to fully degrade 100 mg L^{-1} BDDA, whereas it took 150 hours to degrade 100 mg L^{-1} BDDA when it was mixed with only 10 mg L^{-1} BDTA. Mixing with higher concentrations of BDTA (25 mg L^{-1}) further delayed the degradation of BDDA (50 mg L^{-1}) to 200 hours. In contrast, degradation of 150 mg L^{-1} of BDDA took over 300 hours because this concentration was very close to the toxicity limit of the compound. The slower rate of BDDA degradation in the presence of BDTA is due to their relative toxicities (Hegstad et al., 2010) and this phenomenon is supported by the corresponding growth curves of the bacterium presented in Fig 3.3a. On the other hand, the presence of BDDA did not affect the biodegradation kinetics of BDTA, which will be discussed further in first order kinetics model (Fig 3.4d).

To determine the rate constant of BDDA biodegradation at their various concentrations and in mixture with BDTA, a first order degradation kinetic model was used as shown in Equation 3.3, where, C_0 is the initial concentration of the compound, C_t is the concentration at different time (t) and k is the rate constant. Pseudo-first order degradation kinetic models for various concentrations of BDDA and BDTA are presented in Fig 3.4(c) and 3.4(d), respectively, where ln C_t/C_0 at each point was divided by instantaneous dry biomass (mg) and plotted against time to find k_{spe} ($mg^{-1}\ h^{-1}$).

$$log\ C_t = \log\ C_0 - \frac{kt}{2.303} \qquad \text{----------(3.3)}$$

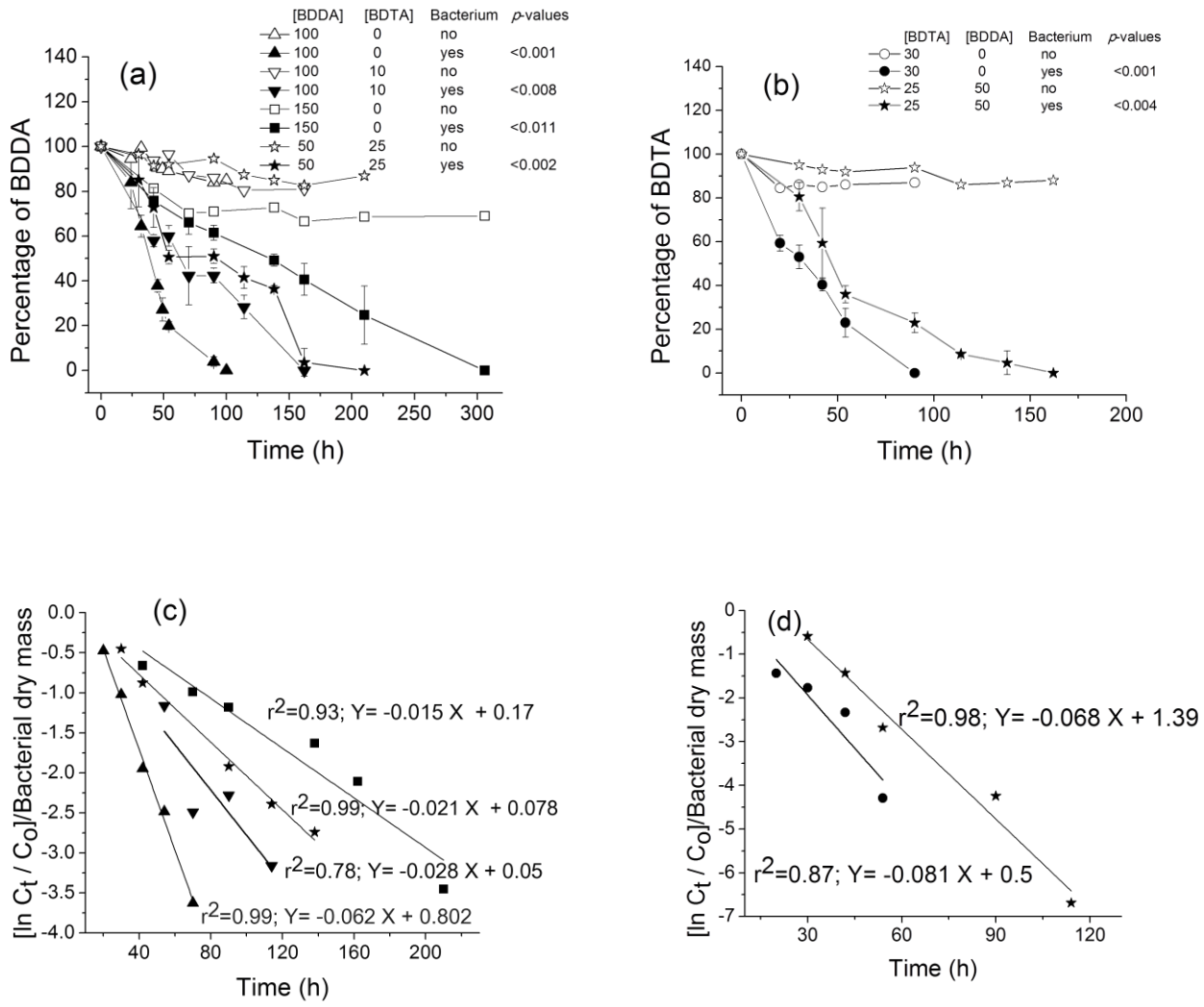

Fig.3.4 Biodegradation kinetics of BACs. The strain C505 utilized BDDA and/or BDTA with various initial concentrations (mg L^{-1}) as the only source of C and N. *p*-values indicate significantly reduced BACs remaining in the presence of strain C505; (a) Percentage of initial BDDA in the medium over the experimental period; (b) Percentage of initial BDTA in the medium over the experimental period; (c) Pseudo-first order kinetics model for BDDA; (d) Pseudo-first order kinetics model for BDTA. Data are presented as the mean and standard deviation of three replicates.

Strain C505 was also able to degrade BDTA, with residual pure BDTA reaching below the detection limit after 90 hours and BDTA in the mixture reaching the same after 162 hours (Fig 3b, $p \leq 0.001$ for each). As mentioned before, the rate of degradation of BDDA at all concentrations was negatively affected by the presence of much smaller concentration of BDTA. The rate constant, k_{spe}, (0.062 mg^{-1} h^{-1}) of 100 mg $L^{-1}$of BDDA, was reduced to 0.028 mg^{-1} h^{-1} in the presence of 10 mg L^{-1} of BDTA. Therefore, the biodegradation of BDDA was inhibited in the presence of BDTA. However, although the rate of BDTA degradation was reduced slightly in presence of BDDA, the k_{spe} values 0.081 mg^{-1} h^{-1} and 0.068 mg^{-1} h^{-1} for BDTA 30 mg L^{-1} and BDTA 25 mg L^{-1} (mixed with BDDA 50 mg L^{-1}) (Fig. 3.4d), respectively, indicate that the effect of BDDA on BDTA degradation was limited. The slightly lower k_{spe} value for $BDTA_{25 \text{ mixed with BDDA } 50}$ compared to $BDTA_{30}$, is because of the competition of BDDA for degradation by strain C505. Preferential biodegradation was observed when benzalkonium chlorides were mixed with glucose in an activated sludge process with mixed cultures. Biodegradation of benzalkonium chlorides did not occur until most of the glucose was used up by the biomass (Zhang et al., 2011). These results and the earlier results with BDDA in presence of different concentrations of BDTA indicate that BDTA is inhibitory to the biodegradation of BDDA and to the growth of strain C505. Although toxic at a lower concentration than BDDA, specific rate of biodegradation of BDTA at initial concentration of 30 mg L^{-1} was slightly higher than BDDA at 100 mg L^{-1}.

3.3.3 Kinetics model

The linear form of the Hanes-Woolf plot (Equation 3.2) was used to calculate the $V_{max(spe)}$ and $K_{m(spe)}$ values. According to the equation, the slope and intercept of the regression line are 1/ $V_{max(spe)}$ and $K_{m(spe)}$ / $V_{max(spe)}$, respectively. The Hanes-Woolf plots are presented in Fig 3.5 and the calculated values of $V_{max(spe)}$ and $K_{m(spe)}$ are presented in Table 3.2.

From Table 3.2, the decreasing order of the $V_{max(spe)}$ for different concentrations of BDDA was $BDDA_{100}$ > $BDDA_{100\ mixed\ with\ BDTA\ 10}$ > $BDDA_{150}$. Similar trends for the specific growth rates (Fig 3.3b) and the specific rate constant (k_{spe}) values (Fig 3.4c) are consistent with this result. In the case of BDTA, the decreasing order of $V_{max(spe)}$ was $BDTA_{30}$ > $BDTA_{25\ mixed\ with\ BDDA\ 50}$ (Table 3.2); a similar but limited effect of BDDA on BDTA was seen in terms of specific rate constant values (Fig 3.4d).

The correlation coefficients (r^2) for the linear regression of degradation models of all BDDA and/or BDTA combinations are presented in Table 3.2. In all experimental treatments, the Hanes-Woolf model fitted the experimental data well ($r^2 \geq 0.87$) except for the biodegradation of 50 mg L^{-1} BDDA, which was inhibited by the addition of 25 mg L^{-1} BDTA. The variation in rate data from the kinetic study causes the poor fit ($r^2 = 0.41$).

The value of $K_{m(spe)}$ is an inverse measure of the affinity between the substrate and the enzyme; the higher the value of $K_{m(spe)}$, the lower the affinity (Eckard et al., 2012). The $K_{m(spe)}$ values presented in Table 3.2 also confirm the inhibition effect of BDTA on the biodegradation of BDDA; the value for $BDDA_{50\ mixed\ with\ BDTA\ 25}$ is 3.2 times higher than the largest $K_{m(spe)}$ value for pure BDDA. The higher $K_{m(spe)}$ values for $BDTA_{25\ mixed\ with\ BDDA50}$ and $BDTA_{30}$, support the greater inhibition effect of BDTA compared to BDDA alone on strain C505.

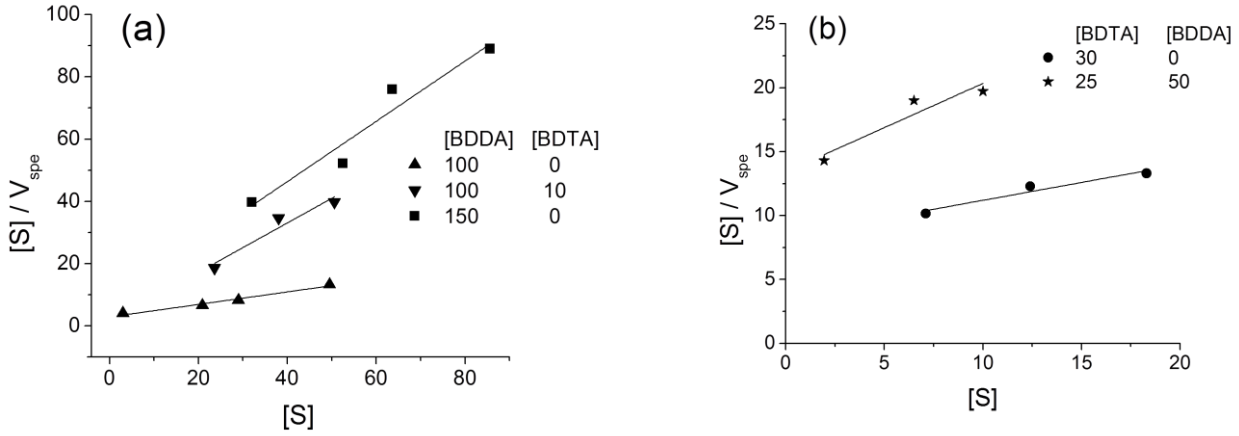

Fig.3.5 Hanes-Woolf models. Models used to calculate kinetics constants (specific V_{max} and K_m) for various initial concentrations of BDDA and/or BDTA in mg L^{-1}; (a) BDDA; (b) BDTA; V_{spe} is specific velocity, normalized to bacterial dry mass.

Table 3.2 Kinetics constants ($V_{max(spe)}$ and $K_{m(spe)}$) calculated using Hanes-Woolf model.

BDDA and/or BDTA, [S] (mg L^{-1})	$V_{max(spe)}$ ($L^{-1}h^{-1}$)	$K_{m(spe)}$ (mg L^{-1})	Regression equations
BDDA (100)	5.0	14.5	$y = 0.2 x + 2.9$; $r^2 = 0.98$
BDDA (150)	1.03	7.9	$y = 0.97 x + 7.67$; $r^2 = 0.94$
BDDA (100)$_{\text{mixed with BDTA(10)}}$	1.27	1.78	$y = 0.79 x + 1.41$; $r^2 = 0.94$
BDDA (50) $_{\text{mixed with BDTA(25)}}$	4.2	46.25	$y = 0.24 x + 11.1$; $r^2 = 0.41$
BDTA (30)	3.6	30.24	$y = 0.28 x + 8.4$; $r^2 = 0.95$
BDTA (25) $_{\text{mixed with BDDA(50)}}$	2.6	36.6	$y = 0.38 x + 13.95$; $r^2 = 0.87$

3.3.4 Identification of transformation products

Extracts from the kinetic experiments that had 150 mg L^{-1} BDDA, 30 mg L^{-1} BDTA , and the 50: 25 in mg L^{-1} mixture of BDDA and BDTA were evaluated by HPLC-MS for the presence and identity of potential transformation products. Chromatograms and mass spectra (MS) of parent BDDA, BDTA and their mixture at time zero (before degradation) are presented in Fig 3.6. The retention times (RT) for BDDA and BDTA were 3.39 min and 3.66 min, respectively. The mass to charge ratio (m/z) for both BACs confirms the presence of parent compounds.

Transformation products of BDDA biodegradation had m/z ratios of 122.09 and 214.25 at retention times of 0.47 and 0.5 min, respectively. The corresponding chromatograms are shown in Fig 3.7. The compounds were identified as benzyl methyl amine (m/z = 122.09) and dodecyl dimethyl amine (m/z = 214.25). Patrauchan and Oriel (2003) detected the production of benzyl methyl amine by an *Aeromonas* sp. in mineral salts medium, and Tezel and Pavlostathis (2009) reported the formation of alkyl dimethyl amine under nitrate reducing conditions in the presence or absence of a mixed mesophilic methanogenic bacterial culture. However, the formation of alkyl dimethyl amine from BDDA by *Pseudomonas* sp. in mineral salts medium has not been reported.

Benzyl methyl amine was further degraded after 210 hours (Fig 3.7a). The MS for the same product (Fig 3.7b) matched the theoretical MS (m/z 122.09) and confirms the molecular formula as $C_8H_{11}N^+H$ (benzyl methyl amine). The same intermediates were identified after the degradation of 30 mg L^{-1} BDTA and the 50:25 mg L^{-1} mixture of BDDA: BDTA (data not shown). The chromatograms for another intermediate, dodecyl dimethyl amine (m/z = 214.25), are presented in Fig 3.7(C) with the corresponding MS in Fig 3.7(d). Dodecyl dimethyl amine accumulated after 42 and 90 hours of BDDA degradation, with relative peak intensities of 8.16×10^6 and 1.83×10^7, respectively (Fig 3.7C). The relative peak intensity for dodecyl dimethyl amine was 7.37×10^5 after 210 hours (data not shown), suggesting that it also degraded during the experiment.

Based on the intermediates discussed above, strain C505 apparently attacks the parent BDDA at two locations (Fig 3.8). In one case, breakage of the bond between the C_{alkyl}– N

bonds of the BDDA molecule was responsible and resulted in the formation of benzyl methyl amine. The breakage of C_{alkyl}– N bonds produced benzyl dimethyl amine, followed by the removal of a methyl group (–CH_3) by N-demethylation to form benzyl methyl amine (Patrauchan and Oriel, 2003; Nishiyama et al., 1995). The breakage between the C_{alkyl}– N bond is the precursor for the access to the nutrient source by microorganisms as described by Bassey and Grigson (2011) for benzyl dimethyl hexadecyl ammonium chloride; for benzyl dimethyl alkyl ammonium chloride (Patrauchan and Oriel, 2003); for dodecyl dimethyl amine (Kroon et al., 1994), and for alkyl trimethyl ammonium salts (Nishiyama et al., 1995). Strain C505 may follow a similar mechanism for the C_{alkyl}– N breakage reaction, which might be catalyzed by an oxygen independent dehydrogenase enzyme (Patrauchan and Oriel, 2003; Bassey and Grigson, 2011).

The second degradation product detected during the biodegradation of BDDA was dodecyl dimethyl amine (m/z = 214.25). The formation of dodecyl dimethyl amine might have followed the cleavage of C_{benzyl}– N bonds. Tezel and Pavlostathis (2009) also found this product, under nitrate reducing conditions in the presence or absence of a mixed mesophilic methanogenic bacterial culture.

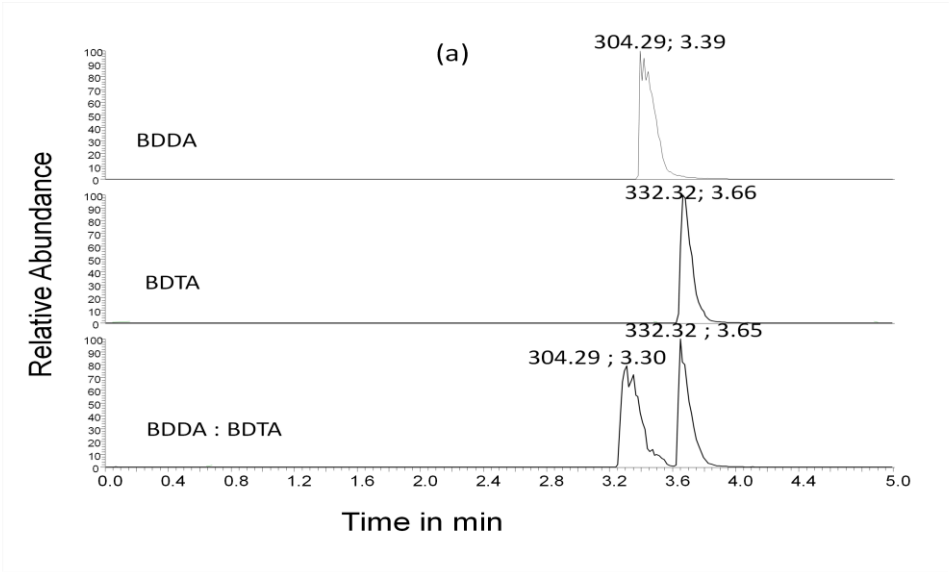

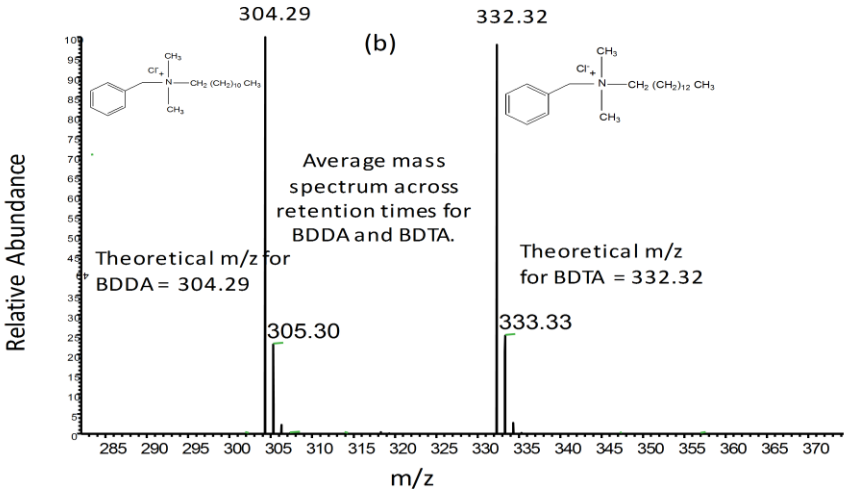

Fig.3.6 Chromatograms and mass spectra of the parent BACs at time zero for BDDA 150, BDTA 30 and BDDA: BDTA at 50:25 mg L^{-1}; (a) Chromatograms; (b) Mass spectra. Relative abundance indicates the electric current proportional to the number of ions going into mass-spectroscopy.

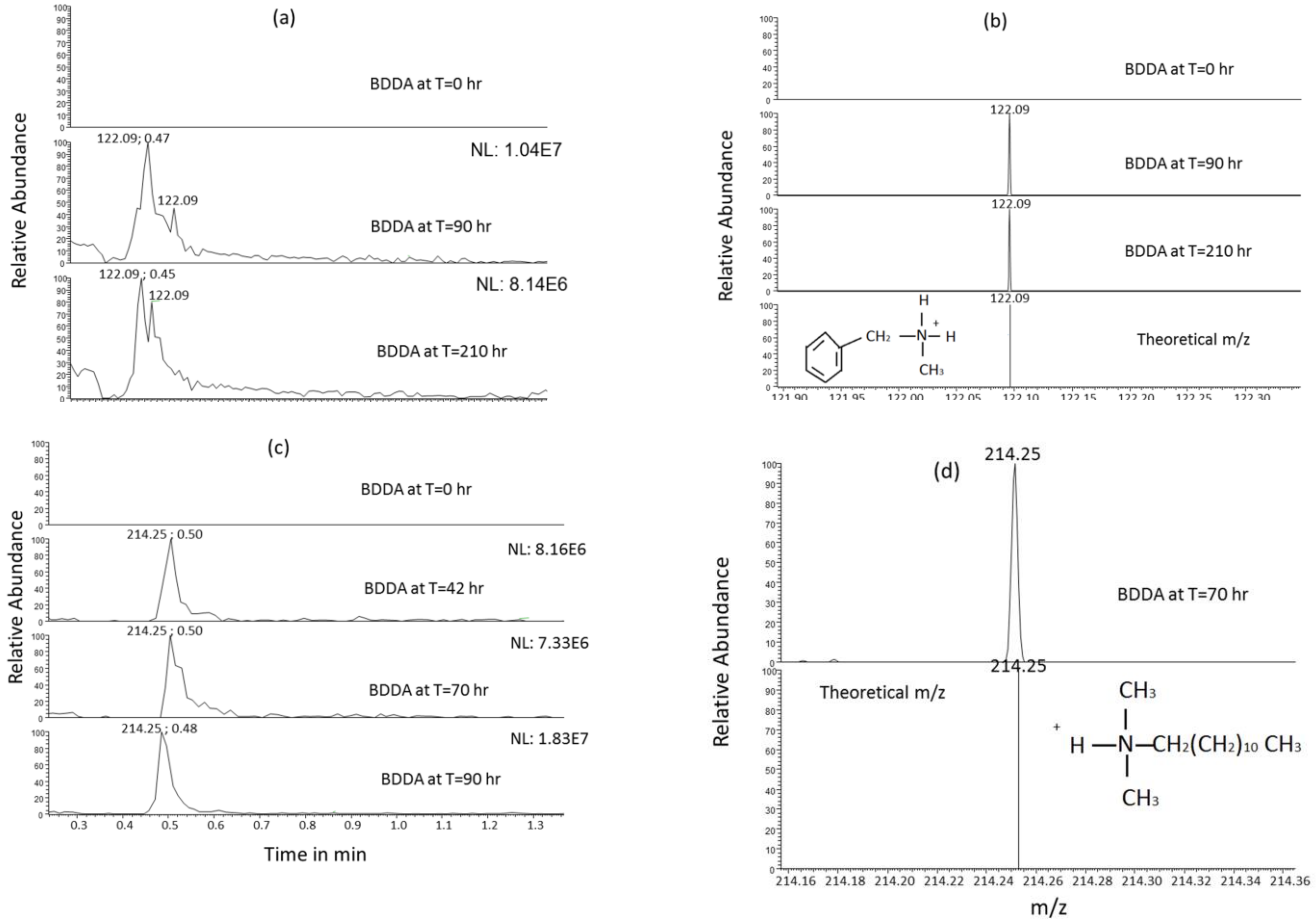

Fig.3.7 Liquid chromatography and MS analysis of transformation products formed during biodegradation of 150 mg L^{-1} BDDA; (a) and (b) Chromatograms and MS of benzyl methyl amine; (c) and (d) Chromatograms and MS of dodecyl dimethyl amine.

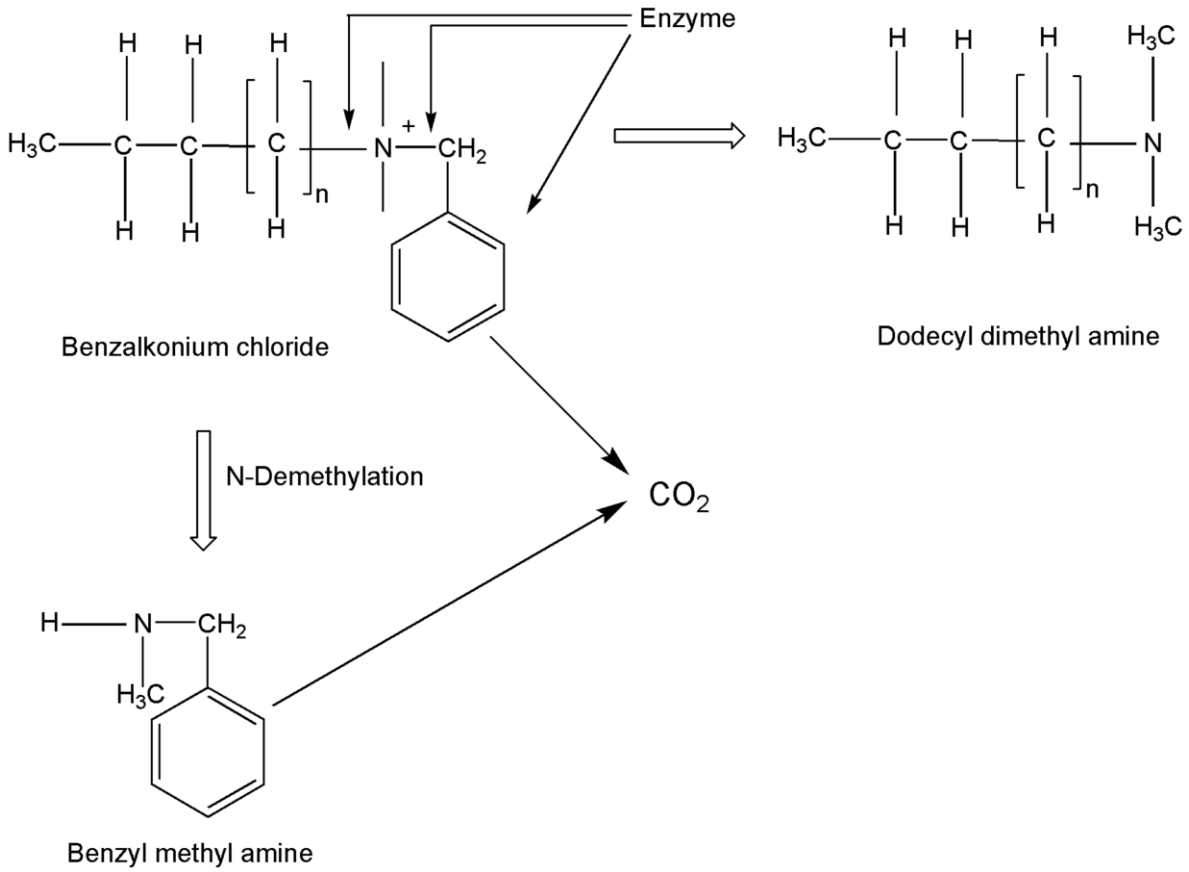

Fig.3.8 Proposed mechanism of BDDA biodegradation by strain C505.

3.3.5 Mineralization of BDDA

The rate of mineralization of [U-benzyl-^{14}C]-BDDA by strain C505 was evaluated. The extent of mineralization increased with increasing incubation time (up to 300 hours) with an initial lag phase of less than 20 hours as shown in Fig 3.9. Almost 85% of the initial ^{14}C isotope in the parent BDDA was detected in the form of $^{14}CO_2$ within 300 hours. An undetectable concentration of $^{14}CO_2$ (other than background level) in the control sample suggests that the strain C505 was capable of almost complete mineralization of BDDA.

According to Fig 3.9, the rate of BDDA degradation was faster than the rate of mineralization and the rate of total ^{14}C degradation versus $^{14}CO_2$ production was not stoichiometric. This could be due to two factors. (1) A certain percentage of total ^{14}C, could have remained with the centrifuged pellet of cells (Lauff et al., 1990) and eventually washed out; the total ^{14}C associated with the pelleted cells was not determined. (2) During the degradation of BDDA, a portion of degradation products was assimilated by the bacterial cells. However, the evolution of $^{14}CO_2$ suggests that the cells utilized the carbon from the BDDA source mainly for the production of energy for their metabolic activity and less likely for the synthesis of cellular molecules.

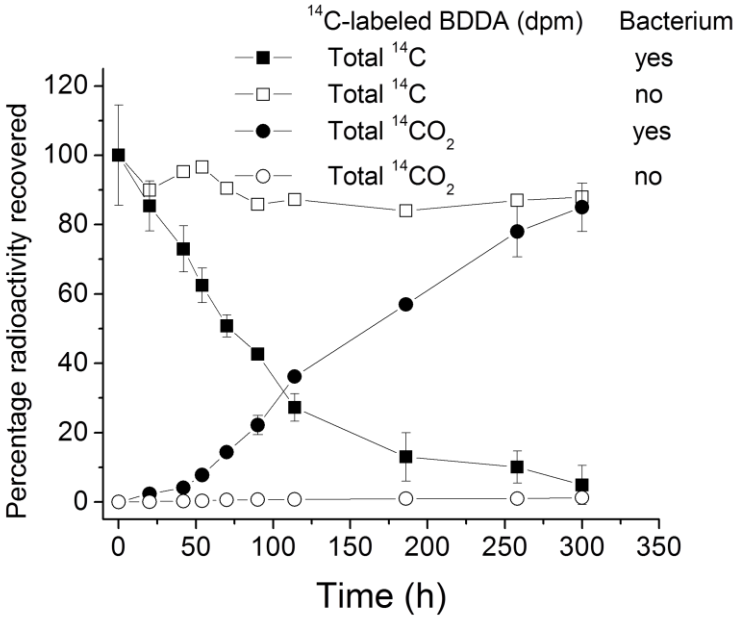

Fig.3.9 Mineralization of ^{14}C-labeled BDDA by the strain C505. Data are presented as the mean and standard deviation of three replicates.

3.4 Conclusions

Strain *Pseudomonas* sp. was able to degrade BDDA and BDTA, individually and in mixture. However, the efficiency of the biodegradation process depends on the initial concentration of the compounds. The strong inhibitory effect of BDTA on the degradation of BDDA suggests that that BACs (and other QACs) in the environment may not degrade as readily as they do under controlled laboratory conditions. Further studies on mixtures of different QACs will be important for an in-depth understanding of the bioremediation possibilities for cationic surfactants in sludge, soil and sediments.

References

Al-Rajab A.J., Sabourin L., Chapman R., Lapen D.R., Topp E., 2010. Fate of the antiretroviral drug tenofovir in agricultural soil. Science of the Total Environment 408, 5559–5564.

Al-Rajab A.J., Sabourin L., Scott A., Lapen D.R., Topp E., 2009. Impact of biosolids on the persistence and dissipation pathways of triclosan and triclocarban in an agricultural soil. Science of the Total Environment 407, 5978–5985.

Bassey D.E., Grigson S.J.W., 2011. Degradation of benzyldimethyl hexadecylammonium chloride by *Bacillus niabensis* and *Thalassospira* sp. isolated from marine sediments. Toxicological and Environmental Chemistry 93, 44-56.

Brycki B., Waligórska M., Szulc A., 2014. The biodegradation of monomeric and dimeric alkylammonium surfactants. Journal of Hazardous Materials 280, 797-815.

Buffet-Bataillon S., Tattevin P., Bonnaure-Mallet M., Jolivet-Gougeon A., 2012. Emergence of resistance to antibacterial agents: the role of quaternary ammonium compounds-a critical review. International Journal of Antimicrobial Agents 39, 381-389.

Dean-Raymond D., Alexander M., 1977. Bacterial metabolism of quaternary ammonium compounds. Applied and Environmental Microbiology 33, 1037-1041.

Eckard A.D., Muthukumarappan K., Gibbons W., 2012. Pretreatment of extruded corn stover with polyethylene glycol to enhance enzymatic hydrolysis: optimization, kinetics, and mechanism of action. Bioenergy Research 5, 424-438.

Ferk F., Misık M., Hoelzl C., Uhl M., Fuerhacker M., Grillitsch B., Parzefall W., Nersesyan A., Micieta K., Grummt T., Ehrlich V., Knasmuller S., 2007. Benzalkonium chloride (BAC) and dimethyldioctadecyl-ammonium bromide (DDAB), two common quaternary ammonium compounds, cause genotoxic effects in mammalian and plant cells at environmentally relevant concentrations. Mutagenesis 22, 363–370.

Garcia M.T., Campos E., Sanchez-Leal J., Ribosa I., 1999. Effect of the alkyl chain length on the anaerobic biodegradability and toxicity of quaternary ammonium based surfactants. Chemosphere 38, 3473-3483.

Gaze W.H., Abdouslam N., Hawkey P.M., Wellington E.M.H., 2005. Incidence of class 1 integrons in a quaternary ammonium compound-polluted environment. Antimicrobial Agents and Chemotheraphy 49, 1802-1807.

Gerba C.P., 2015. Quaternary ammonium biocides: Efficacy in application. Applied and Environmental Microbiology 81, 464-469.

Geftic S.G., Heymann H., Adair F.W., 1979. 14 year survival of Pseudomonas cepacia in a salts solution preserved with benzalkonium chloride. Applied and Environmental Microbiology 37, 505−510.

Gillings M.R., Holley M.P., Stokes H.W., 2009. Evidence for dynamic exchange of *qac* gene cassettes between class1integrons and other integrons in freshwater biofilms. FEMS Microbiology Letters 296, 282-288.

Grabińska-Sota E., 2011.Genotoxicity and biodegradation of quaternary ammonium salts in aquatic environments. Journal of Hazardous Materials 195, 182-187.

Hegstad K., Langsrud S., Lunestad B.T., Scheie A.A., Sunde M., Yazdankhah S.P., 2010. Does the wide use of quaternary ammonium compounds enhance the selection and spread of antimicrobial resistance and thus threaten our health? Microbial Drug Resistance 16, 91-104.

Ismail Z.Z., Tezel U., Pavlostathis S.G., 2010. Sorption of quaternary ammonium compounds to municipal sludge. Water Research 44, 2303-2313.

Kroon A.G.M., Pomper M.A., van Ginkel C.G., 1994. Metabolism of dodecyl dimethyl amine by Pseudomonas MA3. Applied Microbiology Biotechnology 42, 134-139.

Lane D.J., Pace B., Olsen G.J., Stahl D.A., Sogin M.L., Pace N.R., 1985. Rapid determination of 16S ribosomal RNA sequences for phylogenetic analyses. Proceedings of the National Academy of Sciences of the United States of America 82, 6955-6959.

Lauff J.J., Steele D.B., Coogan L.A., Breitfeler J.M., 1990. Degradation of the Ferric Chelate of EDTA by a pure culture of an *Agrobacterium* sp. Applied and Environmental Microbiology 56, 3346-3353.

Li X., Luo X., Mai B., Liu J., Chen L., Lin S., 2014. Occurrence of quaternary ammonium compounds (QACs) and their application as a tracer for sewage derived pollution in urban estuarine sediments. Environmental Pollution 185, 127-133.

Liffourrena A.S., Lopez F.G., Salvano M.A., Domenech C.E., Lucchesi G.I., 2008. Degradation of tetradecyl trimethyl ammonium by Pseudomonas putida A ATCC 12633 restricted by accumulation of trimethyl amine is alleviated by addition of Al^{3+} ions. Journal of Applied Microbiology 104, 396−402.

Martínez-Carballo E., González-Barreiro C., Sitka A., Kreuzinger N., Scharf S., Gans O., 2007. Determination of selected quaternary ammonium compounds by liquid chromatography with mass spectrometry. Part II. Application to sediment and sludge samples in Austria. Environmental Pollution 146, 543-547.

Muyzer G., De Waal E.C.,Uitterlinden A.G., 1993. Profiling of complex microbial populations by denaturing gradient gel electrophoresis analysis of polymerase chain reaction-amplified genes coding for 16S rRNA. Applied and Environmental Microbiology 59, 695-700.

NCBI, 2014; http://www.ncbi.nlm.nih.gov/ (accessed September, 2016)

Nishiyama N., Toshima Y., Ikeda Y., 1995. Biodegradation of alkyltrimethylammonium salts in activated sludge. Chemosphere 30, 593-603.

Nishihara T., Okamoto T., Nishiyama N., 2000. Biodegradation of didecyldimethylammonium chloride by Pseudomonas fluorescens TN4 isolated from activated sludge. Journal of Applied Microbiology 88, 641-647.

Nishiyama N., Nishihara T., 2002. Biodegradation of dodecyl trimethyl ammonium bromide by Pseudomonas fluorescens F7 and F2 isolated from activated sludge. Microbes and Environment 17, 164-169.

Patrauchan M.A., Oriel P.J., 2003. Degradation of benzyldimethylalkylammonium chloride by *Aeromonas hydrophila* sp. *K.* Journal of Applied Microbiology 94, 266-272.

Ritchie R.J., Prvan T., 1996. Current statistical methods for estimating the K_m and V_{max} of Michaelis-Menten kinetics. Biochemical Education 24, 196-206.

Skoog D.A., Holler F.J., Crouch S.R., 2007. Principles of Instrumental Analysis, 6th Edition, Editor- Kiselica S., Brooks/Cole, USA. p: 110-111.

Sullivan D.E., 1983. Biodegradation of a cationic surfactant in activated sludge. Water Research 17, 1145-1151.

Takenaka S., Tonoki T., Taira K., Murakami S., Aoki K., 2007. Adaptation of Pseudomonas sp. Stain 7-6 to quaternary ammonium compounds and their degradation via dual pathways. Applied and Environmental Microbiology 73, 1797-1802.

Tezel U., Tandukar M., Martinez R.J., Sobecky P.A., Pavlostathis S.G., 2012. Aerobic biotransformation of n-tetradecyl benzyl dimethyl ammonium chloride by an enriched *Pseudomonas spp.* community. Environmental Science and Technology 46, 8714−8722.

Tezel U., Pavlostathis S.G., 2009. Transformation of benzalkonium chloride under nitrate reducing conditions. Environmental Science and Technology 43, 1342–1348.

Topp E., Chapman R., Devers-Lamrani M., Hartmann A., Marti R., Martin-Laurent F., Sabourin L., Scott A., Sumarah M., 2013. Accelerated biodegradation of veterinary antibiotics in agricultural soil following long-term exposure, and isolation of a sulfamethazine degrading Microbacterium sp. Journal of Environmental Quality 42, 173-178.

Topp E., Zhu H., Nour S.M., Houot S., Lewis M., Cuppels D., 2000. Characterization of an atrazine-degrading *Pseudaminobacter* sp. isolated from Canadian and French agricultural soils. Applied and Environmental Microbiology 66, 2773-2782.

van Ginkel C.G., Vandijk J.B., Kroon A.G.M., 1992. Metabolism of hexadecyltrimethylammonium chloride in Pseudomonas strain-B1. Applied and Environmental Microbiology 58, 3083−3087.

Weisburg W.G., Barns S.M., Pelletier D.A., Lane D.J., 1991. 16S Ribosomal DNA amplification for phylogenetic study. Journal of Bacteriology 173, 697-703.

Zhang C., Tezel U., Li K., Liu D., Ren R., Du J., Pavlostathis S.G., 2011. Evaluation and modeling of benzalkonium chloride inhibition and biodegradation in activated sludge. Water Research 45, 1238-1246.

Chapter 4

Sorption and Leaching of Benzalkonium Chlorides in Agricultural Soils

[A revised version of this chapter is submitted; Khan et al., 2016. Journal of Environmental Management]

4.1 Introduction

Benzalkonium chlorides (BACs) are a sub-group of quaternary ammonium compounds (QACs), which are cationic surfactants with a positive charge on the nitrogen atom. Widespread use of BACs in many domestic, agricultural and healthcare applications (Gerba, 2015) results in their presence in wastewater treatment plants (Ismail et al., 2010). Due to their polar moieties and alkyl chain, BACs can be partitioned into sludge during wastewater treatment by both electrostatic and hydrophobic interactions. As a result, BACs may enter into a soil environment by the application of biosolids to agricultural fields as fertilizer and by the use of reclaimed wastewater for irrigation (Clarke and Smith, 2011). They can be discharged directly into soil and aquatic systems where the sewage treatment facilities are inadequate. Toxic effects of BACs were found for aquatic invertebrates with an LC_{50} of 5.9 µg L^{-1} (USEPA, 2006). BACs are genotoxic to eukaryotic cells at 1.0 mg L^{-1} (Ferk et al., 2007).

Many environmental and effluent samples indicate the presence of BACs. For example, BACs concentration up to 6.03 mg L^{-1} in hospital effluents in many European countries (Kümmerer et al., 1997), 0.31 mg L^{-1} in wastewater influents in western Austria (Clara et al., 2007), 1.1 mg kg^{-1} in river sediments in China (Li et al., 2014), and 9.0 mg kg^{-1} in sewage sludge (dry weight) in Austria (Martínez-Carballo et al., 2007) have been reported. In a recent study, total BACs in various soils near a cattle farm and migratory bird habitat in Korea ranged from 0.005 to 28.5 mg kg^{-1} (Kang and Shin, 2016). The fate of organic pollutants such as BACs in the soil environment depends on their mobility (diffusion and dispersion), leaching potential, and persistence (Estevez et al., 2014). Sorption properties of BACs on soil can dictate both the mobility and leaching of BACs in surface run-off and infiltration to groundwater. In addition, strong adherence to soil particles can make the compounds less

bioavailable. Due to their positive charge, BACs are expected to strongly adsorb on negatively charged soil particles. Furthermore, the long hydrophobic carbon chains facilitate their adsorption on the organic matter present in soil. The main mechanism to remove BACs from soil can be biodegradation; however, our recent study showed that biodegradation of one BAC under controlled conditions was inhibited in the presence of another BAC (Khan et al., 2015). Co-contamination may explain the persistence and relatively high abundance of BACs in the environment.

García et al. (2006) studied adsorption of BACs on sludge collected from a thickening tank, while Ismail et al. (2010) determined adsorption of BACs on four different types of sludge (primary, waste-activated, mesophilic- and thermophilic-digested sludge). Both studies have reported the adsorption of BACs on sewage sludge was higher with the increase of alkyl chain length. Ismail et al. (2010) also reported the desorption of two cationic surfactants (hexadecyl benzyl dimethyl ammonium chloride and dodecyl tri-methyl ammonium chloride) from sewage sludge after 24 h, to be 5% and 67%, respectively. In another study, desorption of two other QACs (octadecyltrimethyl ammonium bromide and arquad) from different soil samples was found to be 10%-30% and 40%-60%, respectively (Sarkar et al., 2010). These results for QACs indicate that BACs might also leach and become bioavailable in the soil environment and be taken up by plants. In addition, in a parallel study conducted in our lab, two types of plants grown in hydroponic systems using BAC-spiked nutrient solution showed inhibited growth, necrosis, and chlorosis (Khan et. al., 2016), indicating the need to determine the potential for leaching of these compounds in agricultural soil.

To the best of our knowledge, a comprehensive adsorption and leaching study using model BACs and a mixture of agricultural soil and biosolids has not yet been reported, which is the objective of this work. Initially, adsorption parameters of two BACs for three different agricultural soils were determined. Subsequently, soil column leaching experiments using alkaline-stabilized biosolids (a commercial fertilizer) spiked with one of the BACs (BDDA, which is comparatively less adsorptive) along with agricultural soils were conducted to determine the potential for BDDA to leach from biosolids.

4.2 Materials and methods

4.2.1 Chemicals

Individual BACs, such as, benzyl dimethyl dodecyl ammonium chloride (BDDA) and benzyl dimethyl tetradecyl ammonium chloride (BDTA) were purchased from Sigma-Aldrich (St. Louis, MO, USA). BDDA and BDTA had the purity ≥ 99.0% and were used as the certified reference materials for this experiment. HPLC grade acetonitrile (ACN) was purchased from Caledon Chemicals (Georgetown, ON, Canada). Ammonium acetate, HPLC grade (98.3%; Fisher Chemical, New Jersey, USA), was used to prepare the buffer solution for HPLC analysis. Phosphoric acid (85%) was purchased from Caledon Laboratories Ltd, (ON, Canada). Milli-Q water (conductivity 18 MΩ.cm, Millipore water systems, Integral-5, France) was used for experimentation. The physical properties of the two BACs used in this study are presented in Table 4.1.

Table 4.1 Properties of the benzalkonium chlorides used in this study.

Chemical name	Chemical structure	Chemical formula	Molecular weight (g mol^{-1})	Solubility[a] (mg L^{-1} at 25°C)	Log K_{ow}[b]
BDDA	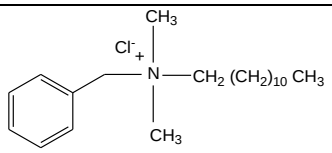	$C_{21}H_{38}NCl$	339.99	5–7.5 x 10^5	0.59±0.04
BDTA	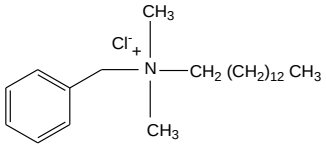	$C_{23}H_{42}NCl$	368.04	5 x 10^5 to 8.5 x 10^{4c}	1.67±0.02

[a] Ismail et al., (2010); [b] Tezel (2009); [c] the solubility of BDTA must be within this range, because the solubility of hexadecyl benzyl dimethyl ammonium chloride is 8.5 x 10^4 (Ismail et al., 2010).

4.2.2 Soil and biosolids

Three types of agricultural soil were collected: two varieties of sandy loam soil (London Loam or LL and Delhi Sand or DS) were obtained from the Agriculture and Agri-Food Canada research farms at London, ON (42°59'N, 81°15'W) and Delhi, ON (42°51'N, 80°29W), respectively. A clay loam soil (Holiday Beach Clay or HB) was obtained from the Essex Region Conservation Authority research farm at Holiday Beach, ON (42°2'N, 83°3'W). The fields from which the soils were collected had no history of biosolids application or amendment. The top 20 cm of each soil type was sampled. Lime-stabilized biosolids were collected from the City of Sarnia, Wastewater Treatment Plant, Sarnia, ON, Canada. This product was generated from anaerobically digested sewage sludge that was further treated with cement kiln dust, then mixed, dried, and pasteurized to produce a granular material that can be used for liming agricultural soil.

After collection, both soils and biosolids were sieved to a maximum particle size of 2 mm (sieve no. 10) and stored at 4°C in a tightly closed polyethylene bag prior to the experiments. Selected properties of the soil and biosolids were determined in triplicate following the methods described in section 4.2.3.1. The composition of clay, silt and sand, organic matter content (OM), total organic carbon (TOC) and pH were measured for each soil. The percentage moisture content, OM, TOC, pH, and the carbon to nitrogen ratio were measured for the biosolids.

4.2.3 Analytical methods

4.2.3.1 Soil and biosolids analysis

The percentages of clay, silt and sand were measured using a hydrometer following the method of Das (2009), and the pH of soil was measured using the method described by the American Society for Testing and Materials (ASTM-D4972–01) and a pH meter (ORION STARA111, Thermo Scientific, USA). The moisture content of biosolids and OM content of soils and biosolids were determined following another ASTM protocol (ASTM-D2974-87). The carbon and nitrogen contents of the biosolids were measured using a CHNS/O analyzer (Flash EA 1112 analyzer; Thermo Scientific, USA), from which the carbon to nitrogen ratio

was calculated. The total organic carbon (TOC) for soils and biosolids was determined by dry combustion of samples at 900°C in a furnace, with the collection and detection of evolved CO_2 using a TOC analyzer (TOC-V analyzer connected with an ANSI-V auto sampler, Shimadzu, Japan) following the methods of Schumacher (2002).

4.2.3.2 BAC extraction from spiked soils and biosolids

In order to determine adsorption and leaching, soil and biosolid samples were spiked with a known concentration of BDDA. Biosolids and soils were oven-dried at 100°C for 1 h, then autoclaved to sterilize, and 50 g of soil or biosolids was placed in a beaker. A stock solution of BDDA in methanol was prepared such that 50 mL of solution would make a final concentration of 0.2 mg BDDA per gram of soil or biosolids sample. The BDDA-methanol solution was added drop-wise to a sample with continuous mixing using a glass rod. Afterwards, the mixture was air-dried at room temperature for 24 h to allow methanol to evaporate and BDDA to interact with the matrix (Ferrer and Furlong, 2002). The spiked soils and biosolids were preserved at 4°C until use.

An ultrasound cleaning bath (Branson Ultrasonic Corporation, USA; Model 5510R-MTH 117V, 50-60 Hz) was employed to extract BDDA because of the simplicity and efficiency of the technique (Khan et al., 2012). 1 g of spiked sample (biosolids or soil) was put in a digestion tube (Kimax Cultures Tubes, reusable with screw cap with 20 mL capacity) and sequentially extracted three times (1 h x 3) using 10 mL of a solvent mixture (acetonitrile and water or acidic methanol) at 68±2°C in the bath (Li and Brownawell, 2009; Li et al., 2014). After each hour of extraction, the supernatant was decanted and passed through a 0.2 µm filter into a Turbo-vap vial (Turbo-vap-II, Caliper Life Sciences, MA, USA) at 50°C and 12 to 18 psi pressure for complete drying. The final solution was diluted to 10 mL with Milli-Q water and the concentration of BDDA was measured using an HPLC-UV system as detailed in section 4.2.3.3. All extractions were carried out in triplicate. One control for each soil type and the biosolids (autoclaved samples without spiking with BDDA) was tested to check the background concentrations of BDDA.

4.2.3.3 Analysis of benzalkonium chlorides

Depending on the concentrations of BACs in the sample, three different analytical instruments, ultra-violet and visible (UV-Vis) spectrophotometer, high performance liquid chromatography-UV (HPLC-UV) or HPLC-MS (mass spectrometry), were used to quantify the BACs.

A UV-Vis spectrophotometer was used to measure BAC concentrations in the range of 10-150 mg L^{-1} for the adsorption study (section 4.2.4). The benzene ring in BAC molecules can absorb UV wavelengths. Several wavelengths in the UV range have been used for the measurement of BACs in solutions, including 262 nm (Fejér et al., 2002), 225 nm (Tezvergil-Mutluaya et al., 2011), and most commonly 210 nm by several researchers (Khan et al., 2015; Tezel and Pavlostathis, 2009). However, there is no evidence that the full spectrum range (starting from 180 nm) has been tested for BACs to determine the maximum absorbance (λ_{max}) wavelength for the selected compounds. A UV-Vis spectrophotometer (Shimadzu, UV-3600 series), with the software UV Probe version 2.21 was set to the following: slit width 5.0, medium scan speed, sampling interval 1 and single scan mode. Quartz type 'Q' cuvettes from Starna Scientific Ltd (UK) were used for spectrophotometric analysis.

The Beer-Lambert law was applied (Equation 4.1) to determine the molar absorptivity (ε = L mol^{-1} cm^{-1}) for individual BACs. In Equation 4.1, *A* is the absorbance (unit less) measured by the UV-Vis spectrophotometer at a given wavelength, *C* is the concentration of the compound in mole L^{-1} or mg L^{-1}, *b* is the light path length in the cuvette in cm (i.e. 1 cm).

$$A = \varepsilon C b \qquad \text{----------(4.1)}$$

The soil column leaching experiments (section 4.2.5) were conducted with only BDDA due to its lower adsorptivity and higher potential to leach from biosolids and soils. The concentrations of BDDA in biosolids and soils after the column leaching experiment were measured using a high performance liquid chromatography (HPLC) coupled with a diode

array UV-Vis detector (Dionex ICS-3000, USA). The separation column was a Luna CN (C-18, 3 µm pore, 100 mm length x 4.6 mm internal diameter; Phenomenex, Canada) and the absorbance was measured at 210 nm. The mobile phase contained a 60:40 (v:v) mixture of acetonitrile and 40 mM ammonium acetate, and was adjusted to pH 5.0 using 1 M H_3PO_4 and filtered (0.2 µm). The isocratic flow rate was 0.8 mL min^{-1} and the injection volume was 100 µL. The retention time for BDDA was 11.5±0.3 min and the limit of quantification was 3.0 mg L^{-1}, with $r^2 > 0.98$ for the standard curve.

Trace levels of BDDA in the leachate after column leaching were identified using an HPLC-MS (mass spectrometer; Q-Exactive Orbitrap by Thermo Scientific). An injection volume of 2 µL at a flow rate of 0.3 mL min^{-1} was used in an Agilent Eclipse plus C-18 RRHD column (1.8 µm pore size, 50 mm length x 2.1 mm internal diameter). The solvent gradient started with 100% H_2O (0.1% formic acid) for 0 to 0.5 min and increased to 100% acetonitrile (0.1% formic acid) over 3.5 min. The organic mobile phase was then held at 100% for 1.5 min before returning to 0% over 30 s followed by another round of 100% H_2O (0.1% formic acid). A top 3, data-dependent tandem MS ($ddMS^2$) analysis combined with a parallel reaction monitoring (PRM) was performed in positive mode. The full MS scans were performed at a resolution of 35,000 and AGC target of 3×10^6. The $ddMS^2$ and PRM scans were performed at a resolution of 17,500 and AGC target of 5×10^5. The spray voltage was held at 3.9 kV, the S-lens at 45 V and the sheath and auxiliary gas were set to 17 and 8 arbitrary units, respectively. The probe temperature and capillary temperature were 450 °C and 400 °C, respectively. The limit of quantification was determined to be 10 ppb (or 10 µg L^{-1}) and the limit of detection was an order of magnitude lower (1 ppb). The data were analyzed using Xcalibur™.

4.2.4 Adsorption kinetics and equilibrium experiments

Adsorption experiments were carried out in triplicate using each type of soil with individual BDDA and BDTA solutions made in Milli-Q water. The soil samples were autoclaved before use at 120°C for 20 min (Autoclave AMSCO Eagle Series 2041 Gravity Steriliz) to avoid possible biodegradation of BACs by soil microbes. About 0.5 g London Loam, 0.5 g Delhi

Sand, or 0.1 g Holiday Beach Clay as adsorbent was placed in a 250 mL Erlenmeyer flask and 150 mL of a selected concentration (25 to 150 mg L^{-1}) of BDDA or BDTA was added. The flasks were sealed with stoppers and shaken at a rate of 190 rpm in an orbital shaker (Thermo Scientific, MAXQ-4000, and USA) at 22°C in the dark.

Kinetic experiments were carried out in triplicate to determine the extent of adsorption with time and the maximum time required for equilibrium adsorption of individual BACs on each soil type. The initial concentration of each BAC was 100 mg L^{-1}. One control (BAC solution without any soil) experiment was conducted to assess the loss of compounds due to adsorption on the container wall. An additional experiment was conducted to determine the interference due to soil organics (Milli-Q water and soil), and this value was subtracted from the absorbance values of the samples during the quantification of BACs using a UV-Vis spectrophotometer. The liquid phase concentrations of the BACs were measured at 0, 0.25, 1, 5, 24 and 48 h; 5 mL of sample was collected at each time interval and passed through a 0.2 μm syringe filter (Pall Corporation, MI, USA) followed by the immediate analysis using the UV-Vis spectrophotometer. The mass of the BACs adsorbed on the soils was calculated as the difference of initial and equilibrium concentrations of the individual BACs.

For the adsorption isotherm experiments, the initial concentrations of BACs were 25, 50, 75, 100, 125 and 150 mg L^{-1} for all three types of soils using the same masses of the soils used in the kinetic experiments mentioned above. Although the BAC concentrations used in the experiments are higher than what is expected in wastewater, they are comparable to the total QACs measured in sewage sludge (167 mg kg^{-1}; Li et al., 2014). All isotherm experiments were conducted in triplicate. One control and one additional experiment (to correct for the background interferences) were also carried out at the same time.

The two most popular isotherm models, Langmuir and Freundlich, were applied to calculate the adsorption parameters. The Langmuir isotherm model assumes monolayer adsorption on an energetically homogenous surface and no sideways interaction between the sorbed molecules (Langmuir 1916). On the other hand, the Freundlich isotherm describes a heterogeneous surface (Freundlich 1906).

4.2.5 Column experiment

Column leaching experiments were carried out according to OECD guidelines (OECD 2004), using a glass column of 4 cm inner diameter and 15 cm length with an outlet control valve. The column length was lower than the OECD recommended minimum of 35 cm as one of the objectives of this research was to evaluate the leaching possibilities of BDDA from biosolids to the rooting zone of plants rather than to the ground water (Ashworth and Alloway, 2004). The leaching experiment was conducted in duplicate and with one control with two types of soil with a top layer of BAC-spiked biosolids. Since the adsorption of the BACs was the highest on clay (Holiday Beach; discussed in section 4.3.6), no leaching experiments were conducted with this soil.

Each column was packed with a plug of glass wool to avoid outflow of particles, then 9 cm of soil (autoclaved and free from any BDDA) topped with 1 cm of spiked biosolids (0.2 mg BDDA g^{-1} of biosolids), for a total of 10 cm sample depth (Fig 4.1). Uniform packing was achieved by adding small portions of soil under gentle vibration of the column (Chen et al., 2006). A piece of coarse filter paper was placed on the top of the soil column to ensure even distribution of artificial rain water.

The bulk density (ρ_{bulk}; density of soil including particles and air trapped inside, calculated by dividing the mass of soil by its volume in the packed column) of London Loam and Delhi Sand was approximately 1.4 g cm^{-3} and 1.5 g cm^{-3}, respectively. Soil particle density ($\rho_{particle}$; material density of only soil particles) for London loam and Delhi sand was 2.5 ± 0.018 g cm^{-3} and 2.58 ± 0.03 g cm^{-3}, respectively, which was further used to calculate the porosity of the soil in the packed column using Equation 4.2. The porosity of packed columns for London loam was 0.44 and for Delhi sand was 0.42. Determination of pore volume is important because the soil must be saturated with water, or the pores must be filled with water, during column leaching. Since the soil volume inside the column was 113 cm^3 (length of soil column was 9 cm), the pore volume was calculated to be 49.5 cm^3 for London Loam and 47.5 cm^3 for Delhi Sand, respectively.

$$Porosity = 1 - \frac{\rho_{bulk}}{\rho_{particle}} \text{ ---------- (4.2)}$$

Artificial rain water (ARW) was prepared with 0.01 M $CaCl_2$ in Milli-Q water. A 200 mm rainfall is equivalent to 250 mL of ARW for a column of 4 cm in diameter (OECD 2004). Before starting the leaching experiment, soil columns were pre-wetted with ARW from bottom to top to remove air trapped inside the soil particles and equilibrated for 12 h (Rabølle and Spliid, 2000). At the beginning of the experiment, water in the soil column was drained (approximately 50 mL based on pore volume). Then, ARW from a controllable separating funnel started dripping from the top under gravity. A total of 300 mL of ARW was added dropewise in two different flow rates 0.1 mL min^{-1} (poured in 48 h), and 0.2 mL min^{-1} (poured in 24 h). Although 250 mL ARW was required, to mimic a rainfall of 200 mm, an additional 50 mL of ARW was needed to maintain the flow overnight. Furthermore, since the pore volume of the soil was about 50 mL, 300 mL of ARW was sufficient to keep the soil column saturated and made sure that 250 mL drip spontaneously. The higher flow rate (0.2 mL min^{-1}) was applied to investigate the possibilities of BDDA leaching from biosolids and passing through soil layers under extreme rain or flash flooding situations. The dripping rate of ARW was monitored every few hours over the duration of the experiment.

About 250 mL of leachate was collected and preserved at 4°C for analysis of BDDA. At the end of the leaching experiment, biosolids applied to the top of the soil layer were removed using a spatula and preserved at 4°C for analysis. The soil inside the column was removed and divided into 3 cm layers (top, middle and bottom), and preserved at 4°C until further analysis. Collected leachate was frozen at –20°C for 48 h prior to freeze drying (FreeZone 4.5, Labconco, MO, USA). The freeze-dried leachate was diluted to 2 mL with Milli-Q water, filtered through 0.2 µm filter and preserved at –20°C until analysis using HPLC-MS. Concentrations of BDDA in soil and biosolids were measuterd after extraction using HPLC-UV.

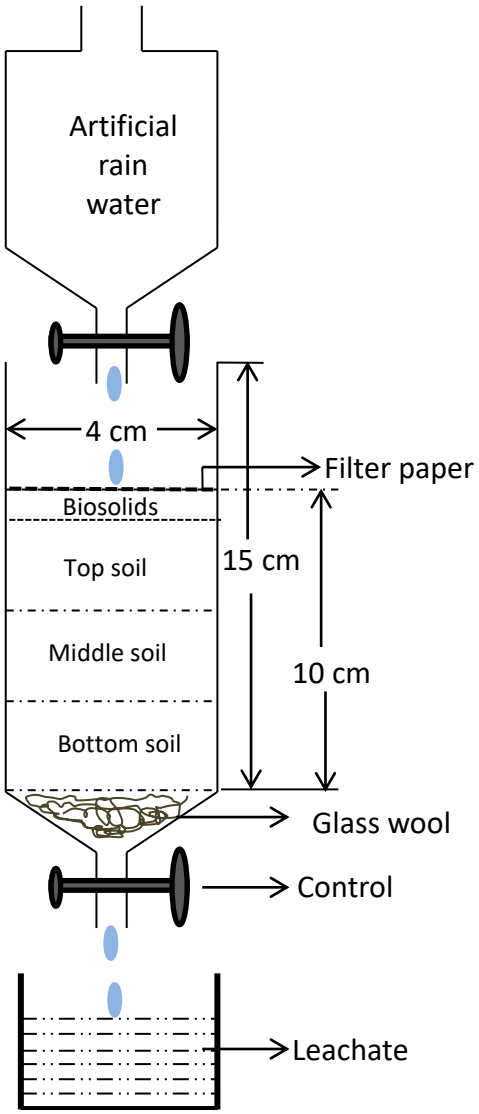

Fig 4.1 Schematic of soil column leaching experiment.

4.3 Results and discussion

4.3.1 Physical characteristics of soils and biosolids

Selected physical characteristics of the three soils (London loam, LL: Delhi sand, DS; Holiday beach, HB) are presented in Table 4.2. Soils in the present study were collected from the same location and/or sources as described by Al-Rajab (2010) and the values determined in this study are comparable to that of Al-Rajab. The cation exchange capacities of the soils as measured by Al-Rajab et al. (2010) are likely the same in our soils: 13.5 for LL, 5.4 for DS and 16.6 for HB (meq 100 g^{-1}). Delhi sand has more sand ($p < 0.05$) and less OM ($p < 0.05$) and cation exchange capacity compared to other two types of soil (Table 4.2). Clay content in HB soil is 4.9 and 3.6 times higher compared to DS and LL; whereas silt content is 6 and 2.7 times higher in HB compared to DS and LL, respectively. Therefore, higher surface area is anticipated for HB compared to DS and LL due to the presence of higher amount of clay and silt percentage in HB. The physical properties of the biosolids were measured to be: moisture content, 20.9±2.1 %; OM, 11.5±1.9 %; TOC, 9.2±0.76 %; pH, 12.5±0.06, and carbon to nitrogen ratio, 12.9:1.

Table 4.2 Selected physical characteristics of the soils. The top 20 cm soil was collected. Soil texture and organic content were measured using oven-dried soil; pH was measured using air-dried soil. Different lower case letters indicate significant differences in each physical properties of three soil, as determined by one-way ANOVA and post hoc Tukey tests (p <0.05). Values are mean±standard deviation, n = 3.

Soil type	Clay (%)	Silt (%)	Sand (%)	Organic matter content (OM) (%)	Total organic carbon (TOC) (%)	pH
London Loam (LL)	7.2±0.6[a]	13.7±1.2[a]	79.1±0.6[a]	3.22±0.06[a]	2.9 ±0.5[a]	7.24±0.01[a]
Delhi Sand (DS)	5.2±1.04[a]	6.3±1.4[b]	88.5±0.6[b]	1.70±0.01[b]	1.02 ±0.2[b]	6.04±0.05[b]
Holiday Beach Clay (HB)	25.6±1.5[b]	37.3±1.2[c]	36.4±1.5[c]	5.21±0.04[c]	2.5± 0.6[a]	4.46±0.18[c]

4.3.2 Quantification of BACs using UV-Vis spectrophotometer

Absorbance of BACs in the UV region (180 to 300 nm) was measured using a UV-Vis spectrophotometer to identify the maximum absorbance wavelengths for BDDA and BDTA, which were 188±0.5 and 187±0.5 nm, respectively (Fig 4.2). The application of the maximum absorbance wavelength for BACs can push the limit of quantification an order of magnitude or more lower compared to using 210 nm, as can be seen in Fig 4.2. The molar absorptivity for BACs was calculated from the slope of the standard curve using Equation 4.1. A series of

BAC concentrations (10, 5, 2.5, 1.25, 0.625, and 0.3125 mg L^{-1}) was used to produce the standard curve and the molar absorptivity was calculated to be 0.1444 and 0.1577 in L mg^{-1} cm^{-1} for BDDA and BDTA, respectively. The correlation coefficient for both BACs was r^2 > 0.99.

4.3.3 Adsorption kinetics

The time to reach equilibrium for the adsorption of 100 mg L^{-1} of BDDA or BDTA to three types of soil was determined from the kinetics experiment (Fig 4.3). Rapid adsorption for both BACs in each type of soil was observed in less than 5 h. There was no change in concentrations between 24 and 48 h for BACs in solutions and/or in soils. Control experiments with BACs but no soils showed no changes over the 48 h of the experiments indicating no adsorption of BACs on the container walls. A similar 24 h equilibrium time was observed for pharmaceuticals and personal care products in agricultural soils (Xu et al., 2009). Both BDDA and BDTA reached maximum adsorption on the three agricultural soils by 5 h, which is slightly slower than the reported adsorption of BACs on sewage sludge, which occurred in less than 3 h (Ismail et al., 2010). Typically, BDTA was adsorbed more on each type of soil than BDDA, with 30–80% of the total BDTA compared to 20–50% of the BDDA was adsorbed, depending on soil type (Fig 4.3). A similar pattern of higher adsorption of BDTA compared to BDDA was observed by García, (2006) on sewage sludge (BDTA adsorption was approximately 9% more than BDDA). An increase in the alkyl chain length increases the hydrophobicity, leading to higher affinity for adsorption of BACs.

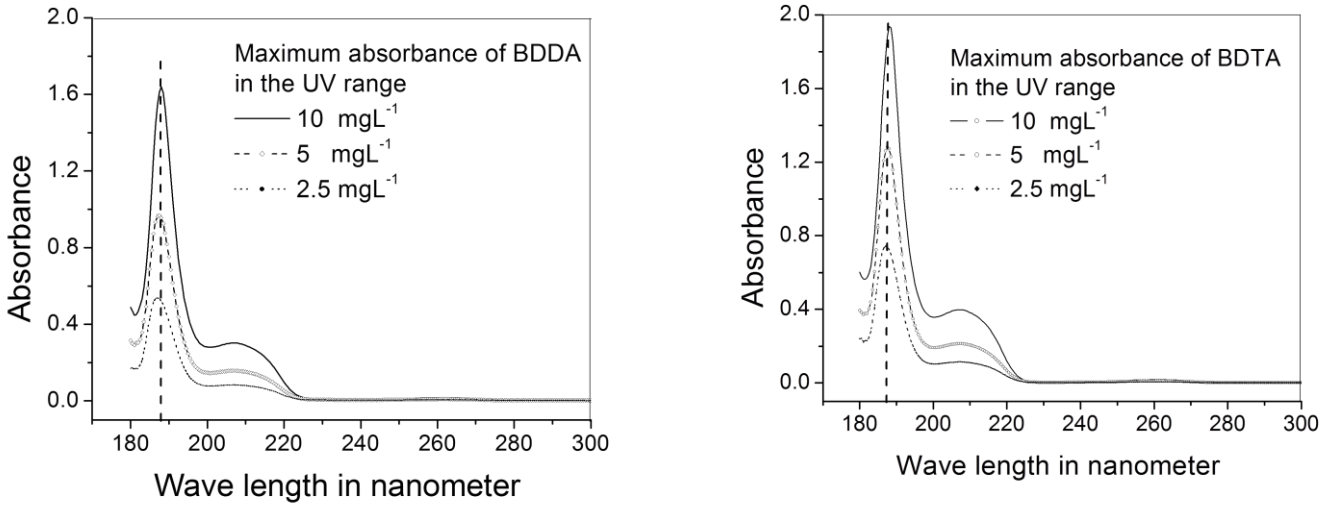

Fig 4.2 Absorption spectrum of BDDA and BDTA. Absorbance was recorded across the range of 180 to 300 nm using a UV-Vis spectrophotometer (Shimadzu, UV-3600 series). The vertical line represents the maximum absorbance (λ_{max}) for BDDA (188±0.5) and BDTA (187±0.5), which is common for three concentrations.

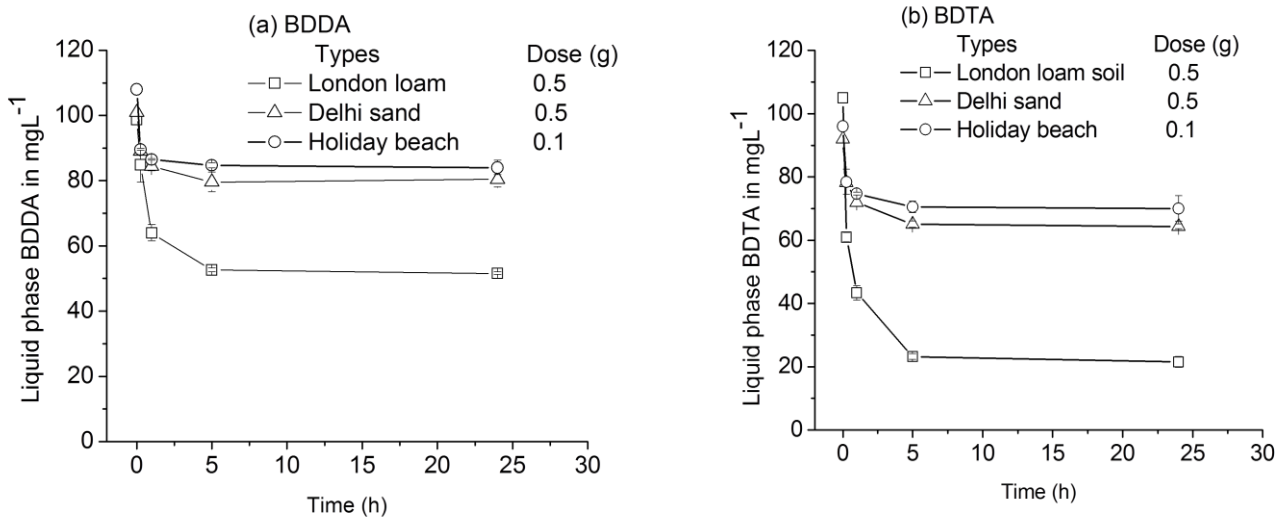

Fig 4.3 Adsorption kinetics of (a) BDDA and (b) BDTA at an initial concentration of 100 mg L^{-1} using three types of soil for 24 h. Error bar represents the standard deviation of triplicate samples. Control lines showed no difference between initial and final concentrations; small differences were subtracted from the concentrations that are plotted.

4.3.4 Adsorption isotherm parameters

A range of BAC concentrations (25 to 150 mg L^{-1}) was investigated to calculate the isotherm parameters and distribution coefficients for the three soil types. Isotherm models (Langmuir and Freundlich) for BDDA and BDTA are presented in Fig 4.4 and the corresponding parameters are presented in Table 4.3.

In the Langmuir model (Equation 4.3), C_e (mg L^{-1}) is the equilibrium concentration of BACs that remain unadsorbed; q_e (mg g^{-1}) is the concentration of BACs adsorbed on soil particles per unit mass ($q_e = [(Co - Ce)V]$/mass of sorbent), where C_0 is the initial BAC concentration (mg L^{-1}) and V is the volume of water (L) used for experiments. Other parameters in the Langmuir model, q_{max} (mg g^{-1}) and b (L mg^{-1}), are the maximum amount of

BACs per unit mass of sorbent to form a complete monolayer on the surface bound at C_e, and a constant related to the affinity of the binding sites, respectively (Hameed et al., 2008). The q_{max} and b of the Langmuir model can be determined from the slope and intercept of the linear plot of C_e/q_e versus C_e. The Freundlich model (Equation 4.4) also describes C_e (mg L^{-1}) and q_e (mg g^{-1}) as the equilibrium concentration of BACs that remain unadsorbed and the concentration of BACs adsorbed on soil particles per unit mass, respectively. The Freundlich constants K_f (mg/g (L/mg) $^{1/n}$) and n indicate the adsorption capacity of the sorbent and an indication of the favourability of the adsorption process, respectively. The magnitude of the exponent 1/n, gives an indication of favourable adsorption when n > 1 (Hameed et al., 2008). The values of K_f and n can be calculated from the intercept and slope of the plot $ln(q_e)$ vs. $ln(C_e)$.

$$\frac{C_e}{q_e} = \frac{C_e}{q_{max}} + \frac{1}{b\, q_{max}} \qquad \text{---------- (4.3)}$$

$$\ln q_e = \left(\frac{1}{n}\right) lnC_e + lnK_f \qquad \text{---------- (4.4)}$$

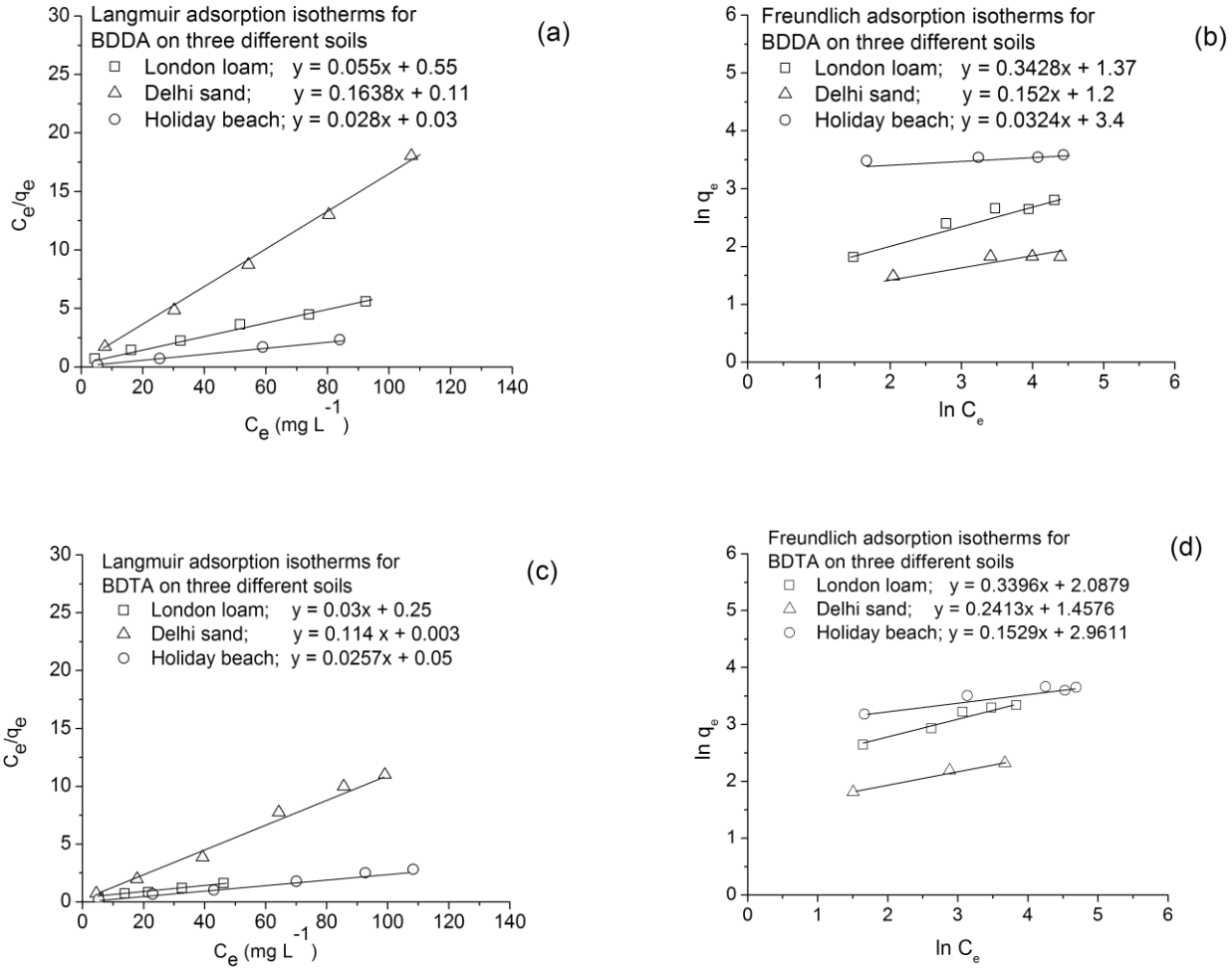

Fig 4.4 Adsorption isotherms for BDDA and BDTA on three soils. Isotherms for BDDA, (a) Langmuir and (b) Freundlich; Isotherms for BDTA, (c) Langmuir and (d) Freundlich.

Table 4.3 Langmuir and Freundlich adsorption isotherm parameters for BDDA and BDTA in three different soils.

Types of soils	Langmuir			Freundlich		
	Isotherms	BDDA	BDTA	Isotherms	BDDA	BDTA
London loam	q_{max} (mg g^{-1})	18.2	33	K_f (mg g^{-1} (L $mg^{-1})^{1/n}$)	3.9	8.2
	b (L mg^{-1})	0.1	0.12	n	2.9	2.9
	r^2	0.993	0.991	r^2	0.956	0.958
Delhi sand	q_{max} (mg g^{-1})	6.25	8.8	K_f (mg g^{-1} (L $mg^{-1})^{1/n}$)	3.3	4.3
	b (L mg^{-1})	1.39	33	n	6.6	4.2
	r^2	0.997	0.992	r^2	0.84	0.984
Holiday beach clay	q_{max} (mg g^{-1})	35.7	38.9	K_f (mg g^{-1} (L $mg^{-1})^{1/n}$)	29.9	19.3
	b (L mg^{-1})	0.9	0.5	n	30.8	6.5
	r^2	0.999	0.994	r^2	0.919	0.926

Adsorption parameters for BACs were better described using the Langmuir model (r^2 > 0.99; Table 4.3) compared to the Freundlich model (r^2 = 0.84 to 0.98) suggesting monolayer adsorption on soil. The Langmuir isotherms for BDDA and BDTA are presented in Fig 4.4(a) and 4.4(c), respectively. The maximum adsorption capacity for BACs, q_{max} (mg g^{-1}) varied from 6.25 to 38.9 (Table 4.3) for the three soils in the order of HB > LL > DS. The presence of OM, clay minerals and cationic exchange capacity (CEC) influence the mobility of organic pollutants (Chen et al., 2006; Chefetz et al., 2008). Percentage of OM, clay minerals and CEC in the HB soil were the highest followed by LL and DS (Table 4.2), which is in agreement with the decreasing trend of q_{max} values calculated for BDDA and BDTA (Table 4.3).

The maximum adsorption (q_{max}) capacity for BDDA and BDTA in sewage sludge (67 and 73 mg g^{-1}, respectively) was higher (García et al., 2006) compared to what we have found in

our study, which might be due to the presence of higher organic matter (38 to 44% by weight) and negative charges on the surface of sewage sludge. However, comparable sorption capacity was determined (22.3 to 39.8 mg g^{-1}) for QACs (broad range of cationic surfactants) in agricultural soil by Sarkar et al. (2010). In another study, a significantly higher sorption capacity was determined for BDDA (182 mg g^{-1}) and BDTA (205 mg g^{-1}) on montmorillonite (Fejér et al., 2013). The high cation exchange capacity of montmorillonite (4.6 times higher compared to the HB soil) might be a major influential factor for high sorptivity of these compounds on clay, which is also seen in this study for soil with higher clay content.

Freundlich adsorption isotherms and the corresponding fitted parameter values (K_f and n) for BACs are presented in Fig 4.4 (b and d) and Table 4.3, respectively. The K_f values obtained for both BDDA and BDTA follow the same desending order for the three soils (i.e., HB > LL > DS) as observed in the Langmuir model. The calculated K_f values lie in the range of 3.3 to 29.9 (mg/g (L/mg) $^{1/n}$) and the magnitude increased with carbon chain length from BDDA to BDTA (except for BDTA in HB soil; Table 4.3). The values (K_f) are comparable to the findings of BAC adsorption to municipal sludge (Ismail et. al., 2010); however, these results suggested that the adsorption affinty depends on both the molecular structure of BACs and physical characteristics of soil. Higher n values (2.9 to 30.8; Table 4.3) indicate that the Freundlich model can be well fitted at the low range of C_e. At higher BAC concentrations (as used in the present study), hydrophobic interactions between the BAC's alkyl chain and soil particles probably dominate over ion exchange interactions where cationic BAC interacts with the negative sites of sorbents (Ismail et al., 2010).

The distribution coefficients (K_d, L kg^{-1}) and organic carbon normalized adsorption coefficients (log K_{oc}, L kg^{-1}) for BACs in the soils are presented in Table 4.4. The linear correlation coefficients between q_e vs C_e, at lower initial concentrations (10 to 25 mg L^{-1}) of BACs were $r^2 > 0.97$, except for BDTA with London loam ($r^2 > 0.94$) (Table 4.4). Distribution coefficients (K_d and log K_{oc}) of BDDA on soils were maximum in HB soil followed by LL and DS but the highest coefficients for BDTA were calculated for DS. Distribution coefficients for BACs to soils ranged from 310 to 3600 L kg^{-1}. A similar high range of K_d was observed for

amines (Ifenprodil and Fluoxetine) and pyrene derivatives (1-Aminopyrene and Pyrene) to river sediments in Japan (Yamamoto et al., 2009). Even higher K_d was determined for galaxolide and tonalide (musk fragrances) for mesophilic digested sludge (K_d was 12200 to 19100 L kg^{-1}) and for thermophilic digested sludge (K_d was from 6709 to 10583 L kg^{-1}), respectively (Carballa et al., 2008). Organic carbon normalized adsorption coefficients (log K_{oc}) for BACs varied between 4.1 to 5.5 among the soils (Table 4.4). A similar range of log K_{oc} was determined for many organic pollutants, including galaxolide (4.48 to 5.96), tonalide (4.67 to 6.04), estrone (3 to 4.18) and 17α-ethinylestradiol (2.9 to 4.16) in various digested sludges (Carballa et al., 2008); as well as for amines (2.5 to 5.4) and pyrene derivatives (3.2 to 6.3) in various river sediments (Yamamoto et al., 2009). For many organic pollutants, high %OM in natural adsorbent leads to higher values of K_d and log K_{oc} (Yamamoto et al., 2009; Estevez et al., 2014). However, adsorbtion of BACs on soil might not only be due to the hydrophobic interaction between the alkyl chain and OM but also due to the electrostatic interactions between the positive charge on its nitrogen atom and the negatively charged soil surface.

4.3.5 Extraction efficiency of BDDA from soils and biosolids

Extraction efficiencies, using an ultrasound assisted extraction process, for BDDA from spiked biosolids and soils using different combinations of solvents are presented in Table 4.5. Extraction of BDDA from solid matrices (biosolids and soil) is difficult because of the strong adsorption of the positively charged BDDA to the biosolids and/or soil particles. To the best of our knowledge, no established analytical methods have been published on the extraction of these compounds from agricultural soil until recently (Kang and Shin, 2016) and lime-stabilized biosolids. The procedures to extract BDDA from soils and biosolids were developed following a few existing methods (Ferrer and Furlong, 2002; Li and Brownawell, 2009) and almost 100% of BDDA from lime-stabilized biosolids was extracted using acetonitrile and water at a ratio of 7:3.

Table 4.4 Solid-liquid distribution coefficient for BDDA and BDTA on different types of soil-water system as adsorbent.

Types of soils	Parameters (BDDA)	Values	Parameters (BDTA)	Values
London loam (LL)	K_d (L kg^{-1}) (r^2)	1210 (0.973)	K_d, (L kg^{-1}) (r^2)	760 (0.945)
	log K_{oc} (L kg^{-1})	4.6	log K_{oc} (L kg^{-1})	4.4
Delhi sand (DS)	K_d (L kg^{-1}) (r^2)	320 (0.985)	K_d, (L kg^{-1}) (r^2)	2900 (0.974)
	log K_{oc} (L kg^{-1})	4.5	log K_{oc} (L kg^{-1})	5.5
Holiday beach clay (HB)	K_d (L kg^{-1}) (r^2)	3600 (0.988)	K_d, (L kg^{-1}) (r^2)	310 (0.987)
	log K_{oc} (L kg^{-1})	5.15	log K_{oc} (L kg^{-1})	4.1

Table 4.5 Percentage BDDA extracted from reference samples (n=3).

Solvent combinations (ratio)	%BDDA extracted ± standard deviation			
	Biosolids	Delhi sand	London loam	Holiday beach
Water: Acetonitrile (3:7)	105±9.5	19.2±1.4	18.3±3.2	ND
0.1 M HCl + Methanol (1:1)	NA	46.6±6.4	ND	ND
1.0 M HCl + Methanol (1:2)	NA	21±3.7	41.7± 4.2	ND

NA = Not applicable; ND = Not detected

Ferrer and Furlong (2002) investigated various combinations of methanol and water using a high pressure solvent extraction technique and the recovery of BDDA was 8 to 85% from sediment samples collected downstream of a wastewater treatment plant. However, in our work with the soil samples, the extraction efficiency was below 50% using HCl and methanol (Table 4.5). The extraction was particularly difficult for HB soil, where no BDDA could be detected in the extract within the limit of quantification (3 mg L^{-1}) of HPLC-UV, probably due to its high CEC. The CEC of HB soil can lead to intercalation of organic cation of the surfactants, such as BDDA, inside the clay structure causing strong adsorbate-adsorbent interactions and subsequent cage formation (Li and Brownawell, 2009). Control soil and biosolids samples were free of any background BDDA within the limit of quantification of HPLC-UV. As a surfactant, BDDA contains both hydrophilic and hydrophobic ends and its solubility varies with various mixtures of aqueous/organic solvents. As a result, further investigation for improved recovery of BDDA from soil matrices is required.

4.3.6 Leaching of BDDA in the soil column experiment

The adsorption of BDTA (q_{max}) was 1.3 to 2.1 times higher compared to BDDA for London loam and Delhi sand (Table 4.3). Additionally, the concentration of BDDA found in natural environment was almost twice the value of BDTA (Li et al., 2014). As mentioned earlier, due to high abundance of BDDA in nature and less adsorption on soils compared to BDTA, only BDDA was tested in the soil column experiment. Similarly, Holiday Beach soil had 2 and 6 times more adsorption capacity (q_{max}, mg g^{-1}) for BDDA compared to London loam and Delhi sand, respectively (Table 4.3). Thus, Holiday Beach soil is more likely to retain BDDA on its particle surfaces and was excluded from the column leaching experiment.

After pouring 300 mL of ARW at two different flow rates (0.1 and 0.2 mL min^{-1}) in soil columns, the biosolids and soils were removed and extracted to determine the amount of BDDA. Since the efficiency of extraction was 100% for biosolids (Table 4.5), it was possible to determine the quantity of BDDA moved from the top biosolids layer to the soil column. Two different flow rates of ARW was applied in two soils (LL and DS) in duplicate topped with spiked biosolids as a top layer; as a result, there was a total of four biosolids samples (n=4)

(for each flow rate two from DS and another two from LL), which were analyzed for BDDA. About 63±19% and 92±9% BDDA moved from the top biosolids layer to the bottom soil layer at flow rates of 0.1 and 0.2 mL min^{-1}, respectively. BDDA might form ionic bonding with organic matter (humic and fulvic acids) or with mineral surfaces in biosolids and be solubilized in the presence of water to leach downwards (Ferrer and Furlong, 2002). As a result, at the higher flow rate (0.2 mL min^{-1}), which is an imitation of a flash flood incident or heavy downpour, approximately 20 to 30% more BDDA leached from biosolids compared to the slower flow rate.

In different layers of the soils (top, middle and bottom), the extraction process was unable to isolate enough BDDA to detect using HPLC-UV. Distribution of BDDA over the large surface area of the soil particles inside the column (9 cm in length), low efficiency (< 50%) of the extraction process for BDDA in soils (Table 4.5), and a higher limit of quantification for BDDA using HPLC-UV, limited the ability to determine the presence of BDDA in soils inside the column. However, leachates were analyzed using HPLC-MS to detect the trace concentrations of BDDA transported through the soil layers. Leachates from the control column were free of any detectable BDDA. At the higher flow rate (0.2 mL min^{-1}) of ARW, BDDA was detected in leachates (duplicate samples) from the BDDA-spiked soil column made of Delhi sand; a representative chromatogram is presented in Fig 4.5. The presence of BDDA in leachates was confirmed by the fragment ions (m/z 91.05, 212.24) produced from the parent BDDA (m/z 304.3). Delhi Sand, which had the lower BDDA adsorption capacity (q_{max}*=6.25* mg g^{-1}) compared to London Loam soil (q_{max} *= 18.2* mg g^{-1}), showed the greater leaching potential. The amount of BDDA in the leachate was estimated to be 0.07 µg (in 2 mL solution prepared for HPLC-MS), which was well below 1% of the total amount of BDDA mixed into the top layer of biosolids (~10 g). No measurable amount of BDDA was leached at the lower flow rate (0.1 mL min^{-1}) due to high adsorbing capacity of both the soils; BDDA may have moved within the soil column but did not pass through the entire 9 cm soil layer. While the BACs in soil amended with biosolids that contain up to 0.2 mg g^{-1} BACs may not be bioavailable in sandy loam soils, there remains the potential for plant uptake if the roots are within the top 9 cm of soil.

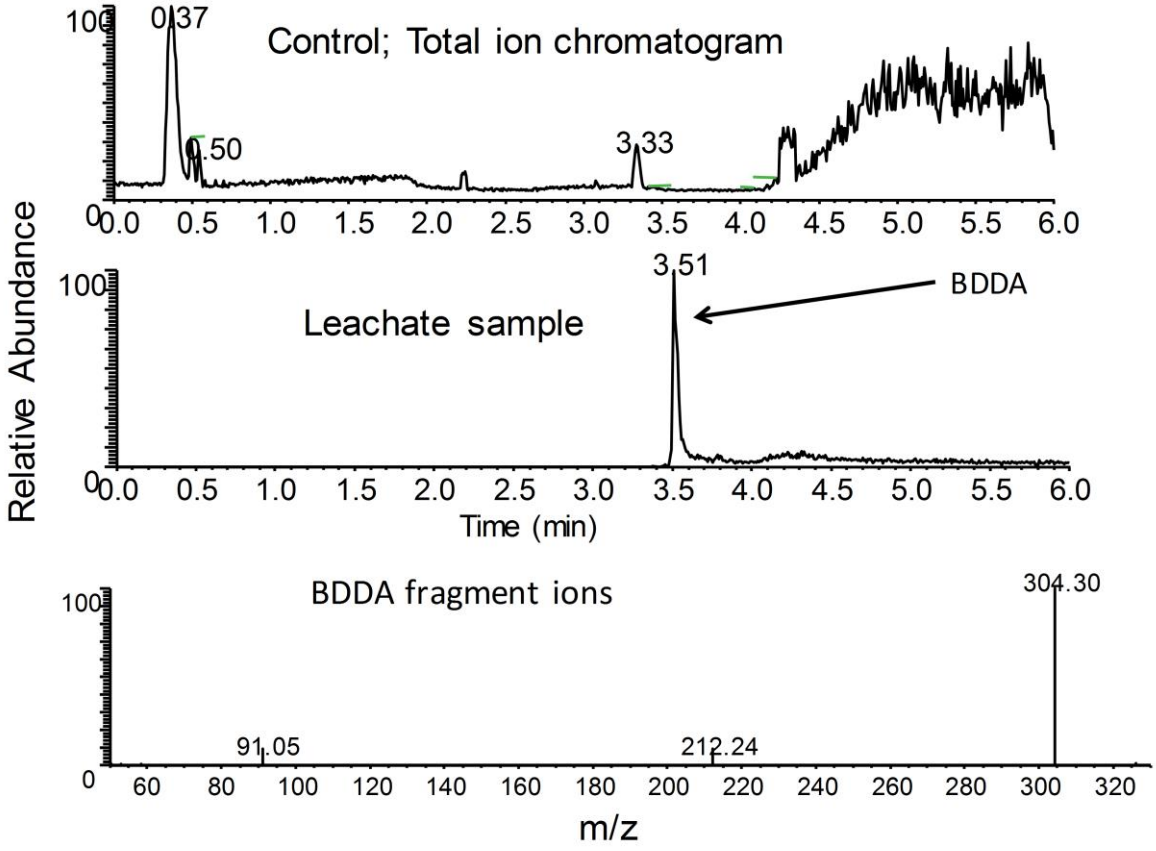

Fig 4.5 Leachate analyzed for BDDA for column packed with Delhi Sand when 300 mL of artificial rain water was poured at 0.2 mL min^{-1}.

4.4 Conclusions

Micropollutants such as BACs may enter agricultural soil through the application of municipal biosolids as a fertilizer and/or by the application of reclaimed wastewater for irrigation. The high q_{max} (mg g^{-1}) of the clay-rich soil (HB) for BDDA and BDTA and the log K_{oc} (L kg^{-1}) > 4.0, suggests that BACs are more likely to be retained inside the soil layers and less likely to move with runoff water. In sandy loam soil, in cases of extreme weather conditions (heavy downpour or flash flood situation), BACs have the potential to leach through the soil layers, although leached amounts are very low when the BACs are at environmentally relevant concentrations.

The positive charge of BACs plays an important role in the sorption and leaching of the compounds. The mobility of BACs in soil depends on how the BACs are interacting with solid matrices. For example, the formation of ionic bonds with humic acid enhances the solubility of BACs in water; conversely, intercalated cation formation in clay or hydrophobic interactions with organic matter on soil reduce the mobility of BACs and they will remain within the soil matrices.

References

Al-Rajab A.J., Sabourin L., Chapman R., Lapen D.R., Topp E., 2010. Fate of the antiretroviral drug tenofovir in agricultural soil. Science of the Total Environment 408, 5559–5564.

Ashworth D.J, Alloway B.J., 2004. Soil mobility of sewage sludge-derived dissolved organic matter, copper, nickel and zinc. Environmental Pollution 127, 137-144.

Carballa M., Fink G., Omil F., Lema J.M., Ternes T., 2008. Determination of the solid–water distribution coefficient (K_d) for pharmaceuticals, estrogens and musk fragrances in digested sludge. Water Research 42, 287–295.

Chefetz B., Mualem T., Ben-Ari J., 2008. Sorption and mobility of pharmaceutical compounds in soil irrigated with reclaimed wastewater. Chemosphere 73, 1335–1343.

Chen W., Song L., Gan N., Li L., 2006. Sorption, degradation and mobility of microcystins in Chinese agriculture soils: Risk assessment for groundwater protection. Environmental Pollution 144, 752-758.

Clara M., Scharf S., Scheffknecht C., Gans O., 2007. Occurrence of selected surfactants in untreated and treated sewage. Water Research 41, 4339–4348.

Clarke B.O., Smith S.R., 2011. Review of 'emerging' organic contaminants in biosolids and assessment of international research priorities for the agricultural use of biosolids. Environment International 37, 226–247.

Das B.M., 2009. Soil mechanics laboratory manual. 7th Edition, Oxford University Press. P 25–36.

Estevez E., Hernandez-Moreno J.M., Fernandez-Vera J.R., Palacios-Diaz M.P., 2014. Ibuprofen adsorption in four agricultural volcanic soils. Science of the Total Environment 468–469, 406–414.

Fejér I., Kata M., Erõs I., Dékány I., 2002. Interaction of monovalent cationic drugs with montmorillonite. Colloid Polymer Science 280, 372-379.

Ferk F., Misık M., Hoelzl C., Uhl M., Fuerhacker M., Grillitsch B., Parzefall W., Nersesyan A., Micieta K., Grummt T., Ehrlich V., Knasmuller S., 2007. Benzalkonium chloride (BAC) and dimethyldioctadecyl-ammonium bromide (DDAB), two common quaternary ammonium compounds, cause genotoxic effects in mammalian and plant cells at environmentally relevant concentrations. Mutagenesis 22, 363–370.

Ferrer I., Furlong E.T., 2002. Accelerated solvent extraction followed by on-line solid-phase extraction coupled to ion trap LC/MS/MS for analysis of benzalkonium chlorides in sediment samples. Analytical Chemistry 74, 1275-1280.

Freundlich H., 1906. Über die adsorption in lösungen (adsorption in solution). Journal of Physical Chemistry 57, 384–470.

García M.T., Campos E., Sánchez-Leal J., Comelles F., 2006. Sorption of alkyl benzyl dimethyl ammonium compounds by activated sludge. Journal of Dispersion Science and Technology 27, 739–744.

Gerba C.P., 2015. Quaternary ammonium biocides: Efficacy in application. Applied and Environmental Microbiology 81, 464-469.

Hameed B.H., Mahmoud D.K., Ahmad A.L., 2008. Equilibrium modeling and kinetic studies on the adsorption of basic dye by a low-cost adsorbent: Coconut (Cocos nucifera) bunch waste. Journal of Hazardous Materials 158, 65-72.

Ismail Z.Z., Tezel U., Pavlostathis S.G., 2010. Sorption of quaternary ammonium compounds to municipal sludge. Water research 44, 2303-2313.

Kang H.I., Shin H.S., 2016. Rapid and sensitive determination of benzalkonium chloride biocide residues in soil using liquid chromatography–tandem mass spectrometry after ultrasonically assisted extraction. Bulletin of the Korean Chemical Society 37, 1219–1227.

Khan A.H., Shange J.Q., Alam R., 2012 Ultrasound-assisted extraction for total sulphur measurement in mine tailings. Journal of Hazardous Materials 235-236, 376–383.

Khan A.H., Topp E., Scott A., Sumarah M., Macfie S.M., Ray M.B., 2015**.** Biodegradation of benzalkonium chlorides singly and in mixtures by a *Pseudomonas* sp. isolated from returned activated sludge. Journal of Hazardous Materials 299, 595–602.

Khan A.H., Winnick D., Libby M., Sumarah M., Macfie S.M., Ray M.B., 2016. Plant uptake of benzalkonium chlorides in a hydroponic system. 66th Canadian Chemical Engineering Conference (Accepted for oral presentation and to be held on October 2016).

Kümmerer K., Eitel A., Braun U., Hubner P., Daschner F., Mascart G., Milandri M., Reinthaler F., Verhoef J., 1997. Analysis of benzalkonium chloride in the effluent from European hospitals by solid-phase extraction and high-performance liquid chromatography with post-column ion-pairing and fluorescence detection. Journal of Chromatography A 774, 281–286.

Langmuir I., 1916. The constitution and fundamental properties of solids and liquids, Part 1 solids. Journal of American Chemical Society 38, 2221–2295.

Li X., Brownawell B.J., 2009. Analysis of quaternary ammonium compounds in estuarine sediments by LC-ToF-MS: very high positive mass defects of alkylamine ions as

powerful diagnostic tools for identification and structural elucidation. Analytical Chemistry 81, 7926–7935.

Li X., Luo X., Mai B., Liu J., Chen L., Lin S., 2014. Occurrence of quaternary ammonium compounds (QACs) and their application as a tracer for sewage derived pollution in urban estuarine sediments. Environmental Pollution 185, 127-133.

Martínez-Carballo E., González-Barreiro C., Sitka A., Kreuzinger N., Scharf S., Gans O., 2007. Determination of selected quaternary ammonium compounds by liquid chromatography with mass spectrometry. Part II. Application to sediment and sludge samples in Austria. Environmental Pollution 146, 543-547.

OECD, 2004. Guideline for testing of chemicals. Leaching in soil columns, Paris.

Rabølle M., and Spliid N.H., 2000. Sorption and mobility of metronidazole, olaquindox, oxytetracycline and tylosin in soil. Chemosphere 40, 715-722.

Sarkar B., Megharaj M., Xi Y., Krishnamurti G.S.R., Naidu R., 2010. Sorption of quaternary ammonium compounds in soils: Implications to the soil microbial activities. Journal of Hazardous Materials 184, 448–456.

Schumacher B.A., 2002. Methods for the determination of the total organic carbon (TOC) in soils and sediments. U.S. Environmental Protection Agency, Washington DC.

Tezel U., 2009. Fate and effect of quaternary ammonium compounds in biological systems. (https://smartech.gatech.edu/handle/1853/28229; accessed September, 2016)

Tezel U., Pavlostathis S.G., 2009. Transformation of benzalkonium chloride under nitrate reducing conditions. Environmental Science and Technology 43, 1342–1348.

Tezvergil-Mutluaya A., Mutluaya M.M., Gub L., Zhangb K., Ageec K.A., Carvalhod R.M., Mansoe A., Carrilhof M., Tayg F.R., Breschih L., Suhe B., Pashleyc D.H., 2011. The anti-MMP activity of benzalkonium chloride. Journal of Dentistry 39, 57-64.

United States Environmental Protection Agency (EPA739-R-06-009), August 2006. Reregistration eligibility decision for alkyl dimethyl benzyl ammonium chloride (ADBAC). (https://archive.epa.gov/pesticides/reregistration/web/html/index-9.html; accessed September, 2016)

Xu J., Wu L., Chang A.C., 2009. Degradation and adsorption of selected pharmaceuticals and personal care products (PPCPs) in agricultural soils. Chemosphere 77, 1299–1305.

Yamamoto H., Nakamura Y., Moriguchi S., Nakamura Y., Honda Y., Tamura I., Hirata Y., Hayashi A., Sekizawa J., 2009. Persistence and partitioning of eight selected pharmaceuticals in the aquatic environment: laboratory photolysis, biodegradation, and sorption experiments. Water Research 43, 351–362.

Zanini G.P., Ovesen R.G., Hansen H.C.B., Strobel B.W., 2013. Adsorption of the disinfectant benzalkonium chloride on montmorillonite. Synergistic effect in mixture of molecules with different chain lengths. Journal of Environmental Management 128, 100–105.

Chapter 5

Uptake and Phytotoxic Effect of Benzalkonium chlorides in *Lepidium Sativum* and *Lactuca Sativa* in a Hydroponic System

[A revised version of this chapter is submitted; Khan et al., 2016. Journal of Environmental Pollution]

5.1 Introduction

Increasing scarcity of fresh water in many parts of the world, due to climate change, and overuse due to urbanization and industrialization, has necessitated recycling water from various effluents. Adequately treated large volumes of municipal wastewater can be used for many purposes, such as irrigation of agricultural land, parks and playgrounds (Bixio et al., 2006; Exall, 2004), and industrial applications. In the United States, approximately 8% of the total generated wastewater has been reused/reclaimed for agricultural and landscaping irrigation, groundwater recharge, etc. (Miller 2006). In southern Europe, 44% of agricultural projects were irrigated with reclaimed wastewater compared to 51% of the environmental projects in northern Europe (Bixio et al., 2006). However, the widespread presence of organic compounds such as pharmaceuticals and personal care products in water after conventional wastewater treatment has been reported all across the world (Gros et al., 2010; Clara et al., 2007). As a result, it is possible that organic pollutants in reclaimed wastewater used for irrigation can be taken up by plants. There may be potential risks that consumers are exposed to due to the uptake of these compounds through food crops.

Benzalkonium chlorides (BACs) are a type of cationic surfactant and represent a subset of quaternary ammonium compounds with long alkyl chains of C_8 to C_{18} (Zhang et al., 2011). The two commonly used BACs are benzyl dimethyl dodecyl ammonium chloride (BDDA; alkyl chain with 12 C atoms) and benzyl dimethyl tetradecyl ammonium chloride (BDTA; alkyl chain with 14 C atoms). Many domestic, agricultural and healthcare applications use BACs as a surfactant and/or a biocide (Gerba, 2015) and the compounds eventually end up in wastewater treatment plants (Ismail et al., 2010). Up to 6.03 mg L^{-1} BACs are found in hospital effluents in several European countries (Kümmerer et al., 1997). During wastewater

treatment processes, a fraction of BACs is removed by biodegradation in combination with adsorption on sewage sludge and the rest is discharged in the effluent. For example, a maximum of 0.002 mg L^{-1} of total BACs was measured in the effluent of a wastewater treatment plant in Austria even though a high concentration (0.31 mg L^{-1}) of BACs was found in the influent (Clara et al., 2007). Conversely, a high concentration of 9.0 mg kg^{-1} (dry weight) BACs was measured in sewage sludge in Austria (Martínez-Carballo et al., 2007), indicating the potential for BACs to accumulate in sludge. Higher concentrations of BACs could be in the reclaimed wastewater in places where the wastewater treatment facilities are inadequate, resulting in higher concentration of these compounds entering the natural environment. BACs are generally biodegradable; however, biodegradation is inhibited when BACs are present in a mixture (Khan et al., 2015). Additionally, most of the commercial products use multiple BACs in their formulation, thereby increasing the probability of discharge of a mixture of BACs rather than an individual compound in an effluent.

There is ample evidence of the presence of BACs in the natural environment. For instance, 1.1 mg kg^{-1} of BACs was found in river sediments in China (Li et al., 2014), 5 to 30 mg L^{-1} was recorded in roof runoff immediately after repair in France, which dropped to 4 µg L^{-1} after 640 mm of rainfall (Gromaire et al., 2015); and 0.005 to 28.5 mg kg^{-1} was measured in soil near a cattle farm and migratory bird habitat in Korea (Kang and Shin, 2016). The toxicity of BACs has been reported for various living organisms. For examples, a concentration of 1.0 mg L^{-1} BACs was genotoxic to eukaryotic cells (Ferk et al., 2007), an LC_{50} of 5.9 µg L^{-1} was reported for acute exposure of aquatic invertebrates (USEPA, 2006), and the EC_{50} of BACs for a natural assemblage of algae in sea water was 36.4 µg L^{-1} in 24 h and 63.9 µg L^{-1} in 72 h (Pérez et al., 2009).

Uptake of organic pollutants (e.g., pharmaceuticals and personal care products) by various vegetable crop plants has been reported (Calderón-Preciado et al., 2012; Tanoue et al., 2012; Dodgen et al., 2013; Wu et al., 2013; Mathews et al., 2014). These studies indicate that even in field conditions, exposure to various micropollutants is possible by way of the consumption of crops grown on soils contaminated either by wastewater irrigation or by biosolids amendment. Wu et al. (2013) reported the uptake of 16 different organic pollutants

by four crop plants (lettuce, spinach, cucumber and pepper) in a hydroponic system. Physical properties such as molecular weight, solubility, and octanol-water coefficient dictate the bioavailability of the pollutants from soils. All of the compounds were found in roots and many of them were found in leaves, including atorvastatin (a lipid-lowering drug with a molecular weight of 558.64 g mol^{-1}).

Benzalkonium chlorides with molecular weights around 300 Dalton (BDDA and BDTA are 339.99 and 368.04 g mol^{-1}, respectively) and with solubility (greater than 5 x 10^5 mg L^{-1} for both compounds) have the potential to be taken up from soil by plant roots. To the best of our knowledge, uptake of BACs by plants has not yet been published in literature. Warren (2013) reported that wheat (*Triticum aestivum*) and banksia (*Banksia oblongifolia*) grown in hydroponic culture were capable of taking up natural quaternary ammonium compounds (QACs) (betaine, carnitine and acetyl-carnitine) with molecular weights less than 250 Dalton, and using them as a source of nitrogen. Therefore, the objective of this study was to evaluate the uptake potential and possible phytotoxicity of two BACs in two plant species that are usually consumed raw: lettuce (*Lactuca sativa* L.) and garden cress (*Lepidium sativum* L.). Lettuce has lower lipid content (0.15% by weight) and higher leaf surface area compared to garden cress (lipid content approximately 0.7% by weight) (United States Department of Agriculture (USDA) Food Composition Databases). The two species might, therefore, interact differently with BACs, which have both hydrophobic (alkyl chain) and hydrophilic (positive charge) characteristics. Phytotoxicity of the test BACs was assessed at three stages of plant development: germination, seedling emergence and during vegetative growth. The effect of BACs on macro and micronutrient content of roots and shoots was also investigated.

5.2 Materials and methods

5.2.1 Germination and emerging seedling experiment

Lettuce (*Lactuca sativa*) and garden cress (*Lepidium sativum*) seeds were purchased from the Ontario Seed Company Ltd. (Kitchener, ON Canada) and were stored in a sealed container in a refrigerator (4°C) before use. To study the toxic effect of BACs, benzyl dimethyl dodecyl ammonium chloride (BDDA) and benzyl dimethyl tetradecyl ammonium chloride

(BDTA) with purity ≥ 99.0% were purchased from Sigma-Aldrich (St. Louis, MO, USA) as certified reference materials.

Twenty seeds of garden cress or lettuce were spread over filter paper (VWR 314) placed in a Petri dish, and the filter paper was moistened with 7 mL of 0, 0.5, 1, 3, 5, 10, 25, 50 or 100 mg L^{-1} of BDDA or BDTA individually, and a 2:1 solution of BDDA:BDTA prepared in reverse osmosis (RO) water, using 3 replicate Petri dishes per treatment. The 10 mg L^{-1} of 2:1 BDDA:BDTA mixed BAC solution contained 6.67 and 3.33 mg L^{-1} of BDDA and BDTA, respectively. This ratio was chosen because the environmental ratio of BDDA:BDTA typically is between 1.5:1 and 2.1:1 (Clara et al., 2007). The Petri dishes were placed in a controlled environment chamber maintained at a 16 h day (photon flux = 205±10 µmol m^{-2} s^{-1}) at 20°C and an 8 h night at 16°C, and constant 60% relative humidity. Percentage germination was measured after 24 h and the emergent seedling length, from radicle tip to end of the emerging cotyledon, was measured after 65 h.

5.2.2 Phytotoxicity of BACs to seedlings

To evaluate the toxic effect of BACs, plants were grown in nutrient solutions that were dosed with BACs. For these experiments, seeds of both plants were germinated as described in section 5.2.1 but without any BACs. When the radicle length was 2 to 3 cm, the seedlings were transferred to pots filled with sand that had been saturated with nutrient solution with the following composition: 1.0 mM $Ca(NO_3)_2.4H_2O$, 1.0 mM K_2HPO_4, 0.4 mM KNO_3, 0.3 mM $Mg(NO_3)_2.6H_2O$, 0.3 mM NH_4NO_3, 0.1 mM K_2SO_4, 10.0 µM $FeCl_3.6H_2O$, 10.0 µM Na_2EDTA, 6.0 µM H_3BO_3, 2.0 µM $MnCl_2.4H_2O$, 0.5 µM $ZnSO_4.7H_2O$, 0.15 µM $CuSO_4.5H_2O$ and 0.1 µM Na_2MoO_4 adjusted to pH 6 (Akhter et al., 2012). Hydroponic nutrient solutions were prepared using reverse osmosis (RO) water. The sand was kept moist with RO water until the shoot length was approximately 4 cm, at which point pairs of seedlings of the same species were transferred to glass jars containing 100 mL nutrient solution. The seedlings were suspended over the solution by a piece of foam.

When the shoots were approximately 7 cm, each seedling pair was transferred to a jar containing 1.4 L of nutrient solution to which environmentally relevant concentrations of

BACs were added: 0, 0.025 or 0.25 mg L^{-1} BDDA and BDTA, either as single compounds or in a mixture with a ratio of 2:1 BDDA:BDTA with 6 replicate jars per treatment. Custom made lids were used to support the seedlings. A control jar (BACs in nutrient solution but without any plants) was included to determine the amount of BACs lost due to adsorption on the container wall. Solutions were aerated using air pumps (TopFinAir 8000) connected to plastic tubing. Each jar was covered with aluminum foil to prevent algal growth in the solution. The volume of solution in each jar was maintained daily using RO water and after 6 d of growth, nutrient solutions were replenished with another dose of $Ca(NO_3)_2.4H_2O$, K_2HPO_4, KNO_3, $Mg(NO_3)_2.6H_2O$, NH_4NO_3, and K_2SO_4 to avoid nutrient deficiency.

Garden cress and lettuce were harvested after 12 d of BAC treatment. Roots were rinsed with RO water then soaked for 30 min in 10 mM $CaCl_2$ solution to desorb any possible BACs on the root surface (Akhter et al., 2012). The shoots were separated from the roots and the tissues were dried to constant mass at 60°C.

5.2.2.1 Macro and micronutrient analysis in plant tissues

Plants were analyzed for five macronutrients (phosphorus, P; potassium, K; calcium, Ca; sulfur, S; and magnesium, Mg) and 6 micronutrients (boron, B; manganese, Mn; iron, Fe; zinc, Zn; molybdenum, Mo; and copper, Cu). Plant tissues were digested following the methods of Akhter et al. (2012) prior to ICP-MS (Inductively coupled plasma-mass spectroscopy) analysis.

Oven-dried plant samples were chopped and ground to 1 mm using a mortar and pestle, and about 0.1 g sample was placed in a 15 mL glass digestion tube with 1 mL OmniTrace® (EM Science, USA) pure nitric acid, and covered with a glass marble. Samples were digested overnight at room temperature. The following day, samples were heated to 103°C on a hot plate until acid digestion was complete. After digestion, samples were cooled to room temperature and each sample was filtered into a 25 mL Falcon tube through a VWR 314 filter paper. Standard reference materials (NIST 1573A tomato leaves and NIST 1570A spinach leaves) were purchased from the National Institute of Standards and Technology (Gaithersburg, MD, USA) and similarly processed to determine the digestion efficiency. The

samples were topped up to 25 mL with RO water and sent to ALS Environmental (London, ON, Canada) for ICP-MS analysis. The limits of quantification (LOQ) for the nutrient elements are presented in Table 5.1.

Nitrogen (N) was analyzed using a LECO CNS-2000 analyzer (LECO, U.S.A.). Dry plant samples were chopped and ground to 1 mm in the same way as described above and were sent to the Laboratory for Geochemical Analysis in the Department of Earth Sciences, University of Western Ontario.

Table 5.1 Limit of quantification (LOQ) for analyzed elements using ICP-MS.

Element	**LOQ (mg L^{-1})**
Boron (B)	0.1
Calcium (Ca)	5
Copper (Cu)	0.01
Iron (Fe)	0.5
Magnesium (Mg)	0.5
Manganese (Mn)	0.005
Molybdenum (Mo)	0.0005
Phosphorus (P)	0.5
Potassium (K)	0.5
Sulfur (S)	5
Zinc (Zn)	0.03

5.2.3 Extraction and detection of BACs from plant tissue

Higher doses of BACs (BDDA at 5 mg L^{-1} and BDDA+BDTA mixture at 5+2.5 mg L^{-1}) were introduced in a hydroponic system to determine if they could be taken up and translocated by lettuce and garden cress. With the exception of the BAC doses, plants were sown and grown as described in section 5.2.2.

After harvest, the extraction of BACs from plant tissues (roots and shoots) was conducted following the method described by Díez et al. (2016) with minor modifications. Due to the variation in mass, the plant dry mass was divided into two parts; specifically, 3 to 7 g (approximate mass of control plants' parts without BACs) and 0.05 to 1 g (approximate mass of plant parts treated with BACs at 5 and 7.5 mg L^{-1}). First, the plants were separated into roots and shoots, and each sample was ground in liquid nitrogen using a mortar and pestle, then transferred into a 50 mL polypropylene centrifuge tube. Afterwards, 10 mL or 5 mL of acidic acetonitrile (acetonitrile with 1% pure acetic acid) were added to control and treated samples, respectively. Samples were mixed manually for 1 min and then placed in a horizontal shaker for 10 min. Afterwards, 3.75 g and 1 g QuEChERS extraction salts (Q-salt) reagent was added in control samples and for treated samples, respectively, and the tubes were shaken for another 2 min. The Q-salt were purchased from Restek Pure Chromatography (http://www.restek.com/), Restek Corporation, U.S.A., for the extraction of BACs from plant tissues. The mixture was then centrifuged at 3700 rpm for 5 min in order to obtain good phase separation. The supernatant was collected and transferred into Turbo-Vap vials to dry in a nitrogen-enriched atmosphere (45°C at 15 psi). After drying, samples in the Turbo-Vap vials were made up to 2 mL volume using Milli-Q water and were filtered through a 0.2 µm PTFE (polytetrafluoroethylene) syringe filter into a 2 mL HPLC vials for HPLC-MS analysis.

An HPLC-MS (Q-Exactive Orbitrap by Thermo Scientific) equipped with an Agilent Eclipse plus C-18 RRHD column (1.8 µm pore size, 50 mm length x 2.1 mm internal diameter) was used at a solvent flow rate of 0.3 mL min^{-1} and an injection volume of 2 µL. The solvent gradient started with ≈100% H_2O (0.1 % formic acid) for 0 to 0.5 min and increased to ≈100% acetonitrile (0.1% formic acid) over 3.5 min. The organic mobile phase was then held at 100%

for 1.5 min before returning to 0% over 30 s and returned to 100% H_2O (0.1 % formic acid). A top 3, data-dependent tandem MS ($ddMS^2$) analysis combined with a parallel reaction monitoring (PRM) was performed in positive ion mode. The full MS scans were performed at a resolution of 35,000 and AGC target of 3×10^6. The $ddMS^2$ and PRM scans were performed at a resolution of 17,500 and AGC target of 5×10^5. The spray voltage was held at 3.9 kV, the S-lens at 45 V and the sheath and auxiliary gas were set to 17 and 8 arbitrary units, respectively. The probe temperature and capillary temperature were 450°C and 400°C, respectively. The limit of quantification (LOQ) for BDDA and BDTA was determined to be 10 ppb (or 10 μg L^{-1}) and the limit of detection was an order of magnitude lower (1 ppb) for both of the compounds, with $r^2 > 0.999$ for each standard curve. Retention times for BDDA and BDTA were 3.51±0.01 and 3.72±0.02 min, respectively. The data were analyzed with Xcalibur™. The relative quantities of BACs in the various plant parts were estimated using the peak areas of the chromatograms from plant samples and the corresponding BAC peak areas were obtained using standards.

5.2.3.1 BACs remaining in solution

In order to close the mass balance, a few samples dosed with higher (due to the limitation of detection limit in a HPLC-UV as described below) concentrations of BACs (BDDA alone at 5 mg L^{-1} and BDDA+BDTA at 7.5 mg L^{-1}) were analyzed to determine the remaining BACs in nutrient solutions after harvesting. However, individual BDTA at higher dose was not examined.

After the plant uptake experiment, nutrient solutions were analyzed for the remaining BACs using high performance liquid chromatography (HPLC) coupled with a diode array UV-Vis detector (Dionex ICS-3000, USA). The method used in the HPLC-UV analysis was adopted from our previous study (Khan et al., 2015), with minor modifications: the isocratic solvent flow rate was 0.8 mL min^{-1} and the injection volume was 100 μL. The retention times for BDDA and BDTA were 7.3±0.1 and 8.1±0.2 min, respectively, and the r^2 values for the standard curves were greater than 0.99 for both compounds. The limit of quantification (LOQ) and limit of detection (LOD) for the BACs were determined to be 3.0 and 2.0 mg L^{-1},

respectively, for both compounds. The mobile phase used in the HPLC-UV separation was prepared by mixing (HPLC) grade acetonitrile (CAN) purchased from Caledon Chemicals (Georgetown, ON, Canada). HPLC grade (98.3%) ammonium acetate (40 mM) (Fisher Chemical, New Jersey, USA) was used to prepare buffer solution and was used at a ratio of 60:40 (acetonitrile: buffer). The pH of the mobile phase was adjusted to 5 using phosphoric acid (85%), which was purchased from Caledon Laboratories Ltd, (ON, Canada). Milli-Q water (conductivity 18 MΩ.cm, Millipore water systems, Integral-5, France) was used for experimentation using HPLC-UV and for sample preparation for analysis using HPLC-MS (HPLC connected to a mass-spectroscopy detector).

Nutrient solutions dosed with 5 and 7.5 mg L^{-1} BDDA were analyzed for the remaining BDDA. The initial dose of BDTA was 2.5 mg L^{-1} (below LOQ) in the BACs mixture and was not quantified. Nutrient solutions were analyzed at time zero and at the time of harvest. A 5 mL solution from each test jar was collected, filtered through a 0.2 µm syringe filter (Pall Corporation, MI, USA) and preserved at –20°C until analysis using HPLC-UV.

5.2.4 Statistical analysis

The effects of BACs on germination, seedling length, plant biomass and nutrient concentrations were assessed using two-way ANOVA, followed by post hoc Tukey tests in cases where ANOVA detected significant (p <0.05) main effects. Statistical analysis was performed using SigmaPlot (version 12.5).

5.3 Results and discussion

5.3.1 Germination and emerging seedlings

Germination of both species was unaffected by both BACs, alone or in mixture, and varied between 98-100% (two-way ANOVA, *p>0.05;* data not shown). Plant seed coats create a barrier between a plant embryo and the culture medium and protect the embryos from contamination until the embryonic roots start to develop (An et al., 2009). The experimental results suggest that BACs were either unable to permeate the seed coat or may have been adsorbed on the seed surface due to their positive charge. A similar nontoxic effect was

observed for the germination of wheat (*Triticum aestivum* L.) when treated with 1000 mg L^{-1} paracetamol (an analgesic and antipyretic drug) (An et al., 2009). However, surfactant-mediated inhibition of the germination of zucchini (*Cucurbita pepo*) seeds was found when 0.2% sodium dodecyl sulphate (an anionic surfactant) was tested (Stampoulis et al., 2009), which was attributed to the ability of surfactants to emulsify cell membranes and other lipid-containing cellular constituents. In this study, the concentration of the BACs used was significantly lower than that of Stampoulis et al. (2009).

Toxic effects of BACs on the emergent seedling increased with the increasing concentration of BACs as measured by the lengths of emerging seedlings of both plants. Significant reductions in seedling length were seen at concentrations ≥ 3.0 mg L^{-1} for lettuce (Fig 5.1a) and ≥ 10.0 mg L^{-1} for garden cress (Fig 5.1b). Seedling lengths were approximately 50% of control length at 10 mg L^{-1} and 25 mg L^{-1} BACs for lettuce and garden cress, respectively, with one exception: garden cress was more resilient to BDTA and the seedling length was inhibited by 50% only when the concentration of BDTA was ≥ 100 mg L^{-1} (Fig 5.1b). Although, BDTA with longer alkyl chain was found to be more toxic to a pure strain of bacterium (Khan et al., 2015), this was not the case for these two species of plants.

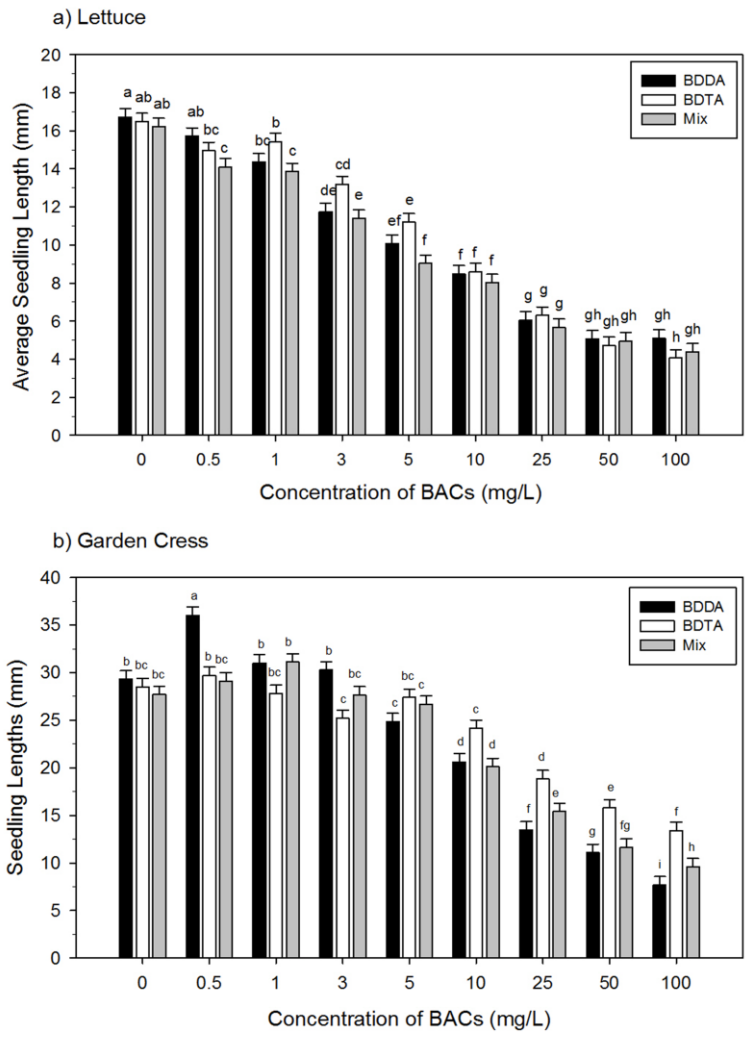

Fig 5.1 Length of emerging seedlings. (a) lettuce and (b) garden cress grown in various concentrations of BACs, individually and in mixture (2:1 BDDA:BDTA). Error bars are standard error of the mean (n=3). Within each species, different lower case letters indicate significant differences in seedling length among the BAC treatments, which was determined by two-way ANOVA and post hoc Tukey tests (p <0.05).

5.3.2 Toxic effect on plant growth

Plants grown in environmentally relevant concentrations of BACs (0.25 or 0.025 mg L^{-1}) were used to determine the plants' tolerance for BACs (Fig 5.2). Lettuce shoot (Fig 5.2a), garden cress root and shoot (Fig 5.2e and 5.2d) were unaffected by 0.025 mg L^{-1} of BACs. However, with 0.25 mg L^{-1} of BACs in solution, the dry mass was 50 to 85% smaller than that of control in both tissues of both plant species (Fig 5.2). On the other hand, dry mass of lettuce root was 25% of that of the control at 0.025 mg L^{-1} of BACs (Fig 5.2b). The experimental results clearly demonstrate that lettuce is more sensitive to BACs than garden cress, at least in hydroponic solution.

The shoot to root dry weight ratio was calculated to determine the sensitivity of plant parts to BACs. Lettuce root was more sensitive compared to shoot (Fig 5.2c) but no tissue-specific sensitivity was observed for garden cress at either concentration of BACs (0.025 and 0.25 mg L^{-1}) (Fig 5.2f). It is interesting to note that the inhibition effect seemed to be slightly more due to BDDA (except in lettuce shoot, Fig 5.2a, at 0.025 mg L^{-1}) than BDTA (Fig 5.2). Such an effect is opposite to what was observed in our previous study on the biodegradation of BACs (Khan et al., 2015); BDTA, with longer alkyl chain, was found to be more toxic than shorter chain BDDA to a pure strain of *Pseudomonas* sp. In this study, due to its lower molecular weight and shorter chain, it might have been easier for the root to take up BDDA compared to BDTA.

Dry mass of dwarf wheat (*Triticum aestivum*) was also reduced by 20 to 25% in the presence of amphoteric (cocamidopropyl betaine) and non-ionic (alcohol polyethoxylate) surfactants at 1.3 and 8 mg L^{-1}, respectively (Garland et al., 2004). Shoot and root weight inhibition from 60 to 85% was also reported for alfalfa (*Medicago sativa* L.) grown in a hydroponic solution dosed with 0.05 mM (approximately 42 mg L^{-1}) or higher oxytetracycline (an antibiotic) (Kong et al., 2007). A possible explanation for this was given by Jing et al. (2012); the positive charge on the nitrogen of the cationic surfactants (such as BACs) damage the living cells by interacting with the negatively charged cytoplasmic membrane, followed by the penetration of the non-polar alkyl chain. By doing so, the negative charges of the

membrane are neutralized and, at the same time, the interaction between lipid components of the cells with hydrophobic alkyl chain changes the fluid circulation inside cell structure.

The toxic effect of BACs was more pronounced for older seedlings for both plant species. About 50% of growth inhibition occurred at 0.25 mg L^{-1} of BACs in both plants (Fig 5.2) but for the same rate of inhibition in the emergent seedling required dosages of 10 and 25 mg L^{-1} of BACs for lettuce and garden cress (Fig 5.1), respectively. These results suggest that BACs might be affecting the metabolic process of plants and are more harmful during the vegetative stage for both lettuce and garden cress rather than their seedling stage. However, the effect of BACs on emergent seedlings could be more profound with longer exposure time than conducted in this experiment.

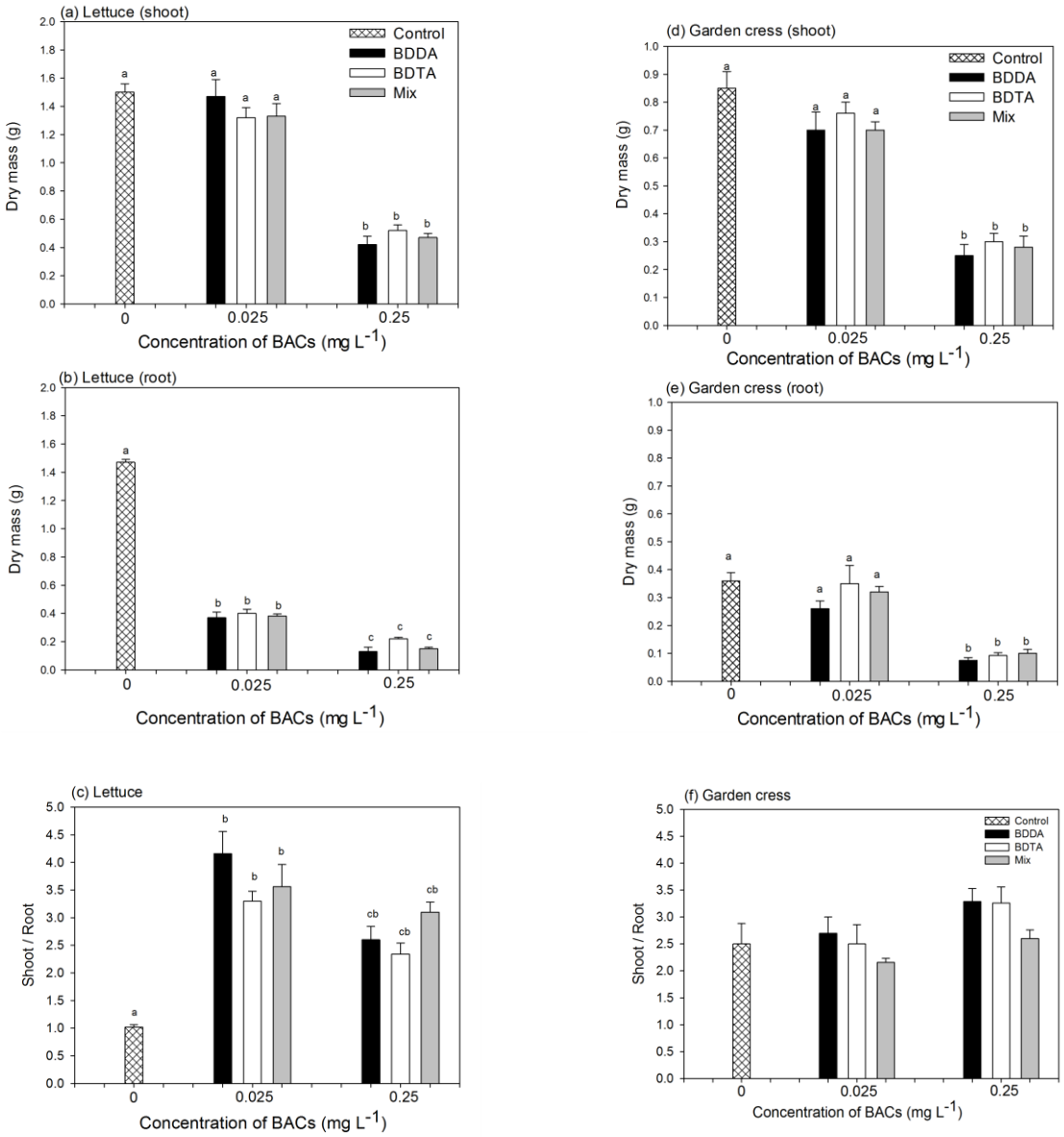

Fig 5.2 Dry mass of lettuce (a,b,c) and garden cress (d,e,f) exposed to BDDA and/or BDTA. Plants were grown hydroponically for 12 d with 0, 0.025 or 0.25 mg L^{-1} BACs, individually and in mixture. Dry mass of shoots (a, d) and roots (b, e) and the shoot: root ratios (c, f) are shown. Error bars are standard error of the mean (n=6). Within each panel different lower case letters indicate significant differences in dry mass (two-way ANOVA and post hoc Tukey tests; p <0.05). Absence of any lower case letters indicates no significant difference among the treatment conditions.

5.3.3 Nutrient analysis in plants

Macro- and micronutrient contents in roots and shoots of lettuce and garden cress are presented in Fig 5.3 and Fig 5.4a to 5.4d, where Fig 5.3 shows the results of N and Mg analysis and the results for other nutrients are presented in Fig 5.4a to 5.4d. Nitrogen concentrations in lettuce shoot (Fig 5.3a) in plants treated with 0.25 mg L^{-1} were 50% lower than that in control plants; on the other hand, N concentration did not vary with BAC treatment in lettuce roots (Fig 5.3b) or either tissue of garden cress (Fig 5.3e and 5.3f). Magnesium concentrations in lettuce shoot and root decline in BAC-treated plants (Fig 5.3c and 5.3d) compared to control plants, and was unaffected by BAC treatment in garden cress (Fig 5.3g and 5.3h). Other than N and Mg, no evidence of possible deficiency was observed for any other nutrients (Fig 5.4a to 5.4d). Conversely, the concentrations of several other nutrients increased in response to 0.025 and/or 0.25 mg L^{-1} BACs. For example, in lettuce shoot, Mo concentration increased, by about 50% at both concentrations of BACs (Fig 5.4a); however, in lettuce root, significant increase was observed for Fe 50%;, P 30%; K 40%; Zn 50% at 0.25 mg L^{-1} of BACs (Fig 5.4b). On the other hand, no significant increase was found for garden cress shoot for any of the macro or micro nutrient content (Fig 5.4c) but in garden cress root, Cu, Fe, Mo, P, K, and S increased significantly at 0.25 mg L^{-1} of BACs (Fig 5.4d). However, most of the concentrations were not high enough to suspect BAC-induced nutrient toxicity. The only exception might be Fe, which increased by 50% in roots of both species in response to BACs (Fig 5.4b and 5.4d). Excess Fe can cause oxidative stress in plant tissue (Kampfenkel et al., 1995), which might be an indirect indication of BAC toxicity. The slight increases in uptake of many elements might be due to the dispersing property of surfactants, as one of their inherent characteristics. Enhanced accumulation of certain elements was also observed in response to non-ionic and anionic surfactants in some studies. For example, Cu uptake was enhanced in the root of *Halimione portulacoides* (Almeida et al., 2009). In another study, natural (tea saponin) and anionic surfactants enhanced the uptake of polychlorinated biphenyls and Cd in corn (*Zea mays* L.) and sugarcane (*Saccharum officinarum* L.), respectively (Xia et al., 2009).

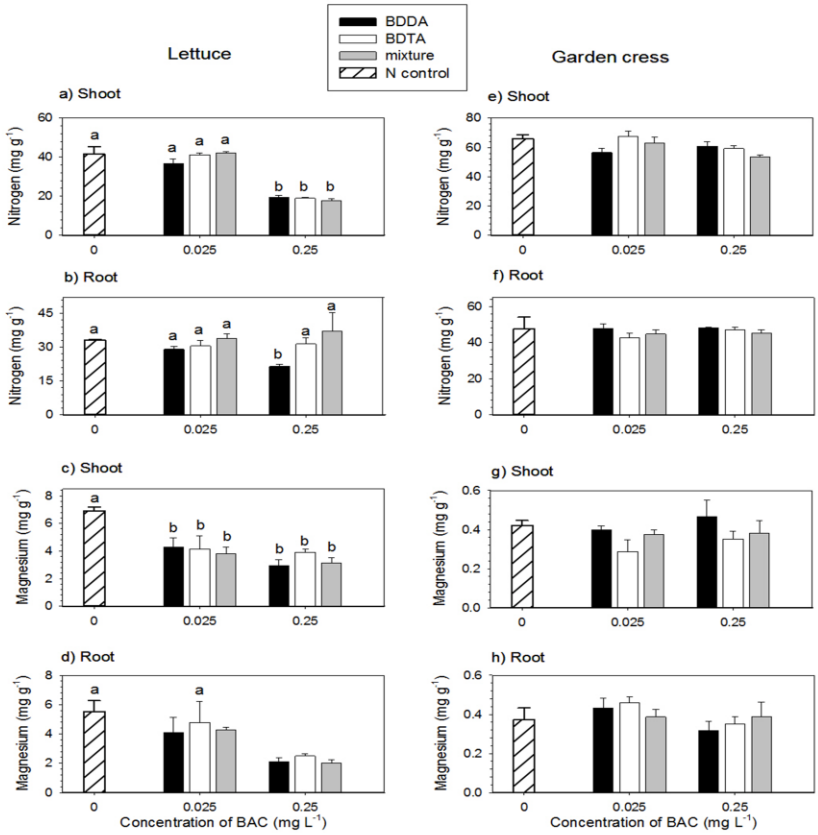

Fig 5.3 N and Mg content of lettuce and garden cress exposed to BDDA and/or BDTA. Plants were grown hydroponically for 12 d with 0, 0.025 or 0.25 mg L^{-1} BACs, individually and in mixture. N content of lettuce and garden cress in shoots (a, e) and roots (b, f); Mg content of lettuce and garden cress in shoots (c, g) and roots (d, h) are shown. Error bars are standard error of the mean (n=3). Within each panel different lower case letters indicate significant differences in N or Mg content (two-way ANOVA and post hoc Tukey tests; p <0.05). Absence of any lower case letters indicates no significant difference among the treatment conditions.

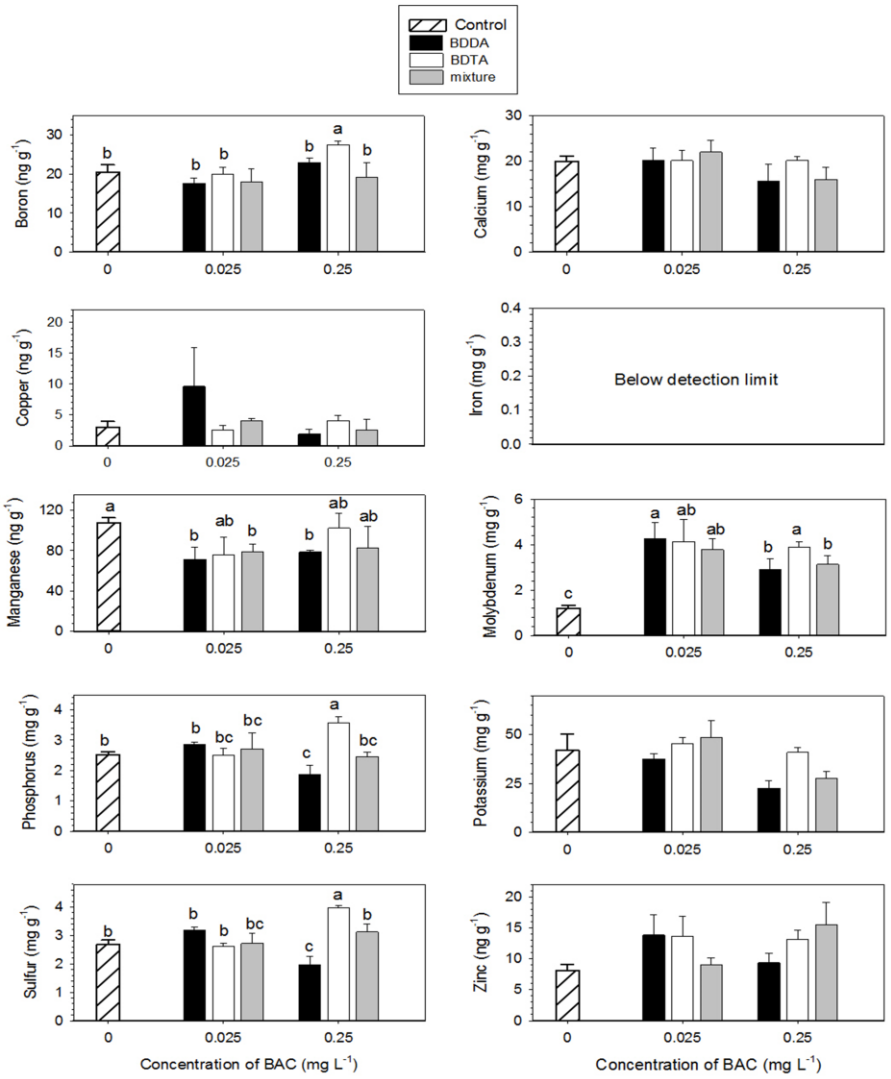

Fig 5.4a Four macronutrients (phosphorus, P; potassium, K; calcium, Ca; and sulfur, S) and 6 micronutrients (boron, B; manganese, Mn; iron, Fe; zinc, Zn; molybdenum, Mo; and copper, Cu) were presented in lettuce shoot exposed to BDDA and/or BDTA. Plants were grown hydroponically for 12 d and treated with 0, 0.025 or 0.25 mg L^{-1} BACs, individually and in mixture. Error bars are standard error of the mean (n=3). Within each panel different lower case letters indicate significant differences in nutrient content (two-way ANOVA and post hoc Tukey tests; p <0.05). Absence of any lower case letters indicates no significant difference among the treatment conditions.

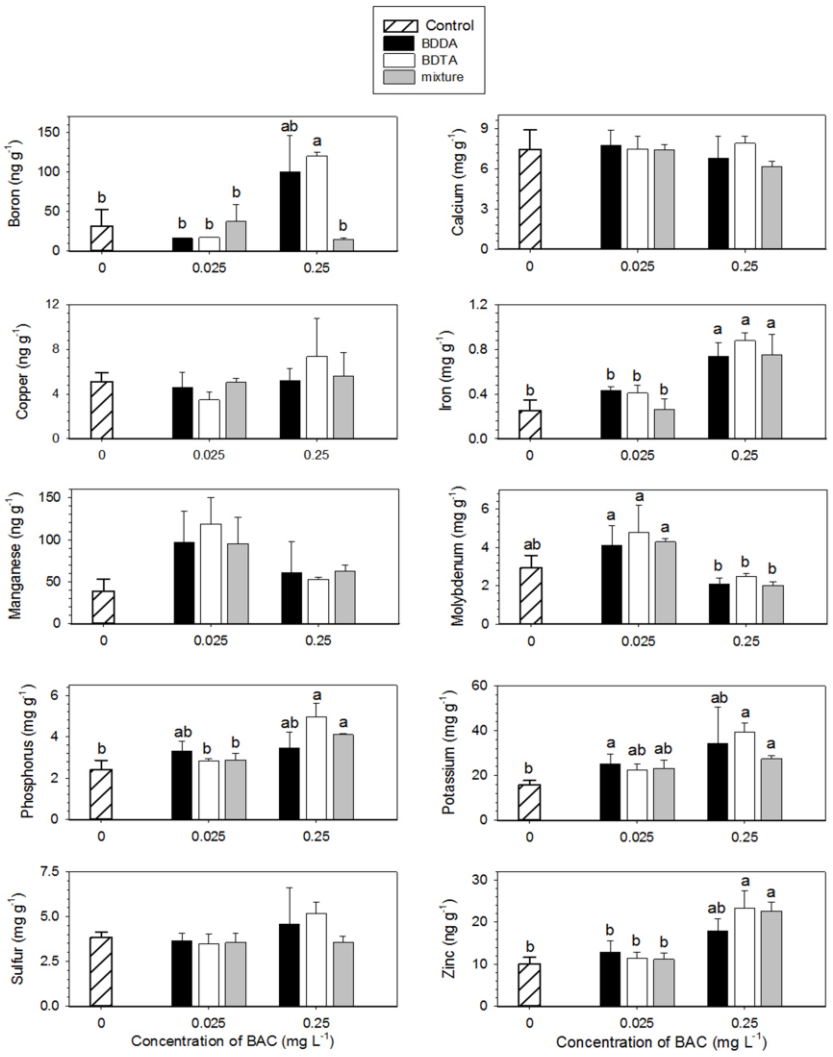

Fig 5.4b Four macronutrients (phosphorus, P; potassium, K; calcium, Ca; and sulfur, S) and 6 micronutrients (boron, B; manganese, Mn; iron, Fe; zinc, Zn; molybdenum, Mo; and copper, Cu) were presented in lettuce root exposed to BDDA and/or BDTA. Plants were grown hydroponically for 12 d and treated with 0, 0.025 or 0.25 mg L^{-1} BACs, individually and in mixture. Error bars are standard error of the mean (n=3). Within each panel different lower case letters indicate significant differences in nutrient content (two-way ANOVA and post hoc Tukey tests; p <0.05). Absence of any lower case letters indicates no significant difference among the treatment conditions.

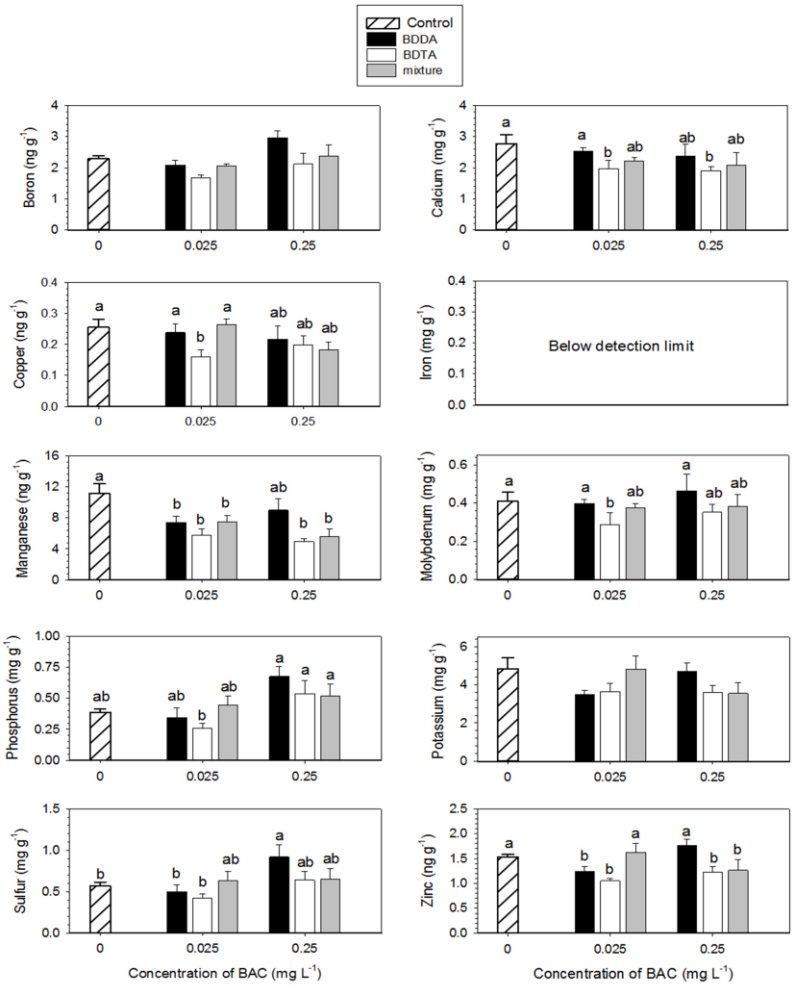

Fig 5.4c Four macronutrients (phosphorus, P; potassium, K; calcium, Ca; and sulfur, S) and 6 micronutrients (boron, B; manganese, Mn; iron, Fe; zinc, Zn; molybdenum, Mo; and copper, Cu) were presented in garden cress shoot exposed to BDDA and/or BDTA. Plants were grown hydroponically for 12 d and treated with 0, 0.025 or 0.25 mg L^{-1} BACs, individually and in mixture. Error bars are standard error of the mean (n=3). Within each panel different lower case letters indicate significant differences in nutrient content (two-way ANOVA and post hoc Tukey tests; p <0.05). Absence of any lower case letters indicates no significant difference among the treatment conditions.

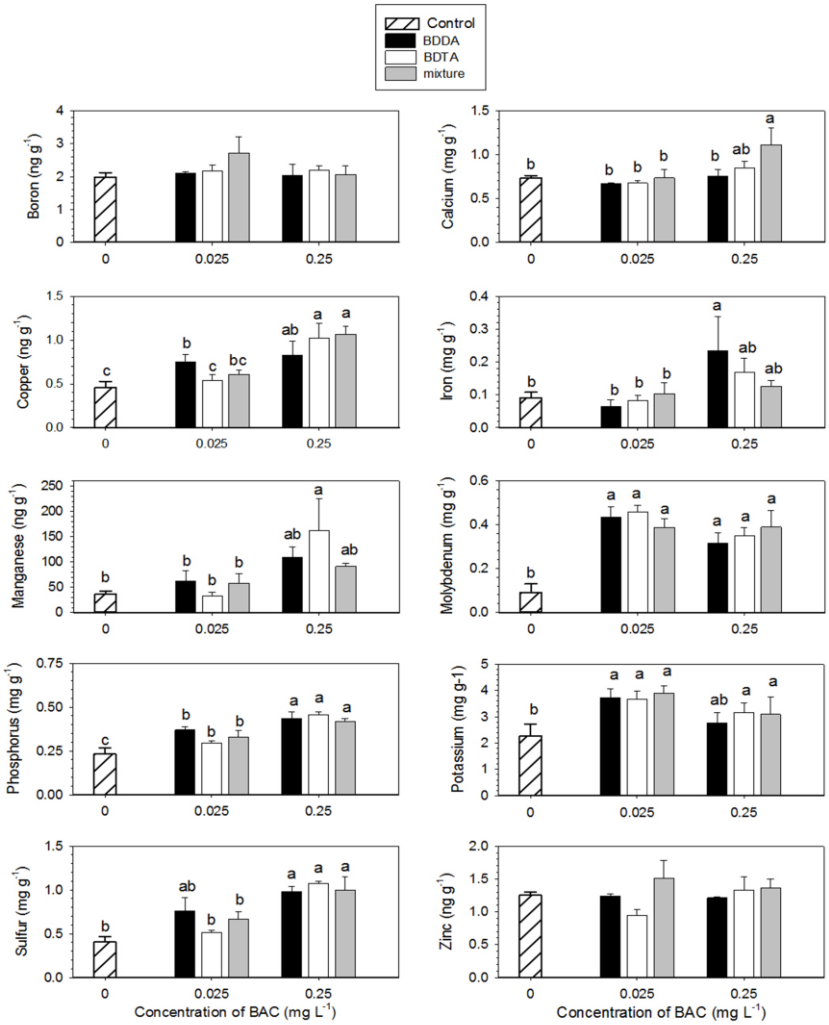

Fig 5.4d Four macronutrients (phosphorus, P; potassium, K; calcium, Ca; and sulfur, S) and 6 micronutrients (boron, B; manganese, Mn; iron, Fe; zinc, Zn; molybdenum, Mo; and copper, Cu) were presented in garden cress root exposed to BDDA and/or BDTA. Plants were grown hydroponically for 12 d and treated with 0, 0.025 or 0.25 mg L^{-1} BACs, individually and in mixture. Error bars are standard error of the mean (n=3). Within each panel different lower case letters indicate significant differences in nutrient content (two-way ANOVA and post hoc Tukey tests; p <0.05). Absence of any lower case letters indicates no significant difference among the treatment conditions.

A number of the visible symptoms of stress observed in BAC-treated lettuce were chlorotic and necrotic older leaves and wilted shoots, which may have been due to N and Mg deficiencies (Salisbury and Ross, 1985). However, similar physical symptoms of stress were seen for BAC-treated garden cress as well, although it had N and Mg concentrations similar to those in control plants. Further work is required to ascertain the mechanisms of BACs induced toxicity and any relationship with the changes in nutrient uptake with the plant stress.

5.3.4 Uptake of BACs by plants

Uptake and translocation of BACs in plants were confirmed and presented in Fig. 5.5. Total ion chromatograms (TIC) of standard BDDA and BDTA along with their fragment ions are presented in (Fig 5.5 a to d). TIC of lettuce for control and treated tissues are presented as, shoot (Fig 5.5e and 5.5g) and root (Fig 5.5f and 5.5h), respectively. Additionally, TIC of garden cress for control and treated tissues are presented as, shoot (Fig 5.5i and 5.5K), and root (Fig 5.5j and 5.5l), respectively.

The chromatograms for the BDDA and BDTA standards (Fig 5.5a and 5.5b) and the corresponding fragment ions (Fig 5.5c and 5.5d) showed the major fragments for BDDA to be (m/z) 91.05, 212.24, and 304.3, and for BDTA to be (m/z) 91.05, 240.27, and 332.33. During extraction and separation of target analytes using an HPLC system, undesired compounds may overlap at the same retention time with the target analytes. As a result, confirmation of target analytes (BACs) in plant tissues was carried out by observing both the indicative mass fragments ions recorded as $ddMS^2$ by parallel reaction monitoring (PRM) and the retention time to the corresponding standards (Wu et al., 2013). The presence of molecules with m/z of 304 and 332 confirms the presence of parent BDDA (Fig 5.5c) and BDTA (Fig 5.5d), respectively. No peaks were detected in control samples at these retention times' 3.51±0.01 min for BDDA and 3.72±0.02 min for BDTA.

Organic pollutants are usually xenobiotic and, as a consequence, plants do not have any membrane transporters for such compounds. However, moderately hydrophobic

compounds (Log K_{ow} 0.5 to 3), such as BACs (Log K_{ow} are 0.59 and 1.67 for BDDA and BDTA, respectively; Tezel, 2009) can attach to the membrane layers and diffuse through the lipid bilayers (Pilon-Smits (2005)). Additionally, after diffusion into the root tissues, the high solubility of BACs might facilitate their translocation into shoot tissues.

The amount of BACs in the various plant parts were estimated and are presented in Table 5.2. Shoots and roots were analyzed separately to confirm the translocation of BACs. Since the dry mass of both species were very low for plants grown at the higher dose of BACs, samples from the three replicates were combined together for analysis (reducing n to 1). The results confirmed that BACs were taken up by the roots of both plant species and eventually translocated into the upper parts of the plants. The concentration of BDDA in the roots was up to 19 times higher in garden cress and 11 times higher in lettuce compared to the corresponding shoots, especially when the BACs were provided as a mixture (Table 5.2). BDTA concentration was also higher in root compared to the shoot; about 19 times higher in garden cress and 7 times higher in lettuce. When comparing the two plant species, the concentrations of BDDA were higher in lettuce and concentrations of BDTA were higher in garden cress. As we have discussed earlier, the shorter chain of BDDA might make it easier to diffuse in plant cells compared to BDTA and growth inhibition of plants was slightly more due to BDDA than BDTA at 0.25 mg L^{-1} of BACs (Fig 5.2). The quantification results of BACs in lettuce root and shoot partially verified this (Table 5.2).

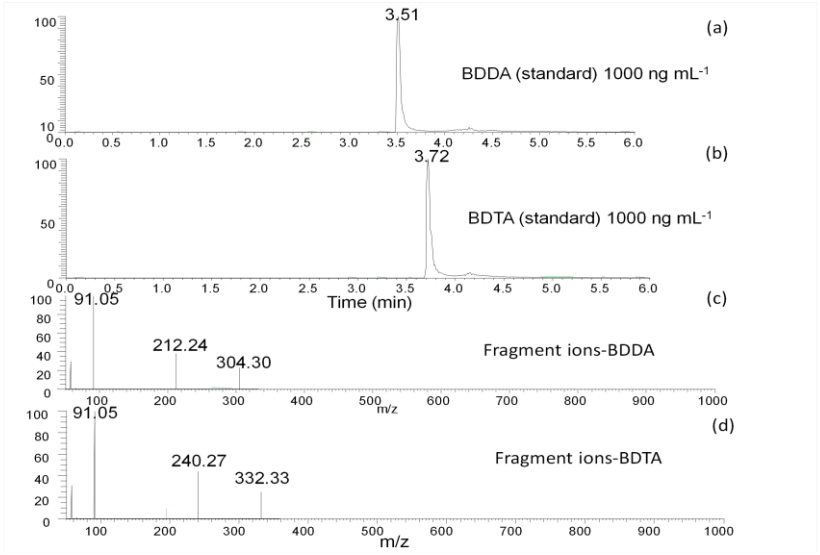

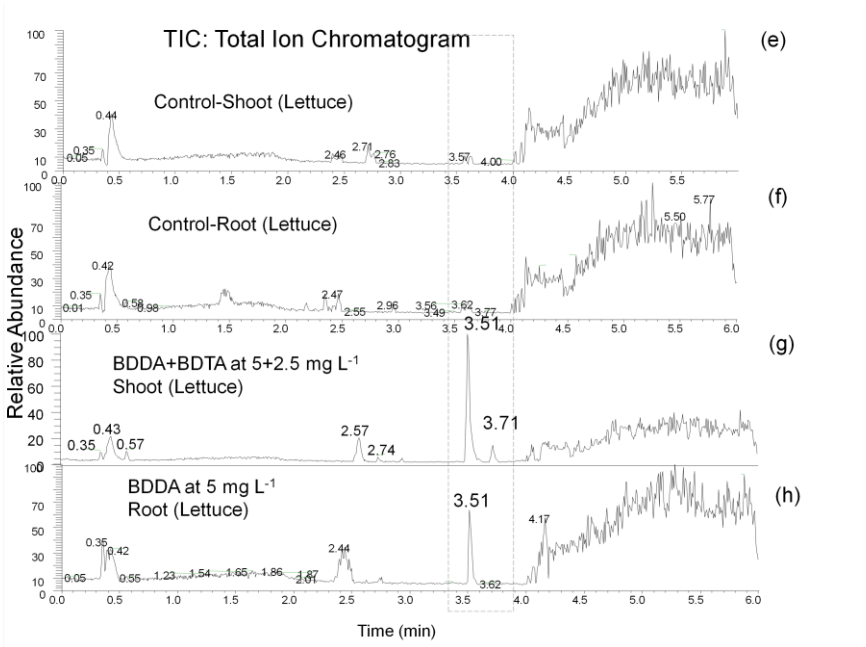

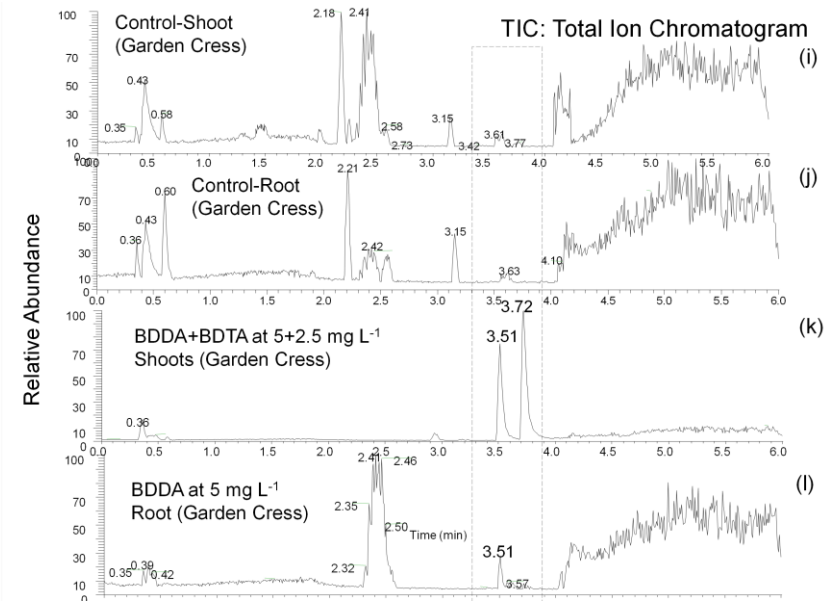

Fig 5.5 Total ion chromatograms of plant tissues (lettuce and garden cress) treated with BACs. Plants were grown hydroponically with 5 mg L^{-1} BDDA or a BDDA:BDTA mixture at 5:2.5 mg L^{-1} and BACs were detected using HPLC-MS. Standards: (a) BDDA, (b) BDTA, (c) fragment ions for BDDA, (d) fragment ions for BDTA; lettuce, where, (e) control shoot, (f) control root, (g) shoot dosed with BDDA:BDTA mixture, (h) root dosed with BDDA; garden cress (i) control shoot, (j) control root, (k) shoot dosed with BDDA:BDTA mixture, and (l) root dosed with BDDA. Rectangle shapes (dotted lines) show the retention times for BDDA and BDTA.

Lipid content in plant roots (tested on five different species, pepper, *Capsicum annuum*; tomato, *Lycopersicon esculentum*; collard, *Brassica oleracea*; lettuce, *Lactuca sativa*; and radish, *Raphanus sativus*) was found to be correlated with the accumulation of the drug carbamazepine (Log K_{ow}, 2.45), which is a moderately hydrophobic compound with a moderate level of solubility (17.7 mg L^{-1}) (Wu et al., 2012). Due to the longer alkyl chain length BDTA is more hydrophobic (Log K_{ow}, 1.67) than BDDA (Log K_{ow}, 0.59), and both compounds are highly soluble in water and exist as a cation in solution (Tezel, 2009). The higher lipid content in garden cress compared to lettuce along with the higher hydrophobicity of BDTA might be the potential reason for higher accumulation of BDTA into the root tissues of garden cress (Table 5.2). Conversely, higher accumulation of BDDA compared to BDTA in lettuce root suggested that smaller molecular structure, and higher solubility (Ismail et al., 2010) of BDDA, along with the lower lipid content in lettuce than garden cress, facilitate the uptake of BDDA. However, BDDA amount was twice higher in garden cress as compared to lettuce when plants were dosed with the mixture of BACs.

The approximate bioconcentration factor (BCF, L kg^{-1}) of BDDA in roots and shoots was calculated as the ratio of BDDA concentration in plant tissue to the concentration in solution at harvest following Wu et al. (2012). The BCF ranged from 3.4 to 110 L kg^{-1} in roots and 1.7 to 5.8 L kg^{-1} in shoots for garden cress, whereas, the BCF was approximately 11 to 49 L kg^{-1} in lettuce root and 4.3 L kg^{-1} in lettuce shoot. BCF of BDTA was not determined because of the concentration of BDTA was below the LOQ in nutrient solution for HPLC-UV. The approximate BCF values determined in this study are comparable to that of many pharmaceuticals and personal care products tested on green vegetables. For example, the BCF of carbamazepine was approximately 10 to 100 L kg^{-1} in both roots and leaves/stems in lettuce grown hydroponically (Wu et al., 2013).

5.3.5 Nutrient solution analysis for BACs

Negligible adsorprtion of BACs on the container wall occurred and the majority of the total BACs remained in solution. The initial concentration of BDTA in solution was 2.5 mg L^{-1} and at the time of harvest BDTA in solution was below the LOQ; as a result, mass balance

was conducted only on BDDA and is presented in Fig 5.6. The BDDA taken up by combined root and shoot tissues was found to be only 0.05 to 1.5% of the initial BDDA solution. The percentage of total BDDA that was unaccounted for during the experiment (about 18 to 24%) could be due to adsorption on the surface of the roots or biodegradation by microbes or may be an analytical error. A similar range of unaccounted triclocarban and triclosan (20 to 70%) was determined for uptake of these compounds by tomato (*Solanum lycopersicum*), celery (*Apium graveolens*) and beet (*Beta vulgaris*) (Mathews et al., 2014) in a hydroponic system. The authors determined the plant uptake of triclocarban and triclosan to be less than %1 to 20% of the total amount in solution. In another study, various pharmaceuticals and personal care products were measured in lettuce grown hydroponically and the mass balance determined the compound distribution as follows: in plant tissue (5 to 65%), in nutrient solution (20 to 60%) and unaccounted (20 to 50%) (Dodgen et al., 2013).

Table 5.2 BACs taken up by garden cress and lettuce. Control plants (without any BACs) and various plant parts (roots and shoots) from plants treated with BACs were analysed using HPLC-MS. Here, ND= not detected; NA=not applicable; and n indicates number of replicates tested. Treatment conditions were BDDA at 5 mg L^{-1} and a BDDA:BDTA mixture at 5:2.5 mg L^{-1}.

BACs (mg L^{-1})	**Tissue samples**	**Plant types**	**BDDA (µg g^{-1})**	**BDTA (µg g^{-1})**
	Control root (n=1)	Garden cress	ND	ND
	Control shoot (n=2)		ND	ND
BDDA (5)	Leaves and shoot (n=1)		5.4	NA
BDDA (5)	Root (n=1)		11	NA
BDDA+BDTA (5+2.5)	Leaves and shoot (n=1)		20.8	34.2
BDDA+BDTA (5+2.5)	Root (n=1)		396	678
	Control root (n=1)	Lettuce	ND	ND
	Control shoot (n=2)		ND	ND
BDDA (5)	Root (n=1)		37.2	NA
BDDA+BDTA (5+2.5)	Leaves and shoot (n=1)		14.6	2.5
BDDA+BDTA (5+2.5)	Root (n=1)		167	17.4

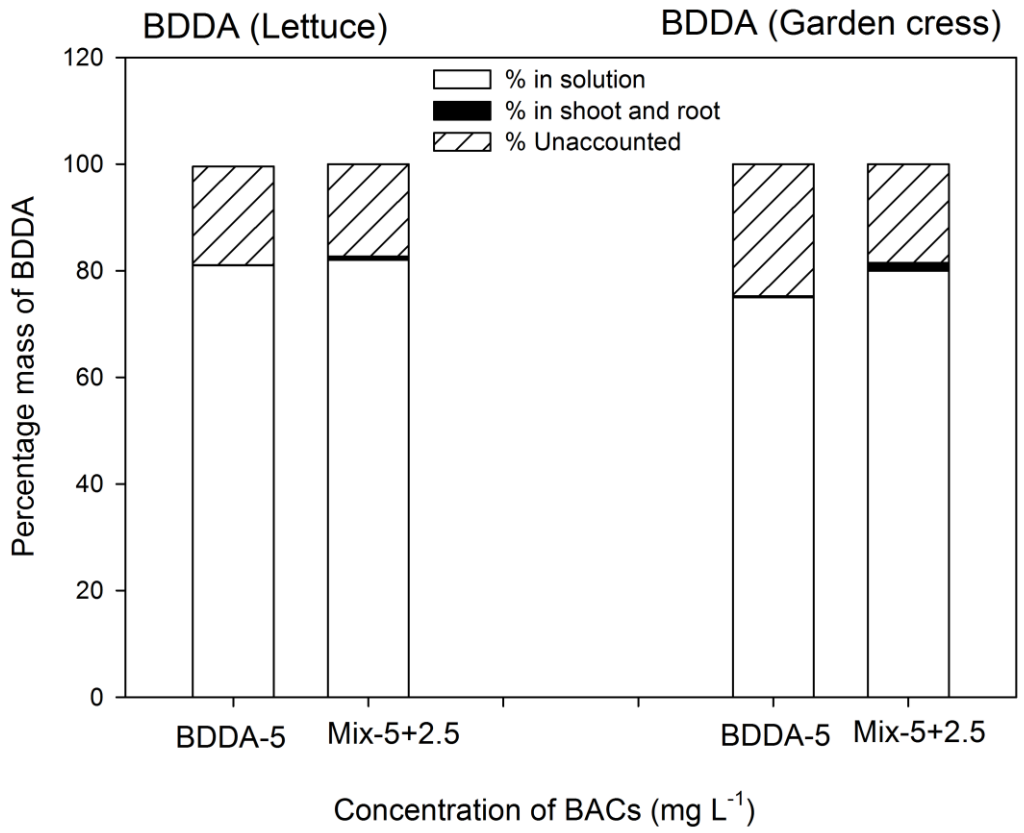

Fig 5.6 Mass balance for BDDA in hydroponic treatments after harvest (12 d for both plants). Lettuce and garden cress were treated with BDDA (5 mg L^{-1}) alone and in mixture of BDDA: BDTA at 5:2.5 mg L^{-1}. Unaccounted mass (%) may represent loss due to adsorption on the plant roots or biodegradation or measurement error.

5.4 Conclusions

Roots of hydroponically grown lettuce and garden cress were capable of taking up BACs and translocating them into their shoots. Environmentally pertinent concentrations of BACs were toxic to both plant species, and BACs were more toxic to lettuce than garden cress. However, bioavailability of BACs in hydroponic solution is higher than that would be in soil and these results cannot simply be extrapolated to an agricultural field. Nutrient analysis in plants does not show any consistent pattern to ascertain the mechanism of BAC toxicity; however, the concentration of Fe increased by 50% in roots of both species, which may cause oxidative stress in plant tissue. Measurement of carbohydrate content, O_2 exchange rate, photosynthetic rate and chlorophyll production might provide some valuable information. This study, however, provides essential information about the potential BAC toxicity to vegetables and highlights the importance of studying the impacts of these compounds in agricultural soils amended with biosolids.

References

Akhter M.F., McGarvey B., Macfie S.M., 2012. Reduced translocation of cadmium from roots is associated with increased production of phytochelatins and their precursors. Journal of Plant Physiology 169, 1821–1829.

Almeida C.M.R., Dias A.C., Mucha A.P., Bordalo A.A., Vasconcelos M.T.S.D., 2009. Influence of surfactants on the Cu phytoremediation potential of a salt marsh plant. Chemosphere 75, 135–140.

An J., Zhou Q., Sun F., Zhang L., 2009. Ecotoxicological effects of paracetamol on seed germination and seedling development of wheat (*Triticum aestivum L.*). Journal of Hazardous Materials 169, 751-757.

Bixio D., Thoeye C., De Koning J., Joksimovic D., Savic D., Wintgens T., Melin T., 2006. Wastewater reuse in Europe. Desalination 187, 89–101.

Calderón-Preciado D., Renault Q., Matamoros V., Cañameras N., Bayona J.M., 2012. Uptake of organic emergent contaminants in spath and lettuce: an in vitro experiment. Journal of Agricultural and Food Chemistry 60, 2000–2007.

Clara M., Scharf S., Scheffknecht C., Gans O., 2007. Occurrence of selected surfactants in untreated and treated sewage. Water Research 41, 4339–4348.

Díez C., Feinberg M., Spörri A. S., Cognard E., Ortelli D., Edder P., Rudaz S., 2016. Evaluation of quantification methods to compensate for matrix effects in the analysis of benzalkonium chloride and didecyldimethylammonium chloride in fruits and vegetables by LC-ESI-MS/MS. Food Analytical Methods 9, 485–499.

Dodgen L.K., Li J., Parker D., Gan J.J., 2013. Uptake and accumulation of four PPCP/EDCs in two leafy vegetables. Environmental Pollution 182, 150–156.

Exall K., 2004. A review of water reuse and recycling with reference to Canadian practice and potential: 2 applications. Water quality research journal of Canada 39, 13–28.

Ferk, F., Misık, M., Hoelzl, C., Uhl, M., Fuerhacker, M., Grillitsch, B., Parzefall, W., Nersesyan, A., Micieta, K., Grummt, T., Ehrlich, V., Knasmuller, S., 2007. Benzalkonium chloride (BAC) and dimethyldioctadecyl-ammonium bromide (DDAB), two common quaternary ammonium compounds, cause genotoxic effects in mammalian and plant cells at environmentally relevant concentrations. Mutagenesis 22, 363–370.

Garland J.L., Levine L.H., Yorio N.C., Hummerick M.E., 2004. Response of graywater recycling systems based on hydroponic plant growth to three classes of surfactants. Water Research 38, 1952–1962.

Gerba, C.P., 2015. Quaternary ammonium biocides: Efficacy in application. Applied and Environmental Microbiology 81, 464-469.

Gromaire M.C., Van de Voorde A., Lorgeoux C., Chebbo G., 2015. Benzalkonium runoff from roofs treated with biocide products–In situ pilot-scale study. Water Research 81, 279–287.

Gros M., Petrovic M., Ginebreda A., BarcelÓ D., 2010. Removal of pharmaceuticals during wastewater treatment and environmental risk assessment using hazard indexes. Environmental International 36, 15–26.

Ismail Z.Z., Tezel U., Pavlostathis S.G., 2010. Sorption of quaternary ammonium compounds to municipal sludge. Water research 44, 2303-2313.

Jing G., Zhou Z., Zhou J., 2012. Quantitative structure–activity relationship (QSAR) study of toxicity of quaternary ammonium compounds on *Chlorella pyrenoidosa* and *Scenedesmus quadricauda.* Chemosphere 86, 76–82.

Kang H.I., Shin H.S., 2016. Rapid and sensitive determination of benzalkonium chloride biocide residues in soil using liquid chromatography–tandem mass spectrometry after ultrasonically assisted extraction. Bulletin of the Korean Chemical Society 37, 1219–1227.

Kampfenkel K., Montagu M.V., Inzé D., 1995. Effects of iron excess on *Nicotiana plumbaginifolia* plants[1] implications to oxidative stress. Plant Ohysiology 107, 725–735.

Khan A.H., Topp E., Scott A., Sumarah M., Macfie S.M., Ray M.B., 2015**.** Biodegradation of benzalkonium chlorides singly and in mixtures by a *Pseudomonas* sp. isolated from returned activated sludge. Journal of Hazardous Materials 299, 595–602.

Kong W.D., Zhu Y.G., Liang Y.C., Zhang J., Smith F.A., Yang M., 2007. Uptake of oxytetracycline and its phytotoxicity to alfalfa (*Medicago sativa* L.). Environmental Pollution 147, 187–193.

Kümmerer K., Eitel A., Braun U., Hubner P., Daschner F., Mascart G., Milandri M., Reinthaler F., Verhoef J., 1997. Analysis of benzalkonium chloride in the effluent from European hospitals by solid-phase extraction and high-performance liquid chromatography with post-column ion-pairing and fluorescence detection. Journal of Chromatography A 774, 281–286.

Li, X., Luo, X., Mai, B., Liu, J., Chen, L., Lin, S., 2014. Occurrence of quaternary ammonium compounds (QACs) and their application as a tracer for sewage derived pollution in urban estuarine sediments. Environmental Pollution 185, 127-133.

Martínez-Carballo E., González-Barreiro C., Sitka A., Kreuzinger N., Scharf S., Gans O., 2007. Determination of selected quaternary ammonium compounds by liquid chromatography with mass spectrometry. Part II. Application to sediment and sludge samples in Austria. Environmental Pollution 146, 543-547.

Mathews S., Henderson S., Reinhold D., 2014. Uptake and accumulation of antimicrobials, triclocarban and triclosan, by food crops in a hydroponic system. Environmental Science and Pollution Research 21, 6025–6033.

Miller G.W., 2006. Integrated concepts in water reuse: managing global water needs. Desalination 187, 65–75.

Pérez, P., Fernández, E., Beiras, R., 2009. Toxicity of benzalkonium chloride on monoalgal cultures and natural assemblages of marine phytoplankton. Water Air Soil Pollution 201, 319–330.

Pilon-Smits E., 2005. Phytoremediation. Annual Review of Plant Biology 56, 15–39.

Salisbury F.B., Ross C.W., 1985. Plant physiology. Third Edition, Belmont, California: Wadsworth Publishers.

Stampoulis D., Sinha S.K., White J.C., 2009. Assay dependent phytotoxicity of nanoparticles to plants. Environmental Science and Technology 43, 9473–9479.

Tanoue R., Sato Y., Motoyama M., Nakagawa S., Shinohara R., Nomiyama K., 2012. Plant uptake of pharmaceutical chemicals detected in recycled organic manure and reclaimed wastewater. Journal of Agricultural and Food Chemistry 60, 10203–10211.

Tezel U., 2009. Fate and effect of quaternary ammonium compounds in biological systems. (https://smartech.gatech.edu/handle/1853/28229; accessed September, 2016).

United States Environmental Protection Agency (EPA739-R-06-009), August 2006. Reregistration eligibility decision for alkyl dimethyl benzyl ammonium chloride (ADBAC).

(https://archive.epa.gov/pesticides/reregistration/web/html/index-9.html; accessed September, 2016)

Warren C.R., 2013. Quaternary ammonium compounds can be abundant in some soils and are taken up as intact molecules by plants. New Phytologist 198, 476–485.

Wu C., Spongberg A.L., Witter J.D., Sridhar B.B.M., 2012. Transfer of wastewater associated pharmaceuticals and personal care products to crop plants from biosolids treated soil. Ecotoxicology and Environmental Safety 85, 104–109.

Wu X., Ernst F., Conkle J.L., Gan J., 2013. Comparative uptake and translocation of pharmaceutical and personal care products (PPCPs) by common vegetables. Environment International 60, 15–22.

Xia H., Chi X., Yan Z., Cheng W., 2009. Enhancing plant uptake of polychlorinated biphenyls and cadmium using tea saponin. Bioresource Technology 100, 4649–4653.

Zhang C., Tezel U., Li K., Liu D., Ren R., Du J., Pavlostathis S.G., 2011. Evaluation and modeling of benzalkonium chloride inhibition and biodegradation in activated sludge. Water Research 45, 1238-1246.

Chapter 6

Toxicity Reduction and Improved Biodegradability of Benzalkonium Chlorides by Ozone/Hydrogen Peroxide Advanced Oxidation Process

[A revised version of this chapter is submitted; Khan et al., 2016. Journal of Hazardous Materials]

6.1 Introduction

Benzalkonium chlorides (BACs), cationic surfactants, are a subgroup of quaternary ammonium compounds (QACs) and contain benzyldimethyl ammonium chlorides with an attached alkyl chain of C_8 to C_{18}. The commercial use of various surfactants (anionic, cationic, non-ionc and amphoteric) was 12 million tonnes in 2010 of which approximately 15% were QACs (Brycki et al., 2014). About 75% of the QACs, including BACs, end up in wastewater treatment plants (WWTP) (Ismail et al., 2010) following use in various fields such as domestic, agricultural and healthcare (Gerba, 2015). Although benzalkonium chlorides are biodegradable at low concentration (they are bactericidal at higher concentration) (Brycki et al., 2014; Bassey and Grigson, 2011), significant amounts of the total BACs have been measured in various environmental samples all around the world. BAC concentrations ranged from 0.05 mg L^{-1} to 6.03 mg L^{-1} in hospital effluents in many European countries (Kümmerer et al., 1997). In some WWTP, BACs were measured in the range of 0.02 to 0.31 mg L^{-1} in influents and 0.00009 to 0.002 mg L^{-1} in effluents suggesting that more than 90% of total BACs were removed either through biodegradation or adsorption on the sewage sludge during biological treatment (Clara et al., 2007). BACs in sewage sludge were found at 3.6 mg kg^{-1} (dry weight) in China confirming that BACs can accumulate into sewage sludge during biological wastewater treatment (Li et al., 2014). Even higher concentrations (2 to 9 mg kg^{-1}, dry weight) of various BACs were measured in sewage sludge in Austria (Martínez-Carballo et al., 2007). BACs were also found in river sediments close to WWTP or urban areas in the range of 0.022 to 0.21 mg kg^{-1} in USA (Ferrer and Furlong, 2002), and from 0.05 to 1.1 mg kg^{-1} in China (Li et al., 2014).

BACs have been found to be toxic to aquatic life (Carbajo et al., 2016) and genotoxic to eukaryotic cells in the environmentally relevant concentration of 1.0 mg L^{-1} (Ferk et al., 2007). Microalgae are more sensitive to the toxic effect of BACs. The EC_{50} for a natural assemblage of algae in sea water was 36.4 µg L^{-1} in 24 h and 63.9 µg L^{-1} in 72 h (Pérez et al., 2009). Given the sensitivity of aquatic organisms to BACs and their widespread use, it is important to reduce concentrations of BACs in the natural environment.

Although, advanced oxidation processes (AOPs) are widely used for remediation of waste streams particularly for the removal of organic contaminants, only a few researchers have studied the degradation of BACs using AOPs. In a pioneering work, Hidaka et al. (1992) reported that the TiO_2 photocatalytic degradation rate of benzyldimethyl dodecyl ammonium chloride (BDDA) was lower than that of an anionic surfactant, sodium dodecyl benzene sulfonate. Photodegradation of BAC using TiO_2 nanoparticles was carried out in two other studies (Loveira et al., 2012; Suchithra et al., 2015). Loveira et al. (2012) found some toxic by-products of TiO_2 photocatalysis as a pretreatment of BACs for biological treatment. In another study ultraviolet/H_2O_2 pretreatment improved the biodegradability of BACs (Adams and Kuzhikannil, 2000) while higher O_3 doses were found to enhance aquatic toxicity when NiO nanoparticles were used as a catalyst (Carbajo et al., 2016).

Complete chemical mineralization of a compound using AOPs can be expensive compared to biodegradation. Since BACs are toxic to microorganisms at high concentration, a combined approach of pretreatment of TiO_2 photocatalysis followed by biological treatment improved the overall removal of BDDA from water (Loveira et al., 2012). Ultraviolet/H_2O_2 pretreatment improved the biodegradability of BACs measured in terms of total organic carbon (TOC) when 90% of initial TOC was removed in a process combining advanced oxidation and biodegradation (Adams and Kuzhikannil, 2000). Ozonation of wastewater with or without NiO nanoparticles was tested for the removal of BACs (Carbajo et al., 2016) and the authors found intermediate products due to ozone pretreatment and tested NiO toxicity on different bacterial species.

Photocatalysis processes are effective in degrading organic pollutants in transparent water; however, the use of UV irradiation is compromised in water containing suspended

particulate matter (SPM) due to poor penetration of light, even at a low turbidity < 2 NTU (Cantwell and Hofmann, 2011). Moreover, residual nanoparticles are found to be toxic to variety of microorganisms (Otero-González et al., 2014; Lovern and Klaper, 2006; Garner and Keller, 2014). As a result, photocatalysis as a pretreatment process before biological treatment for the degradation of BACs may not be an appropriate choice. In this context chemical oxidation using ozone in combination with H_2O_2 could be a better advanced oxidation pretreatment method for BACs. On the other hand, ozone either singly or in combination with other oxidants such as hydrogen peroxide is frequently used in both water and wastewater treatments. Ozonation is relatively unaffected by suspended particles (Huber at al., 2005) and it has a low potential for formation of harmful (e.g. chlorinated) intermediates (Carbajo et al., 2016). Additionally, ozone based chemical oxidation (e.g. O_3 or O_3/H_2O_2) is less expensive compared to UV based photochemical or sonochemical processes for the removal of many organic pollutants (Mahamuni and Adewuyi, 2010; Sarkar et al., 2014). The addition of H_2O_2 during ozonation enhances the formation of •OH radicals (Andreozzi et al., 1999) and broadens the potential applicability of ozone based advanced oxidation processes to medium to high strength effluents (Alaton et al., 2004).

BACs or QACs are generally found in mixture of various structures and C-chain lengths in commercial products; high abundance of these compounds in nature is probably due to poor biodegradability of the mixture of BACs. Therefore, the objective of this research is to determine the efficacy of advanced oxidation pretreatment of a mixture of two BACs to improve the biodegradability of the mixture. To the best of our knowledge, AOP with O_3/H_2O_2 of benzyl dimethyl dodecyl ammonium chloride (BDDA) and benzyl dimethyl tetradecyl ammonium chloride (BDTA) has not been tested before. A central composite design was used to optimize the oxidation parameters to obtain maximum oxidation rate constant in the range of operating conditions. Biodegradability of the BACs after various treatments was evaluated and the toxicity of the treated solutions was determined using fresh water algal species. Transformation products were identified and the degradation pathways were postulated. The experiments were conducted with BACs spiked in Milli-Q water and finally, the optimum condition was applied in preliminary influent from a local

wastewater plant. A preliminary analysis was also conducted to determine the cost of AOP pretreatment for the mixture of BACs.

6.2 Material and methods

6.2.1 Chemicals

Certified reference materials (purity ≥ 99.0%) benzyl dimethyl dodecyl ammonium chloride (BDDA) and benzyl dimethyl tetradecyl ammonium chloride (BDTA) were purchased from Sigma-Aldrich (St. Louis, MO, USA). Catalase from bovine liver was also purchased from Sigma-Aldrich (St. Louis, MO, USA). HPLC grade acetonitrile (AcN) was purchased from Caledon Chemicals (Georgetown, ON, Canada). Hydrogen peroxide, 30% (w/w), RICCA Chemicals, (Arlington, TX, USA) was diluted to desired concentrations with Milli-Q water (conductivity 18 MΩ.cm, Millipore water systems, Integral-5, France). A hydrogen peroxide (H_2O_2) measuring kit was obtained from HACH LANGE GmbH (Willstätterstrasse, Germany). Ammonium acetate, HPLC grade (98.3%) was used to prepare buffer solution (Fisher Chemical, New Jersey, USA). Phosphoric acid (85%) was purchased from Caledon Laboratories Ltd, (ON, Canada). Potassium indigotrisulfonate was purchased from Acros Organics (New Jersey, USA). All other chemicals used were of analytical reagent grade unless otherwise stated.

6.2.2 Experimental set-up for AOP

Oxidation experiments were performed in a bench-scale annular batch reactor of 750 mL capacity (26.7 cm in length and 9.5 cm inner diameter) using a 500 mL solution made with Milli-Q water. A cooling water jacket was used to maintain a constant 20°C reaction temperature and the reactor contents were thoroughly mixed using a magnetic stirrer (VMS-C7; VWR International, USA). Ozone was produced by an ozone generator (model TG-40, Ozone Solution, Hull, IA, USA) using compressed oxygen (ultra-pure) at a pressure of 20 psi. During an experiment ozone was bubbled continuously in the reactor through a round shape diffuser (inner diameter 8.9 cm with nine small holes) located at the bottom of the reactor. Ozone in the gas phase was measured using an ozone analyzer (model UV-100, Eco Sensors,

Newark, California, USA). The flow rate of ozone in the reactor was 4 L min^{-1}, with a constant gas phase concentration of 2700 ppm. Hydrogen peroxide, 30% (w/w) was spiked at various dosages (Table 6.1) and the reaction time for AOP was kept constant at 2 h. Samples of 5 mL volume were collected from the centre of the reactor for HPLC-UV and HPLC-MS analyses. Solution pH was determined using a pH meter (ORION STARA111, Thermo Scientific, USA). Optimization of the AOP and the kinetic data were extracted from the mean value of three replicates (n=3). All other experiments, were conducted in duplicate (n=2).

6.2.3 Selection of factors and ozone doses for AOP

The concentrations of the two BACs were determined based on our previous biodegradation study, which suggested that 50:25 mg L^{-1} BDDA:BDTA was the minimum concentration and ratio that was resistant to biodegradation using *Pseudomonas* sp. (Khan et al., 2015). Additionally, the ratio of BDDA:BDTA in the natural environment is approximately 2:1 (Li et al., 2014). Therefore, the same mixture of BDDA and BDTA was selected for AOP in this study. Preliminary experiments were conducted and the rate of degradation was low at pH ≤ 9 and only less than 70% of BACs was degraded after 2 h of AOP. As a result, the optimization of AOP was conducted applying a central composite design (CCD) at pH 11 and 9 as high and low levels, respectively. Few assumptions were made to select the H_2O_2 and O_3 dose for the optimization process. The dosage of H_2O_2 was selected based on Equations 6.1 to 6.3. Equation 6.1 is the simplest expression to determine hydroxyl radical formation in O_3/H_2O_2 reactions (Staehelin and Hoigné, 1982); however, a different dissociation mechanism for the production of hydroxyl radical between O_3/H_2O_2 was proposed using thermo-kinetic study (Merényi et al., 2010). The pH of the solution also affects the dissociation rate of O_3 (shown later). The combined effect of H_2O_2 and pH on O_3 dissociation was not experimentally determined and the Equation 6.1 was considered to calculate the maximum concentration of H_2O_2 required for hydroxyl radical production for complete mineralization of the mixture of BACs (although complete mineralization was not the aim of this study). The stoichiometry for complete mineralization of BDDA and BDTA as given in Equations 6.2 and 6.3 was used to calculate the upper limit of H_2O_2 and the lower limit of O_3

only for the optimization process. In reality pH and H_2O_2 will act together to provide various propagation reactions; however, study of the reaction mechanism of ozone degradation is beyond the scope of this study. Therefore, 0.15 mM BDDA (i.e., 50 mg of BDDA) and 0.07 mM BDTA (i.e., 25 mg of BDTA) required 4.1 mM of H_2O_2, which is equivalent to 140 mg L^{-1} of H_2O_2. Thus, the high and low levels of H_2O_2 concentration were selected as 200 and 100 mg L^{-1}, respectively, for optimization of the process.

$$H_2O_2 + 2O_3 \rightarrow 2 \bullet OH + 3O_2 \text{ ---------- (6.1)}$$

$$C_{21}H_{38}NCl\ (BDDA) + 61\ (2 \bullet OH) \rightarrow 21\ CO_2 + 80\ H_2O + N + Cl \text{ ---------- (6.2)}$$

$$C_{23}H_{42}NCl\ (BDTA) + 67\ (2 \bullet OH) \rightarrow 23\ CO_2 + 88\ H_2O + N + Cl \text{ ---------- (6.3)}$$

Equations 6.2 and 6.3 were also used to calculate the minimum ozone doses, which were kept fixed throughout the experiment. According to these equations, 18 mM of O_3 is required for complete mineralization for the same mass of BDDA and BDTA, which is equivalent to 864 mg of ozone. At a flow rate of 4 L min^{-1} of O_3 flow with 2700 ppm gas phase O_3 concentration (240 L per h = 9.92 mole (at NTP 1 mole gas = 24.2 L) = 9.92 x 0.0027 x 48 = 1.28 g O_3 per h), a total of 1.28 g ozone was supplied in one hour indicating sufficient ozone was present to oxidise the target compounds. Additionally, the ozone concentration in the water phase was measured experimentally as described in section 6.2.5.1. The AOP reaction time was selected as 2 h as almost complete degradation of BACs occurred by this time during the preliminary experiments at pH 11. Ozone concentration was not used as a variable since it was difficult to vary the concentrations produced by the O_3 generator due to poor resolution in the controller.

6.2.4 Experimental design for AOP optimization

Response surface methodology (RSM) was employed to optimize variables such as the dosage of H_2O_2 at constant ozone concentration, and pH for BACs degradation. The optimization was conducted to obtain the maximum degradation rate constant using kinetic experiments. Rate constant values are important for cost analysis of AOP. RSM applies multiple regression analysis to solve multivariable data and is capable of expressing individual and cumulative effects of test variables on the response with a limited number of experiments (Prakash et al., 2008). The graphical representation of such techniques (i.e., response surface) can be achieved by various factorial designs; among them, central composite design (CCD) is the most popular when the number of variables are ≤ 3 (Chang et al., 2011; Cho and Zoh, 2007).

Variables considered for the study were optimized using CCD at five different levels and they were coded as: high (+1), low (–1), central (0), extreme high (+α) and extreme low (–α). The CCD for two factors contains a set of full factorial design (i.e., four cubic points) with central points that are augmented with a group of star points (i.e., four axial points) located at a distance ±α from its central points (Myers and Montgomery, 2002). Factorial points determine the interaction effects among the low and/or high levels of the factors. The central point determines the experimental error and the reproducibility of the data. The star points determine the extreme high (+α) or low values (–α). The star points and total number of experimental runs for CCD are determined by Equations 6.4 and 6.5 (Khan et al., 2014).

$$\alpha = 2^{k/4} \quad \text{----------} \quad (6.4)$$

$$N = 2^k + 2k + N_0 \quad \text{----------} \quad (6.5)$$

where, k is the number of factors, N is the number of experimental runs, N_O is the number of central points, 2^k is the total factorial points (cubic points) and 2k is the total axial points. In the present study, α = 1.414 and N = 13 (k = 2 and N_0 = 5). The uncoded values for various levels of the selected variables were calculated using Equation 6.6, where, x is the

coded form of the variables, X_H and X_L are the high and low values of the selected variables in their uncoded form (Table 6.1). The uncoded or the natural value of the experimental factors was denoted by *X* (Chang et al., 2011).

$$x = \frac{X - (X_H + X_L)/2}{(X_H - X_L)/2} \quad \text{---------- (6.6)}$$

The experimental data were optimized with statistical and graphical software Minitab 15. Regression analysis was used to calculate the coefficient of regression (second-order equations), and individual equations were developed for % removal of BDDA and BDTA. The second order equations were further used to calculate the predicted values and compared with the experimental values to determine model adequacy. The optimization results from CCD were also confirmed by examining the observed data using analysis of variance (ANOVA). Fisher's statistical test (*F*-test) and *p*-values (probability values) obtained by ANOVA were evaluated for the individual (linear), squared (quadratic) and interaction effects to the % removal of individual BACs of the variables (Myers and Montgomery, 2002). The *F*-values were determined by the ratio of the mean square of the parameter in the study to the mean square of the error term (data not presented) and compared with the F_{critical} values obtained from an *F*-distribution chart to justify the model. Two dimensional response surfaces in terms of contour plot were used to identify the region, where the factors are responsible for 90% removal of the target pollutants during the AOP.

Contour plots were used to select two different treatment processes (upper and lower region) for 90% removal of BACs in 2 h. A kinetic study was performed to calculate the rate constants for the upper and lower region of AOP. During the kinetic study 15 mL AOP samples were collected at 10, 20, 30, 40, 60, 90, and 120 min and the degradation constants were determined using first-order kinetic plots. The rate constant values were used for the cost analysis of the AOPs.

6.2.5 Analytical methods

6.2.5.1 Ozone concentration in liquid phase

Ozone concentration in Milli-Q water was measured by using decolourization of potassium indigotrisulfonate as described by Bader and Hoigné (1981) at various pH. The sulfonated indigo molecule contains only one C=C double bond, which reacts with one mole of O_3 and decolourizes indigo. The absorbance of decolourized indigo solution was measured using a UV-Vis spectrophotometer (Model-Cary 60; Agilent technologies, CA, USA).

Various ozone doses in gas phase (450, 1200, 2340 and 3560 ppm) were measured using an O_3 analyzer and were supplied in 500 mL Milli-Q water for 30 min (for saturation of the solution with ozone). Ozone concentration in solution did not increase after 15 min of supply. Afterwards, solution was collected to measure the subsequent ozone concentration in the liquid phase (mg L^{-1}) at pH 7, 9 and 11.

Table 6.1 Experimental and predicted % removal of BACs using a central composite design (CCD) matrix (runs 1 to 13) for the factors H_2O_2 and pH. The design matrix contained coded (within brackets) and actual values for CCD. Ozone doses were constant at 1.28 g h^{-1} for 2 h.

Run #	H_2O_2 (mg L^{-1}) (coded) Actual value	pH (coded) Actual value	% BDDA removed Experimental	Predicted	% BDTA removed Experimental	Predicted
1	(-1) 100	(-1)9	62.1±1.82	43.4	66.4 ±1.6	48.8
2	(+1)200	(-1)9	72.9±0.61	62.4	76.5±1.4	66
3	(-1)100	(+1)11	99.9±0.1	96.9	99.2±0.3	99.2
4	(+1)200	(+1)11	100±0	94.4	100±0	97.8
5	(-1.414) 79	(0) 10	80.8±2.3	73.1	85±1.3	82.2
6	(+1.414) 220.7	(0) 10	89.4±1.2	84.7	92.9±0.7	93.4
7	(0) 150	(-1.414) 8.58	60.6±3.2	39.4	57.9±3.3	39
8	(0) 150	(+1.414) 11.4	100±0	99.9	100±0	97
9	(0) 150	(0) 10	94.1±1.42	92	94.2±0.6	91.3
10	(0) 150	(0) 10	91.5±2.1	92	91.6±0.6	91.3
11	(0) 150	(0) 10	92.7±1.8	92	90±1.7	91.3
12	(0) 150	(0) 10	92±0.4	92	90.2±2.0	91.3
13	(0) 150	(0) 10	90.3±1.1	92	91.4±1.0	91.3
Additional runs in the presence of H_2O_2 or O_3 to evaluate their individual effects on the % removal of BACs at pH 11						
(i)	H_2O_2 = 200 mg L^{-1} O_3= 0	11	4.4±2.4		12±5	
(ii)	H_2O_2 = 0 O_3= 1.28 g h^{-1}	11	65.7±0.6		70.7±6.3	

6.2.5.2 Quantification of BACs and their intermediate products

Quantification of BACs was carried out using a high performance liquid chromatography (HPLC) coupled with a diode array UV-Vis detector (Dionex ICS-3000, USA). The separation column was a Luna CN (C-18, 3µm pore, 100 mm length x 4.6 mm internal diameter) (Phenomenex, Canada) and the absorbance was measured at 210 nm (Tezel and Pavlostathis, 2009). Acetonitrile and 40 mM ammonium acetate (adjusted to pH 5.0 using 1 M H_3PO_4 and filtered using a 0.2 µm filter) at a ratio of 60:40 passed through HPLC column isocratically at a flow rate of 0.8 mL min^{-1} and an injection volume of 100 µL. The retention times for BDDA and BDTA were 12±0.2 min and 13.5±0.2 min, respectively. Standard curves for BDDA and BDTA were made using six concentrations (3.125, 6.25, 12.5, 25, 50, and 100 mg L^{-1}); each had r^2 = 0.998. Zero absorbance was measured for a reagent blank (solution without BDDA or BDTA) solution at the same retention time of BDDA and BDTA. The lower limit of quantification (LOQ) was determined to be 3 mg L^{-1}, and was defined as the value corresponding to a signal to noise ratio ≤ 3. One control (i.e. same O_3 dose and pH without BACs; where necessary) and all other quantification of BACs mixture was carried out in triplicate.

Intermediates produce during the AOP experiments were identified using HPLC-MS (mass spectrometry) with a Q-Exactive Orbitrap (Thermo Scientific), using an Agilent Eclipse plus C-18 RRHD column (1.8 µm pore size, 50 mm length x 2.1 mm internal diameter) at a flow rate of 0.3 mL min^{-1} and an injection volume of 2 µL. The solvent gradient used started with 100% H_2O (0.1 % formic acid) for 0 to 0.5 min and increased to 100% acetonitrile (0.1% formic acid) over 3 min. The organic mobile phase was then held at 100% for 1 min before returning to 0% over 30 s and returned to 0.1% formic acid solution. A top 5, data-dependent tandem MS ($ddMS^2$) analysis was performed in positive mode combined with a parallel reaction monitoring (PRM). The full MS scans were performed at a resolution of 70,000 and AGC target of 1 x 10^5. The $ddMS^2$ scans were performed at a resolution of 17,500 and AGC target of 1 x 10^5. The spray voltage was held at 3.6 kV, the S-lens at 65 V and the sheath and auxiliary gas were set to 20, and arbitrary units, respectively. The limit of quantification was

determined to be 10 ppb (or 10 µg L^{-1}) and the limit of detection was an order of magnitude lower (1 ppb) with an $r^2 > 0.999$ obtained from the standard curves of BACs. The data were analyzed with Xcalibur™.

6.2.5.3 Toxicity analysis of effluents using algae

Algal cultures were grown in high salt minimal media (HSM, Sueoka, 1960) in 125 mL conical flasks with sponge stoppers, placed in an incubation shaker (Multitron Pro; Bottmingen, Switzerland) at 150 rpm, 25°C, and under the light source (140 µmol $m^{-2}s^{-1}$; Sueoka, 1960). Pure cultures of *Chlorella vulgaris* strain no. UTEX 2714 and *Chlamydomonas reinhardtii* strain no. CC125 were obtained from the University of Texas at Austin, and the Chlamydomonas center, respectively. Growth of the strains was measured by their optical density at 600 nm (OD_{600}) using a spectrophotometer (Infinite 200PRO series; Männedrof, Switzerland).

Prior to the toxicity test, the cultures were acclimatized in HSM. Two rounds of acclimatization were run and the cell densities at exponential phase were used for the experiments. For the toxicity tests, about 400 µL of AOP treated or untreated BDDA:BDTA mixtures (initial concentrations BDDA:BDTA = 50:25 mg L^{-1}) and 200 µL of acclimatized culture inoculum were added to 50 mL of HSM. The control treatment used HSM only and all experiments were conducted in duplicate (n=2). Inoculated culture solutions with an OD_{600} of 0.04 at their mid-logarithmic phase had average cell counts of 1.2×10^7 and 3×10^6 cell mL^{-1} for *C. vulgairs* and *C. reinhardtii*, respectively.

The growth rate (GR) of the algae species was calculated using Equation 6.7, where OD_0 is the measure of OD_{600} at the beginning, while OD_t is the optical density on day t (Wang et al., 2010).

$$ln\frac{OD_t}{OD_0} = GR * t \quad \text{----------} \quad (6.7)$$

6.2.5.4 Biodegradability test

After AOP, residual H_2O_2 dissociates to oxygen, which interferes with the measurement of BOD_5. Bovine catalase is preferred for quenching H_2O_2 compared to sodium hypochlorite, sodium thiosulfate and sodium sulphite (Liu et al., 2003) and was used in this study. Before quenching, H_2O_2 was measured in the solution using drop wise titration and a H_2O_2 measuring kit (provide supplier details) as described in the HACH manual (Model HYP-1, Cat. No. 22917-000). According to Liu et al. (2003), 2 to 4 mg L^{-1} of catalase can quench up to 142 mg L^{-1} H_2O_2 in less than 30 min. In this study, about 0.5 mL of catalase solution was added to quench the residual H_2O_2 (tested using H_2O_2 measuring kit; blue color indicates the presence of H_2O_2 in solution) in each AOP vials containing 15 mL of AOP sample collected during the kinetic study. After addition of catalase, the vials were shaken twice and the cap was kept open for 30 min to remove O_2 generated by dissociating residual H_2O_2. After quenching, the presence of H_2O_2 was measured using H_2O_2 measuring kit and no blue color was observed. Residual O_3 was not measured after treatment because O_3 dissociation is several order faster at high pH and in presence of H_2O_2 than normal rate of dissociation and ozone is not expected in the solution after quenching with bovine catalase. Quenched AOP samples were used for the following biodegradability experiments.

Biodegradability of AOP treated samples was measured by the ratio of the BOD_5 to the chemical oxygen demand (COD). Standard protocols were followed for the BOD_5 (method No. 5210) and COD analyses (APHA et al., 2005; Kim et al., 2015). About 2 mL sample was added to the HACH kit for high concentrations (20 to 1500 mg L^{-1}) of COD, mixed thoroughly and digested at 150°C for 2 h using a digester DRB 200 (HACH, USA). After digestion, the kit vials were cooled for 15 min and COD in mg L^{-1} was measured using a spectrophotometer DR2800 at 620 nm (HACH, USA) (Kim et al., 2015). A reagent blank for COD was tested and its absorbance was subtracted from the sample values.

For BOD_5 analysis, 10 mL sample was added to 3 mL of BOD seed inoculum solution (Interlab, Woodlands Texas, USA), followed by the addition of nutrient solution to make a total volume of 300 mL in the BOD bottle. The nutrient solution consisted of the following (per liter): K_2HPO_4 54.3 mg, $CaCl_2$ 27.5 mg, $FeCl_3.6H_2O$ 0.25 g, $MgSO_4.7H_2O$ 22.5 g. The

nutrient solution was aerated for 24 h before addition to the BOD bottle to achieve saturated oxygen concentrations. Dissolve oxygen (DO) concentration in mg L^{-1} was measured using a DO meter, HQ30d, flexi (HACH, USA). The seed inoculum solution was prepared in nutrient solution (one seed in 500 mL), aerated for 3 h and was used for BOD_5 analysis as mentioned above. Reagent blanks were also prepared and the sample bottles were incubated at 20°C for 5 d. Equation 6.8 was used to calculate the BOD_5.

BOD_5 (mg L^{-1}) = ($DO_{final\ blank}$ – $DO_{final\ sample}$)* Dilution factor ---------- (6.8)

6.2.5.5 Growth of mixed bacterial culture in AOP treated wastewater

Mixed bacterial culture, collected from returned activated sludge (RAS) were tested for their normal growth in BACs contained influent wastewater samples before and after of AOP treatment. The qualitative assessment was performed to evaluate the AOP as pretreatment before biological treatment.

Influent wastewater (IWW) was collected from the Adelaide Pollution Control Plant in London, ON, Canada. IWW was collected after the grit removal and before primary settling tank and was characterized as: pH 7.7 ± 0.04, chemical oxygen demand (COD) 421 ± 71.7 mg L^{-1}, TSS (total suspended solid) 209.7 ± 3.5 mg L^{-1}, and turbidity 150 ± 2.6 NTU (turbidity meter 2100n, HACH, USA) using triplicate samples. Total organic carbon (TOC) due to the addition of BACs was ~56 mg L^{-1}, which is less than the average TOC (80 to 260 mg L^{-1}) of untreated domestic wastewater influent (Metcalf and Eddy, 2014). After collection, IWW was autoclaved at 120°C for 20 min and stored at 4°C until AOP was conducted. Returned activated sludge with a VSS (volatile suspended solids) concentration of 12 mg mL^{-1}, was collected from Guelph Wastewater Treatment Plant, Guelph, ON, Canada. In a wastewater treatment plant, RAS is generally used for seeding the activated sludge process and was used in this study to check the growth of mixed bacterial cultures on influents spiked with BACs before and after AOP. Petri dishes were plated with LB-agar and supplemented with 0.5 mL of sample solutions of following compositions (a) BDDA:BDTA at 50:25 mg L^{-1} in Milli-Q water; (b) BDDA:BDTA at 50:25 mg L^{-1} spiked in wastewater before AOP; (c) spiked

wastewater after 30 min of AOP; (d) spiked wastewater after 60 min of AOP and (e) Milli-Q water (control). Afterwards, 40 µL of RAS (20 times dilution of the initial concentration) was added, streaked and incubated at 37°C for 24 h on each of the Petri dishes.

6.2.6 Cost estimation

The efficiency of AOPs for the removal of many organic pollutants in various wastewater streams is well established; however, the cost of the technology compared to biological treatment methods is a drawback for their implementation in many real applications. As a result, it is important to estimate the cost of AOP to assess the feasibility of this technology for future adoption; the most likely application would be to combine AOP with a downstream biological treatment.

The cost estimation of the scaled up AOP process used in this study was carried out following the detailed procedure described by Mahamuni and Adewuyi (2010). Four assumptions were made for the cost estimation: (i) wastewater flow rate of 1000 L min^{-1} (ii) the degradation of BACs in mixture followed first order kinetics, (iii) the ozone generator will be replaced every year, and (iv) AOP will remove 90% of initial BACs. The residence time required for the AOP as pretreatment is essential for the cost estimation process and can be calculated using Equation 6.9; where t_{90} is the 90% removal of BDDA or BDTA and k is the degradation rate constant.

$$t_{90} = \frac{2.302}{k} \qquad \text{----------} \quad (6.9)$$

The cost calculations included the capital cost for an O_3 generator, costs of operation and maintenance (O & M), part replacement, labour, as well as analytical, chemical, and electrical costs to find the overall annual cost for AOP. The details are described as the supplementary materials at the end of this chapter.

6.3 Results and discussions

6.3.1 Ozone concentration in liquid phase at different pH

The concentrations of O_3 in liquid phase (Milli-Q water) and gas phase were measured to ascertain that a sufficient amount of O_3 was supplied for the AOP and to characterise O_3 doses for this system. Ozone is unstable in solution and its solubility is highly dependent on the solution pH (Vandersmissen et al., 2008). Ozone in liquid phase was measured using a decolourization technique (Bader and Hoigné, 1981) for various gas phase ozone doses at different pH and the results are presented in Fig.6.1.

Ozone concentration in liquid increased linearly with up to 3500 ppm in the gas phase at pH 7 and 9. At pH 11, less than 0.1 mg L^{-1} was measured in the liquid phase even at higher ozone doses (3500 ppm) suggesting that ozone decomposes very fast at higher pH. Other reports also suggested that faster decomposition of ozone occurs at pH ≥ 9.5 compared to the acidic pH (i.e., < 4) (Gardoni et al., 2012). At elevated pH (> 10) hydroxide ions (OH^-) react with ozone to produce a super-oxide anion radical ($O_2^{\bullet-}$) and a hydroperoxyl radical ($HO_2^{\bullet}$), which further react to form ozonide anion radical ($O_3^{\bullet-}$) that decomposes to a hydroxyl radical (•OH) (Munter R., 2001). Ozone dissociated even faster due to the synergistic effect of H_2O_2 at elevated pH and was not determined. As a result, entire amount of O_3 supplied during AOP (1.28 g h^{-1}) is expected to convert in the following radical ions ($O^{\bullet-}$; $HO_2^{\bullet}$; $O_3^{\bullet-}$; •OH) during various stages of propagation reactions (Poyatos et al., 2010).

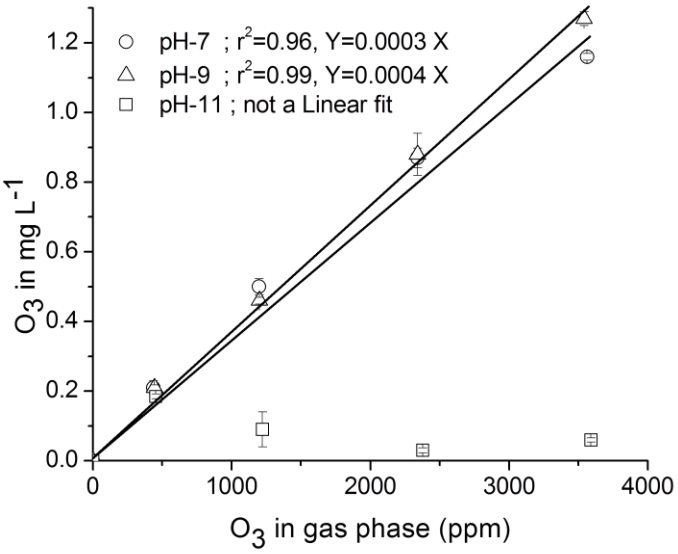

Fig.6.1. Relationship between gas and liquid phase ozone concentration at steady-state and pH 7, 9 and 11 in Milli-Q water.

6.3.2 Optimization of the AOP

The optimum concentration of H_2O_2 and pH for the removal of BACs from water using AOP was carried out using a CCD. The experimental plan for CCD with 13 experimental runs (4 cubic points, 4 axial points and 5 central points) is presented in Table 6.1 along with the experimental and predicted % removal of BDDA and BDTA. The predicted values were calculated using the quadratic model equations obtained from the regression analysis of the data (discussed in subsection 6.3.2.1). Five levels of CCD distributed the factors from extreme low to extreme high values, which were 79 to 220.7 mg L^{-1} for H_2O_2 and 8.5 to 11.4 for pH.

Two additional experiments, other than CCD, were performed to assess the individual effects of H_2O_2 and O_3 on the % removal of BACs (runs i and ii in Table 6.1) at pH 11 because

at pH ≥ 11 the maximum removal of BACs was achieved (removal ≥ 99%; Table 6.1, run # 3, 4 and 8). The maximum % removal of BACs after 2 h of ozonation (without any H_2O_2) was around 70% (Table 6.1, run ii) but the removal of BACs was reduced to ≤ 12% when 200 mg L^{-1} H_2O_2 (without O_3) was used (Table 6.1, run i). As a result, the combined effect of O_3 and H_2O_2 is obvious and required for maximal removal of BACs.

6.3.2.1 Regression analysis and ANOVA for CCD

Multiple regression analysis was performed using the quantitative data obtained from the experimental results using the CCD, and the *p*-values, constant, coefficients and standard error of coefficients are shown in Table 6.2. Regression analysis aims to determine a mathematical relation between the independent (H_2O_2 and pH) and dependent variables (% removal of BACs); as a result, the regression coefficients for the regression constant as well as for individual, squared and interaction effects of the factors for the % removals of BACs are calculated.

According to the regression analyses, each of the individual, squared and interaction terms for the factors (H_2O_2 and pH) affecting the % removal of BACs are significant ($p \leq 0.05$), except for the squared term of H_2O_2. A positive coefficient indicates the synergistic effect of the factors for the % removal of BACs and an antagonistic effect is indicated by a negative coefficient (Prakash et al., 2008). The positive coefficients for the individual factors indicate that there will be an increase in the % removal of BACs with an increase in these factors. All other coefficients obtained for the squared and interaction terms for % removal of BDDA and BDTA were negative, which indicates that the simultaneous increase of H_2O_2 and pH are adverse for the reaction (Cho et al., 2007). However, the significance of the squared terms [$(H_2O_2)^2$ and pH^2], except for [$(H_2O_2)^2$] in case of % removal of BDTA (p = 0.18) (Table 6.2), suggested that there is a curvilinear relationship between % removal of BACs and squared factors (Prakash et al., 2008). To confirm the overall contribution of squared terms on the % removal of BACs, ANOVA of the regression model was calculated and presented in Table 6.3 (see next paragraph). High r^2 (adjusted) values (> 98%) of the regression model (Table 6.2)

indicates good correlation between experimental and predicted values for % removal of BACs.

Analysis of variance (ANOVA) of the regression model is assessed based on the *F* (Fisher's statistical test) and *p*-values (probability values) and the summary of the ANOVA is shown in Table 6.3. High values of *F* ($F > F_{critical}$) and low values of *p* (< 0.05) suggested that the regression model and all other contributions of individual, square and interaction terms of the factors (H_2O_2 and pH) are significant for % removal of BACs (Myers and Montgomery, 2002). As a result, all coefficients calculated in the regression model (Table 6.2) can be incorporated to obtain the quadratic model equations (Equation 6.10 and 6.11), which is well described (Myers and Montgomery, 2002). No residual error in the ANOVA (Table 6.3) for the % removal of BACs also suggested a good fit of predicted values (obtained from Equation 6.10 and 6.11) with experimental results (Prakash et al., 2008).

$$\% \text{ BDDA removal} = 91.95 + 4.13 * H_2O_2 + 21.4 * pH - 6.53 * (H_2O_2)^2 - 11.16 * pH^2 - 5.35 H_2O_2 * pH \quad \text{----- (6.10)}$$

$$\% \text{ BDTA removal} = 91.33 + 3.94 * H_2O_2 + 20.54 * pH - 1.76 * (H_2O_2)^2 - 11.62 * pH^2 - 4.65 H_2O_2 * pH \quad \text{---- (6.11)}$$

Predicted values calculated by using Equation 6.10 and 6.11 for % removal of BDDA and BDTA are presented in Table 6.1 along with the experimental values. All variables were in their coded form according to the run number of CCD. High r^2 values (0.97) between the experimental and predicted results (Fig 6.2) for the % removal of BACs indicate that the quadratic equations (Equation 6.10 and 6.11) are good fit (Chang et al., 2011).

Table 6.2 Regression coefficients for the models and *p*-values obtained from CCD for the % removal of BACs.

Source	BDDA			BDTA		
	Coefficient	Standard error of coefficient	*p-values*	Coefficient	Standard error of coefficient	*p-values*
Constant	91.95	0.78	0.000	91.33	0.7	0.000
H_2O_2	4.13	0.87	0.002	3.94	0.78	0.001
pH	21.4	0.87	0.000	20.54	0.78	0.000
H_2O_2* H_2O_2	-6.53	1.32	0.002	-1.76	1.18	0.180
pH * pH	-11.16	1.32	0.000	-11.62	1.18	0.000
H_2O_2* pH	-5.35	1.74	0.018	-4.65	1.56	0.020
Correlations	r^2 = 0.99; r^2 (predicted) = 0.95; r^2 (adjusted) = 0.98			r^2 = 0.99; r^2 (predicted) = 0.97; r^2 (adjusted) = 0.98		

Table 6.3 Analysis of variance of the fitted model for the % removal of BACs.

Source	*DF*	$F_{critical}$	BDDA		BDTA	
			F	*p-values*	*F*	*p-values*
Regression model	5	3.97	144.26	0.000	164.55	0.000
Individual contribution	2	4.74	314.72	0.000	360.89	0.000
Squared contribution	2	4.74	43.42	0.000	48.49	0.000
Interaction contribution	1	5.59	9.47	0.018	8.89	0.020
Residual error	7					

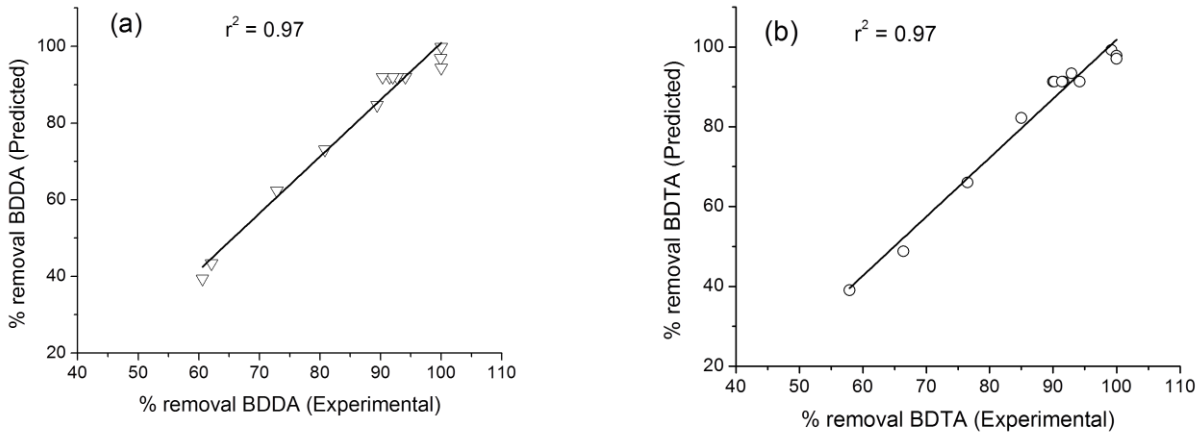

Fig.6.2 Predicted values plotted against experimental values for the % removal of BACs; (a) BDDA, and (b) BDTA.

6.3.2.2 Contour plots to identify the optimum AOP region for BAC removal

Contour plots based on quantitative analysis following the CCD are presented in Fig 6.3, where the combined effects of H_2O_2 and pH are shown for the % removal of BDDA (Fig 6.3a) and BDTA (Fig 6.3b), respectively. According to the contour plots, an incremental change in both variables induces a change in % removal of BDDA and BDTA. A similar trend can be expected from the positive coefficient values calculated in the regression model (Table 6.2). Greater than 90% removal occurred at pH ≥ 10 and H_2O_2 ≥ 150 mg L^{-1}.

6.3.3 AOP kinetics study

Two different AOP treatment conditions were selected from the contour plots (Fig. 6.3) for a kinetic study to determine the degradation rate constants for BACs. The AOP treatment conditions included 200 mg L^{-1} of H_2O_2 at pH 11 (Treatment-1 or T-1) and 150 mg L^{-1} of H_2O_2 at pH 10 (Treatment-2 or T-2) at a constant O_3 dose (1.28 g h^{-1}) for 2 h. Since individual factors (H_2O_2 and pH) were highly significant with their positive coefficients (Table 6.2); T-1

was expected to be more effective compared to T-2. Treatments 1 and 2 were applied to obtain the degradation rate constants for BDDA and BDTA (Fig. 6.4). It should be noted the degradation experiments were conducted with a mixture of BDDA and BDTA at initial concentrations of BDDA:BDTA of 50:25 mg L^{-1}. Control experiments were conducted without any H_2O_2 or O_3 at an ambient pH (pH = 6.8, solution pH without any further adjustment); negligible loss of BACs due to adsorption on the reactor wall was observed (denoted by the round symbol in Fig 6.4a, 6.4c). The time dependent % removal of the BACs, as shown in Fig 6.4a for BDDA and Fig 6.4c for BDTA, for two different treatment conditions (T-1 and T-2), clearly demonstrate that the T-1 was more effective compared to T-2 in terms of BACs removal. T-1 was able to degrade 90% of the initial BACs in less than 40 min, while T-2 took about 2 h to degrade the same amount of BACs.

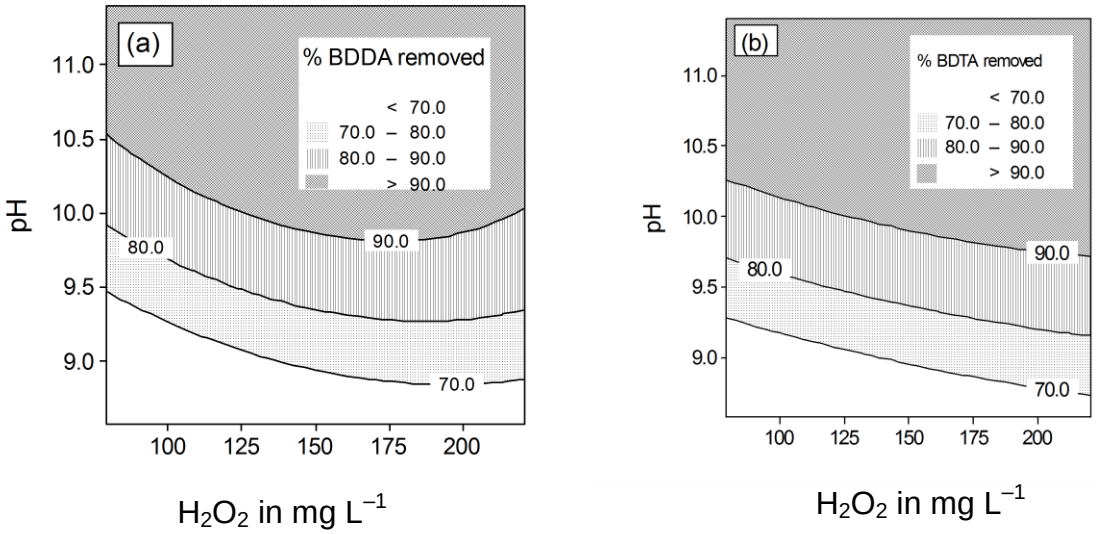

Fig.6.3 Contour plots of the combined effect of pH and H_2O_2 for the % removal of BACs using CCD; (a) BDDA and (b) BDTA. Ozone doses and reaction time were kept constant at 1.28 g h^{-1} and 2 h, respectively.

First order degradation kinetic models were applied for both treatments to calculate the rate of degradation of BACs and are presented in Fig 6.4(b) for BDDA and Fig 6.4d for BDTA. The rate constants were 0.091 min^{-1} and 0.082 min^{-1} for BDDA and BDTA, respectively, for T-1 and are comparable to the overall rate constant obtained for estrone removal using various combination of O_3/UV/H_2O_2 (Sarkar et al., 2014). The rate constants were approximately 4 times lower for T-2. Earlier, Loveira et al. (2012) reported aTiO_2 based photocatalytic degradation rate constant for BDDA as k = 0.023 min^{-1} for initial BDDA concentration of 70 to 390 mg L^{-1}; this value is very close to the rate constant obtained for T-2.

Ozone oxidation of undesired organic compounds and disinfection of water has been a well applied technique for several decades (Hoigné and Bader, 1976). Direct ozonation is very specific for the oxidation of C=C or N=N unsaturated bonds of compounds (Khadhraoui et al. 2009) and the process is known to be very slow compared to indirect ozonation (i.e. •OH radical production through the addition of other catalyst during ozone treatment) (Vandersmissen et al., 2008). In this study, H_2O_2 reacts with O_3 to contribute to the •OH radical production at optimum pH (Munter, 2001; Poyatos et al., 2010). As a result, a sufficient amount and ratio of H_2O_2/ O_3 are important for efficient oxidization of the target compounds. The ratio varies from 0.04 (Alsheyab and Muñoz, 2006) to 0.45 (Paillard et al., 1988) for various compounds and for various treatment conditions, such as ozone dose, contact time, alkalinity of water, etc.

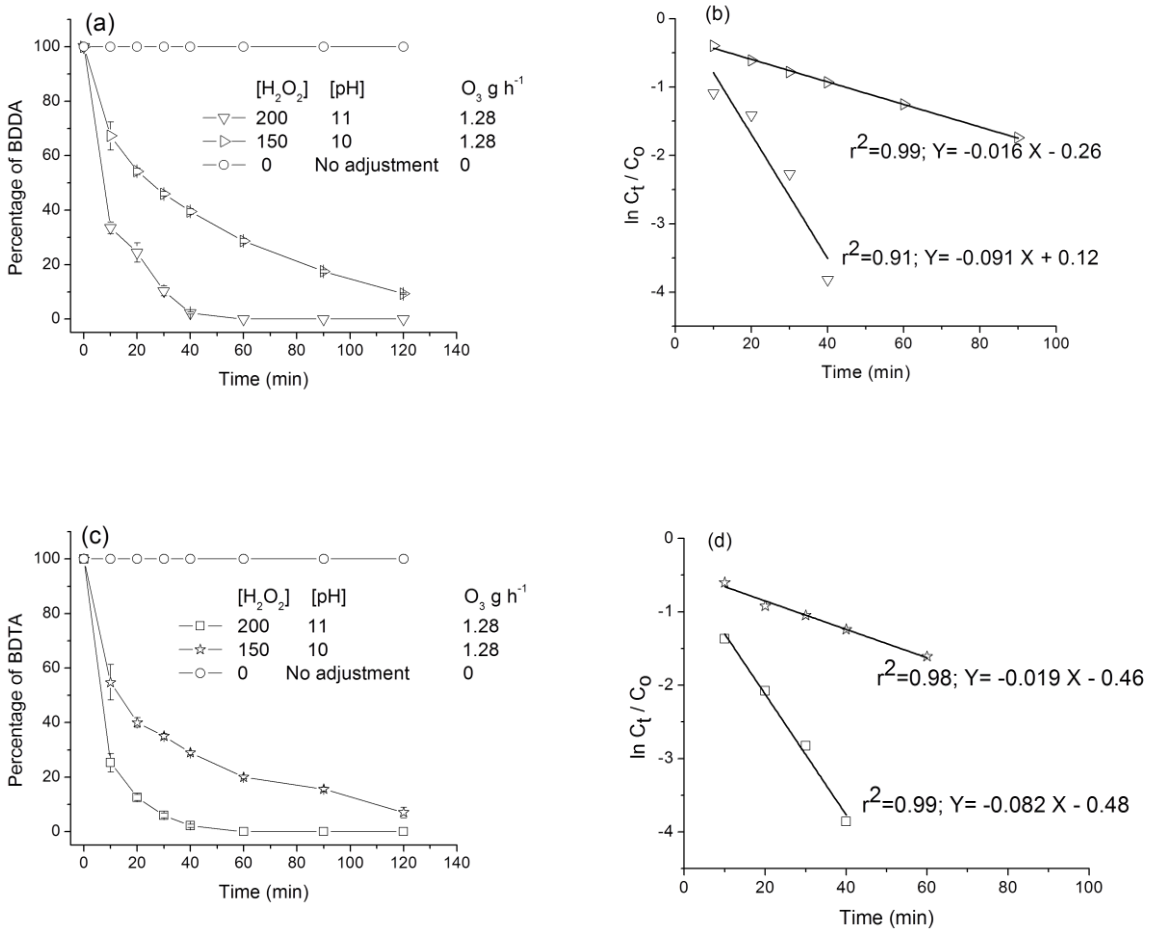

Fig.6.4 Kinetics of BACs degradation in two different AOP conditions and their first order degradation models. Treatment-1 had 200 mg L^{-1} H_2O_2 at pH 11 and treatment-2 had 150 mg L^{-1} H_2O_2 at pH 10. (a) Degradation of BDDA; (b) first order degradation model for BDDA; (c) degradation of BDTA; (d) first order degradation model for BDTA. Ozone doses were constant at 1.28 g h^{-1}. The experiments were conducted in mixture of BDDA: BDTA at 50: 25 mg L^{-1} as the initial concentration in Milli-Q water.

In this study, >90% removal of the initial BACs occurred in less than 40 min for T-1 (Fig 6.4a and 6.4c) and was achieved with the initial molar ratio of H_2O_2 to ozone of 0.23 (calculated considering 30 min of ozone dose; 0.64 g O_3 supplied in 30 min = 0.0133 mole of O_3 and initial H_2O_2 for T-1 was 100 mg in 0.5 L= 0.003 mole of H_2O_2. Therefore, H_2O_2/O_3= 0.003/0.0133=0.23). Although, O_3 dissociates immediately after it is in solution, the ratio of H_2O_2/O_3 indicates that O_3 doses were sufficient and the H_2O_2/ O_3 ratio complies with other literature (Paillard et al., 1988). Additionally, utilization of O_3 during AOP for the production of •OH radical (or other radicals, $O^{\bullet-}$; $HO_2^{\bullet}$; $O_3^{\bullet-}$) is important, and the pH of the solution significantly dictates the rate of ozone decay. The decay rate constant of O_3 at pH 9 was found to be *k1* = 4.0* 10^{-3} s^{-1} (Vandersmissen et al., 2008). The rate increases with increasing solution pH (Gardoni et al., 2012). In this experiment, 0.0133 mole of O_3 was supplied during the first 30 min of AOP in T-1 which was expected to decompose entirely to contribute to the AOP.

6.3.4 Formation of intermediates and degradation pathways

Intermediate products of AOP were confirmed by observing the indicative mass fragments ions recorded as $ddMS^2$ by parallel reaction monitoring (PRM). Every cases, fragment ions were produced by splitting of the parent intermediate. Twenty five intermediates were identified in six different (proposed) degradation pathways during O_3/H_2O_2 advanced oxidation of BACs. The TOC (total organic carbon) analysis (data not presented) showed a 10 to 15 % reduction of organic carbon content after 2 h of AOP for T-1, which supported the formation of large number of intermediates. A similar extent of mineralization was observed by Loveira et al., (2012) when TiO_2 based heterogeneous photocatalysis was applied for 3 h to remove BDDA from synthetic water matrices. Empirical formulae of various intermediates, their mass to charge ratio (m/z) with retention time, m/z of fragments ions produced and mass accuracy in ppm are presented under six different degradation pathways from P-1 to P-6 (Table 6.4). Empirical formulae for intermediates indicated the presence of one to five molecular oxygen in their structure. Elution times of intermediates were faster during HPLC separation compared to parent BACs because of their

lower molecular weight compared to BACs and/or the intermediates lead to more polar molecules due to oxygen attachment in their molecular structure (Table 6.4). Mass accuracy was calculated using Equation 6.12, and was found to be less than ±1.2 for all empirical formulae. Lower values of mass accuracy suggest that more accurate empirical formulae were obtained.

$$Mass\ accuracy\ (ppm) = \frac{m/_z(experimantal) - m/_z(theoritical)}{m/_z(theoritical)} * 10^6 \quad \text{----------(6.12)}$$

Relative profiles of the intermediates, determined using the software Xcalibur, with respect to the peak area of parent BACs for the two treatment methods are shown in Fig 6.5 (a to l). The effectiveness of T-1 is evident also in the case of degradation of intermediates. It can be seen that most intermediates formed by T-1 reach a peak concentration within 10 min and degrade significantly faster than T-2. Some of the intermediates show either 2 peaks or a plateau before they degrade in T-2. All intermediates formed in less than 30 min for T-1 regardless of the degradation pathways (P-1 to -6). This observation is consistent with the kinetic results because the degradation rate constant for T-1 was four times higher than that of T-2 (Fig. 6.4). It is interesting to observe that, for P-4, -5 and -6 for T-1, a gradual decline in intermediates was observed but the intermediates under P-6 a, b for T-1 (Fig. 6.5k) were found to increase up to 100 min of treatment. In contrast, various intermediates produced during T-2 continued to form up to 120 min (Fig. 6.5 b, d, f, h, and j). The formation patterns of intermediates were different between T-1 and T-2 because of their different rates of degradation of the parent compounds.

Table 6.4 Identified intermediates (including two parent BACs) due to AOP on BACs. Oxidation pathways, empirical formulae, mass to charge ratio (m/z) with retention time, m/z fragments and mass accuracy (ppm). Six degradation pathways are denoted as P-1 to P-6.

Pathways of degradation	Empirical formula	m/z (Retention time in min)	m/z confirmation fragments for possible structure	Mass accuracy (ppm)
Parent compounds	$C_{21}H_{38}N$ (BDDA)	304.2995 (3.7)	91; 212; 304	-1.13
	$C_{23}H_{42}N$ (BDTA)	332.3309 (3.88)	91; 240; 332	-0.92
P-1	$C_{21}H_{36}ON$	318.2789 (3.36)	91; 183; 226; 318	-0.75
	$C_{23}H_{40}ON$	346.3105 (3.6)	91; 211; 254; 346	-0.32
	$C_{21}H_{34}O_2N$	332.2583 (2.98)	91; 240; 332	-0.318
	$C_{23}H_{38}O_2N$	360.2895 (3.27)	91; 225; 268; 360	-0.51
P-2	$C_9H_{14}N$	136.1121 (2.12)	91; 136	0.47
	$C_9H_{14}ON$	152.1069 (2.19)	91; 152	-0.2
P-3*	$C_{14}H_{32}N$	214.2527 (3.26)	158; 214	-1.05
	$C_{14}H_{32}ON$	230.2476 (3.27)	62; 230	-0.96
	$C_{14}H_{30}O_2N$	244.2271 (3.0)	183; 244	0.018
P-4	$C_{12}H_{18}O_2N$	208.1333 (2.15)	91; 116; 208	0.59
	$C_{13}H_{20}O_2N$	222.1486 (2.21)	87; 91; 222	-0.97
	$C_{14}H_{22}O_2N$	236.1643 (2.29)	91; 101; 236	-0.82
	$C_{15}H_{24}O_2N$	250.1801 (2.42)	91; 115; 158; 250	-0.30
	$C_{16}H_{26}O_2N$	264.1957 (2.57)	91; 128; 264	-0.248
P-5	$C_{16}H_{24}O_3N$	278.1751 (2.32)	91; 143; 278	0.35
	$C_{17}H_{26}O_3N$	292.1904 (2.42)	91; 157; 292	-0.78
	$C_{18}H_{28}O_3N$	306.2060 (2.54)	91; 171; 306	-1.14
	$C_{19}H_{30}O_3N$	320.2216 (2.62)	91; 185; 320	-1.15
P-6**	$C_{12}H_{24}O_3N$	230.1749 (2.14)	169; 230	-0.43
	$C_{13}H_{26}O_3N$	244.1909 (2.24)	183; 244	0.491
	$C_{14}H_{28}O_3N$	258.2062 (2.51)	197; 258	-0.38
	$C_{16}H_{32}O_3N$	286.2377 (2.87)	225; 286	0.10
P-6a	$C_{14}H_{26}O_4N$	272.1854 (2.21)	211; 272	-0.78
	$C_{16}H_{30}O_4N$	300.2167 (2.47)	127; 197; 239; 300	-0.54
P-6b	$C_{12}H_{22}O_5N$	260.1492 (2.05)	153; 199; 260	-0.07

*P-3 produced from BDDA; ** P-6 produced from BDTA; (P-1,-2,-4,-5; intermediates could produce from either BDDA or BDTA)

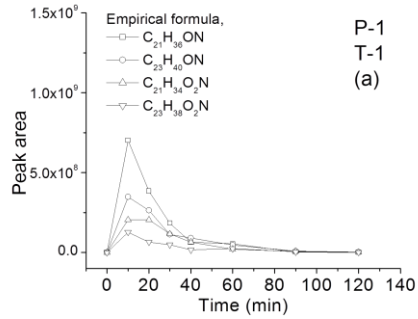
Empirical formula,
$C_{21}H_{36}ON$
$C_{23}H_{40}ON$
$C_{21}H_{34}O_2N$
$C_{23}H_{38}O_2N$
P-1
T-1
(a)
Peak area
Time (min)

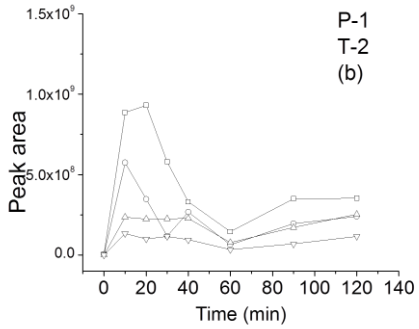
P-1
T-2
(b)
Peak area
Time (min)

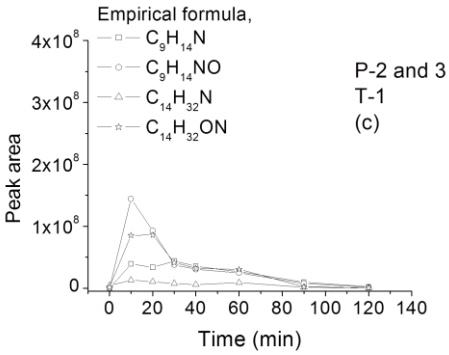
Empirical formula,
$C_9H_{14}N$
$C_9H_{14}NO$
$C_{14}H_{32}N$
$C_{14}H_{32}ON$
P-2 and 3
T-1
(c)
Peak area
Time (min)

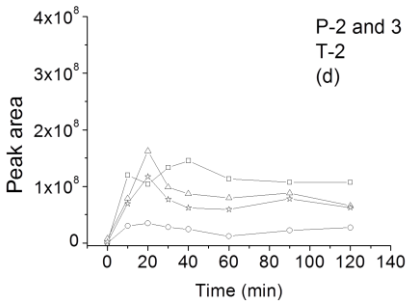
P-2 and 3
T-2
(d)
Peak area
Time (min)

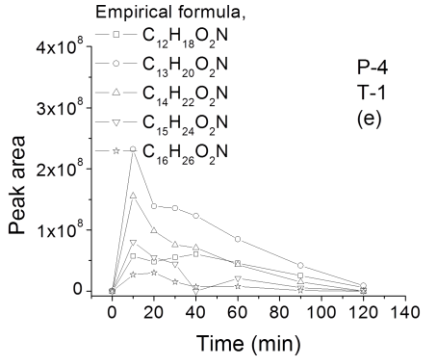
Empirical formula,
$C_{12}H_{18}O_2N$
$C_{13}H_{20}O_2N$
$C_{14}H_{22}O_2N$
$C_{15}H_{24}O_2N$
$C_{16}H_{26}O_2N$
P-4
T-1
(e)
Peak area
Time (min)

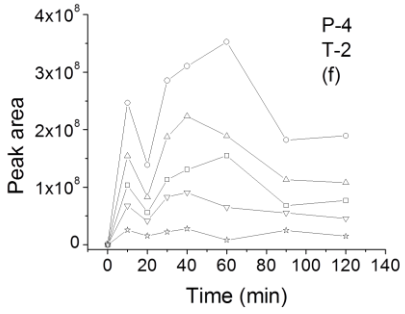
P-4
T-2
(f)
Peak area
Time (min)

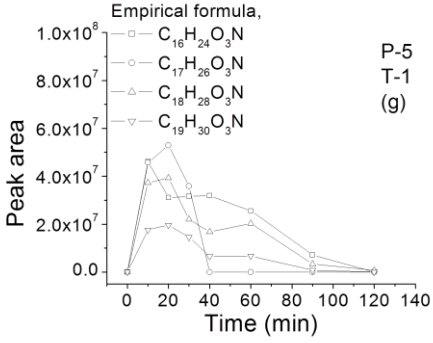
Empirical formula,
$C_{16}H_{24}O_3N$
$C_{17}H_{26}O_3N$
$C_{18}H_{28}O_3N$
$C_{19}H_{30}O_3N$
P-5
T-1
(g)
Peak area
Time (min)

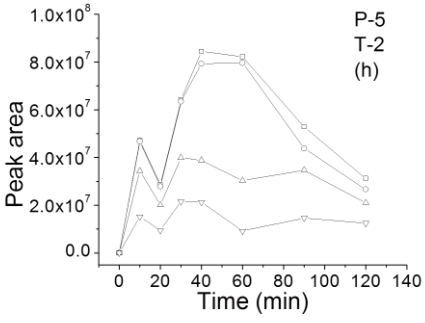
P-5
T-2
(h)
Peak area
Time (min)

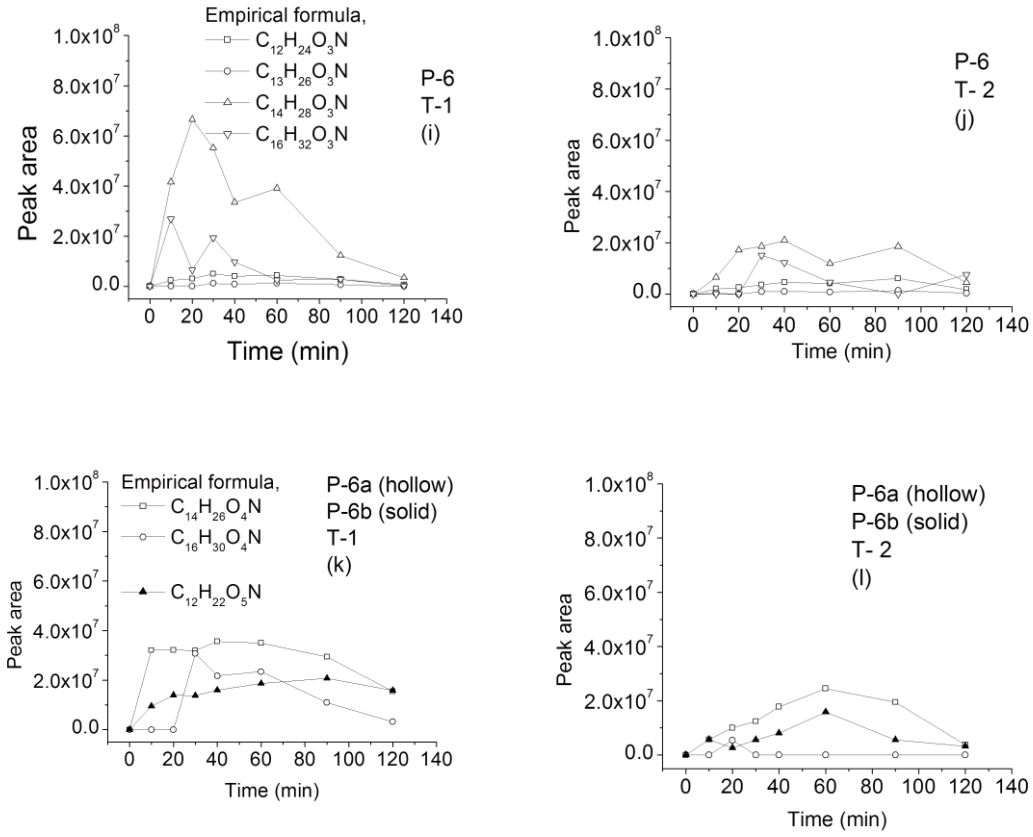

Fig.6.5 Relative quantification of intermediates for T-1 and T-2 with respect to the peak areas of parent BACs.

Degradation pathways corresponded to the structures of BACs; among them P-1, -4 and -5 (Fig. 6.6) occur keeping the hydrophilic (benzyl and ammonium moiety) and hydrophobic part (alkyl chain) intact, while P-2, -3, and -6 involved the cleavage of hydrophilic and hydrophobic parts. Degradation pathways similar to P-1, -2 and -3 were recently identified by Carbajo et al. (2016) when BACs were treated with O_3; although, the authors did not report the pathways P-4, -5, -6 and two additional consecutive paths produced from P-6 are also presented as P-6a and 6b (Fig 6.6). The oxidation of BACs is expected to occur by hydroxyl radical (•OH) and hydroperoxyl radical ($HO_2^{\bullet}$) as they both are formed during ozonation in the presence of H_2O_2 (Munter R., 2001). Hydroperoxyl radicals ($HO_2^{\bullet}$) are unstable and react with O_3 giving a series of chain reactions to produce hydroxyl radical (•OH) (Poyatos et al., 2010). At higher pH, O_3 dissociates faster, providing less opportunity for hydroperoxyl radicals to react with O_3 and higher probability for the BACs to oxidize to form carboxylic groups. On the other hand, hydroxyl radicals (•OH) react with organic compounds in two ways: either hydroxylation (addition to aromatic ring) or abstraction of H atom from C–C saturated bonds through the formation of a carbon centred radical, and both ways lead to the formation of organic carboxylic acids (Geluwe et al., 2011). The initial pH of T-1 (pH 11) and T-2 (pH 10) fell to pH 5.2 ± 0.3 after 2 h of AOP suggesting that organic acids were formed during the process.

The structural confirmation of intermediates was carried out by observing the diagnostic mass fragments ions (Table 6.4) obtained as $ddMS^2$ by parallel reaction monitoring after analyzing the extracted ion chromatograms of putative intermediates detected. Since, the AOP experiments were conducted as a mixture of BACs and both BDDA/BDTA have the same alkyl chain with an exception of an additional two carbon atoms in BDTA, intermediates as identified after AOP could be from any of the BACs. As presented in Fig 6.6, intermediates in P-1, -2, -4 and -5 could be produced from both BACs but the P-3 and P-6 (6, 6a and 6b) were derived from BDDA and BDTA, respectively (Fig 6.6).

All intermediates under P-1, -2, -4 and -5 contained the fragment 91 ($–C_7H_7$) (Table 6.4), suggesting that the oxidation occurred without debenzylation (cleavage of C_{benzyl}–N bonds) of the BACs molecules and the intermediates contained a benzene ring in their

structure. The remaining P-3 and P-6 occurred due to the oxidation of alkyl chain after the cleavage of C_{benzyl}–N bonds (debenzylation) of BDDA and BDTA. In both pathways (i.e., P-3 and -6), hydroxylation with an ammonium moiety and hydrogen abstraction from the alkyl chain produced all 10 intermediates as presented in Table 6.4 and Fig. 6.6. Hydrogen abstraction in the alkyl chain produced carbon centred radicals, which further reacted with dissolved oxygen to form peroxyl radicals and subsequently decomposed to carbonyl compounds (Geluwe et al., 2011). Carbonyl compounds may form at different positions of the carbon chain producing different isomers and was not further investigated. A similar hydrogen abstraction mechanism has been proposed for P-1 for all four intermediates (Table 6.4 and Fig. 6.6). Degradation pathway P-2 involved the breakage of C_{alkyl}–N bonds (dealkylation) and hydroxylation occurred with ammonium moiety ($C_9H_{14}ON^+$, m/z 152.1069).

The initial steps for P-4 and -5 involved the splitting of a portion of an alkyl chain (for P-4, $–C_5H_{10}$ from BDDA or $–C_7H_{14}$ from BDTA; and for P-5, $-C_2H_4$ from BDDA or $–C_4H_8$ from BDTA) and further oxidation of the alkyl chain formed all 9 intermediates. In both cases, for P-4 and -5, m/z fragments of intermediates (Table 6.4) supported the conclusion that a –COOH group (molecular mass = 45) was attached to the intermediates and hydroperoxyl radicals ($HO_2^{\bullet}$) could be responsible for the oxidation of hydrocarbons ($–CH_3$ groups in the alkyl chain) to the carboxylic acid group. For example, in P-5, the first intermediate, $C_{19}H_{30}O_3N$ (m/z=320) had the fragments such as, 91+ 185+ (–COOH), which is equal to the protonated m/z of the parent intermediate. A further hydrogen abstraction mechanism took place for P-5 in the alkyl chain.

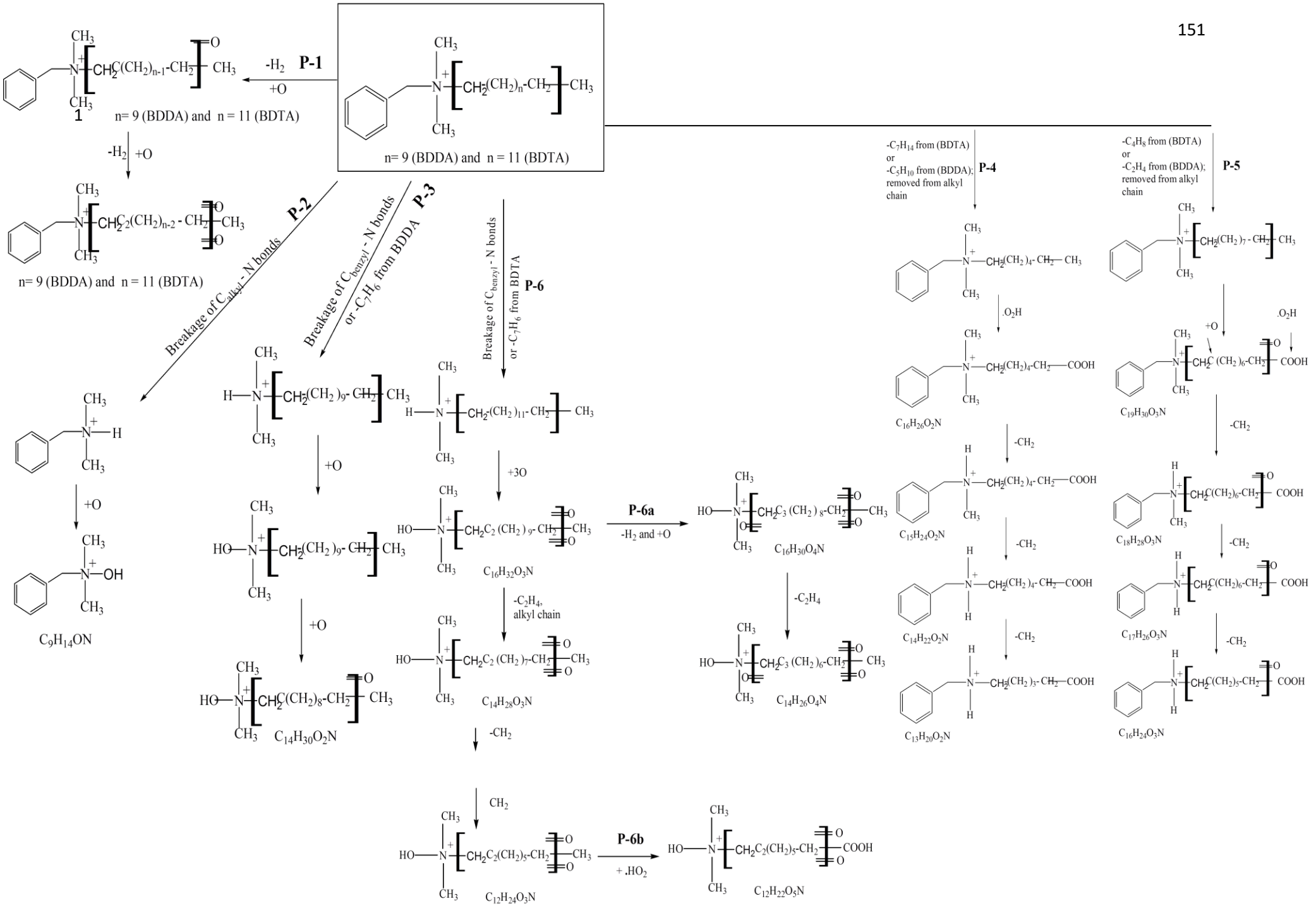

Fig.6.6 Proposed degradation pathways during AOP using O_3/H_2O_2.

Degradation pathways of P-4, -5, -6 and 6a produced a number of intermediates which differed by $–CH_2$ units (CH_2 = 14.01565 Da, IUPAC mass). It was possible to visualize and group related intermediates that differ by the number of CH_2 units by scaling the observed m/z to the Kendrick mass and plotting that against the Kendrick mass defect (Hughey et al., 2001). To do that, the monoisotopic mass of intermediates under P 4, 5, 6 and 6a was converted to Kendrick mass scale by multiplying the monoisotopic mass with the ratio of 14/14.01565 (i.e. based on ^{12}C atomic mass as exactly 12 Da) (Hughey et al., 2001) and further Kendrick mass defect was calculated using the following Equation 6.13;

Kendrick mass defect = (nominal Kendrick mass – exact Kendrick mass) ---------- (6.13)

A visual presentation of the Kendrick plot for P-4, -5, -6 and -6a is presented in Fig. 6.7. The horizontal distribution of intermediates under each degradation path suggested that they were produced from the same initial oxidation process.

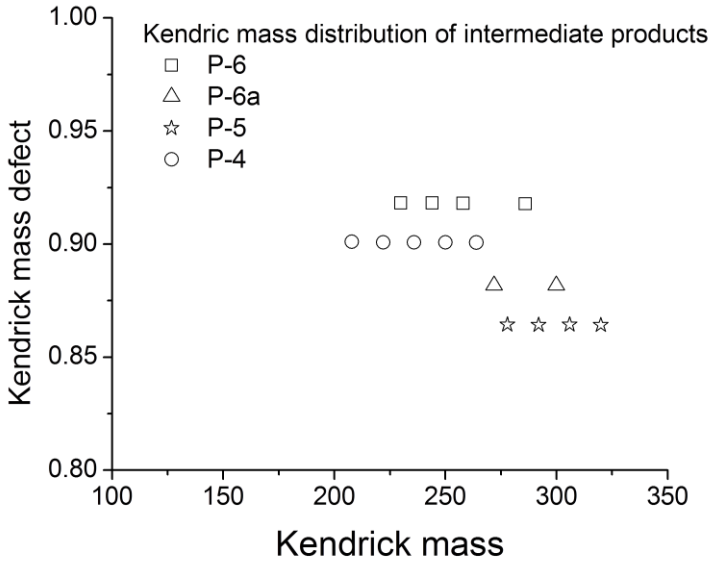

Fig.6.7 Kendrick mass defect vs Kendrick mass for visual interpretation for P-4,-5,-6 and -6a. The vertical separation of the compound represents the mass defect and simultaneous horizontal distribution indicates the separation of CH_2 groups from the initial intermediates.

6.3.5 Toxicity of AOP treated solutions

Two freshwater algae species, *Chlorella vulgaris* and *Chlamydomonas reinhardtii,* were used to evaluate the toxicity of the AOP-treated BAC solutions. According to the Organisation for Economic Cooperation and Development guidelines (OECD, 1984), *C. vulgaris* can be used for toxicity analysis because of their fast growth rate and they have been used to test many compounds, such as pentachlorophenol (Silva et al., 2001). The other species, *C. reinhardtii* has been used earlier to assess the toxicity of perfluorooctanoic acid (Hu et al., 2014) and pentachlorophenol (Silva et al., 2001).

Toxicity was measured in terms of the growth rate of the algal species during their exponential phase and the results are presented in Fig 6.8(a) for *C. vulgaris* and Fig 6.8(b) for *C. reinhardtii*. Growth of both algal species was completely halted (growth rate ≤ 0.014 d^{-1}) after 8 d of incubation when grown in the initial, untreated mixture of 0.4:0.2 mg L^{-1} BDDA:BDTA. On the other hand, the growth rates of *C. vulgaris* control, and solutions after AOP treatment (T-1 and T-2) were 0.41 d^{-1}, and 0.37 d^{-1}, respectively (Fig 6.8a). Similar high growth rates were measured for *C. reinhardtii* in control and AOP-treated samples (Fig 6.8b). The similar growth rates for control and AOP-treated solutions suggest that AOP treatment completely removed the toxic effect of BACs in water. Apparently, the concentration range for toxic effects (i.e., LC_{50}) of BACs was > 120 μg L^{-1} in 24 h for the monoalgal cultures of *Isochrysis galbana* and *Chaetoceros gracilis* (Pérez et al., 2009).

The presence of ≤ 10% of the initial BACs after 2 h of AOP in T-2 did not have a toxic effect on the algal species; as a result, it can be expected that the same amount of BACs remaining (Fig 6.4a and 6.4c) after 30 min of AOP using T-1 would also be free of any toxic effect. However, no time-dependent toxicity experiments were conducted for the selected AOPs. It is encouraging to note that despite the presence of numerous intermediates (25 identified intermediates in the range of 1 to 2 orders of magnitude lower than the initial BACs concentration) using T-1 and T-2, the resulting solutions are non-toxic to the algae.

6.3.6 Biodegradability of AOP treated solutions

Biodegradability of BACs in solution was determined after AOP for two different treatment conditions (T-1 and T-2). Biodegradability was measured as the ratio of BOD_5 to COD and is presented in Fig 6.9. In the same figure, a time dependent H_2O_2 concentration for T-1 has been presented to determine the amount of catalase required to quench the residual H_2O_2 necessary for biodegradability tests (Fig 6.9 solid symbols). After 2 h of AOP, nearly 60 mg L^{-1} of H_2O_2 remained unreacted for T-1; indicating approximately 140 mg L^{-1} was consumed during the AOP.

Biodegradability of BACs increased with time for both treatments (Fig 6.9). After 30 min of AOP, the BOD_5 to COD ratio increased to 0.3 for T-1 and 0.2 for T-2 from the initial

ratio of less than 0.1. A ratio ≥ 0.5 indicates the waste is easily biodegradable; a ratio ≤ 0.3 indicates the waste either has some toxic components or may require acclimated microorganisms (Metcalf and Eddy, 2014). Improvement of biodegradability after various oxidation processes has been found for other sources of contaminants (Melero et al., 2009; Preethi et al., 2009). These results and our toxicity results (Section 6.3.5) support the suitability of O_3/H_2O_2 oxidation at elevated pH as a pretreatment before biological treatment for the treatment of wastewater, including various industrial effluents (such as hospital effluents or effluents from food industries) that contain BACs.

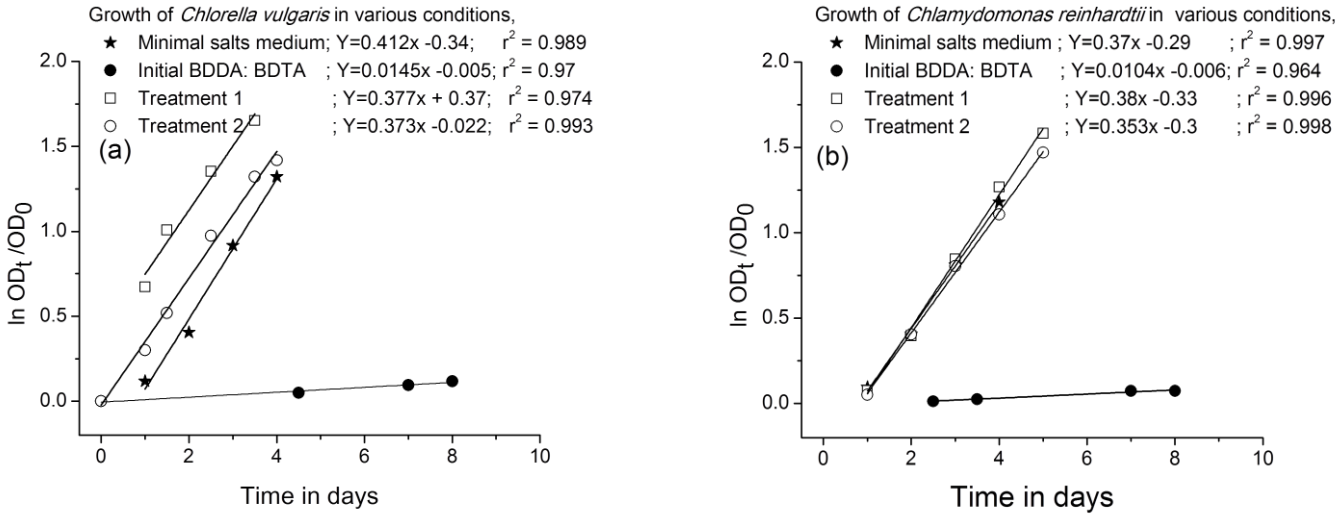

Fig.6.8 Toxicity test of AOP treated solutions using (a) *Chlorella vulgaris* and (b) *Chlamydomonas reinhardtii* in duplicate. The initial concentration of BDDA:BDTA for the experiment was 0.4:0.2 mg L^{-1}. Treatments 1 (T-1) and 2 (T-2) indicate solutions after AOP treatment. Conditions in T-1 were 200 mg L^{-1} H_2O_2, pH-11 and in T-2 were 150 mg L^{-1} H_2O_2, pH-10; ozone was constant at 1.28 g h^{-1} for 2 h.

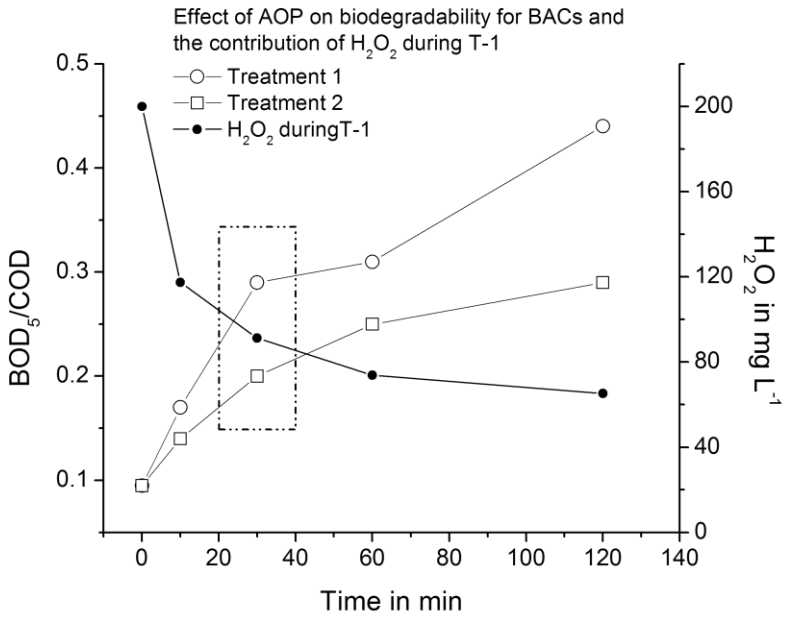

Fig.6.9 Effect of AOP on the biodegradability of solutions containing BACs and the contribution of H_2O_2 during T-1 of the AOP in duplicate samples. Conditions in T-1 were 200 mg L^{-1} H_2O_2, pH-11 and in T-2 were 150 mg L^{-1} H_2O_2, pH-10; ozone was constant at 1.28 g h^{-1} for 2 h. The rectangle with dotted line shows the improvement of biodegradability after 30 min of AOP between T-1 and T-2.

6.3.7 AOP applied in wastewater influent

Toxicity of primary wastewater influent spiked with BACs was assessed after AOP using RAS and the results were compared without the AOP (Fig 6.10). LB-agar was used to stimulate bacterial growth, imitating an activated sludge process containing enough food for sufficient growth of mixed bacterial cultures. To assess the effectiveness of AOP on wastewater spiked with BACs a qualitative assessment has been presented.

In Fig 6.10a, the mixed bacterial cultures did not grow on LB-agar in presence of the BACs mixture prepared in Milli-Q water; in contrast, very little growth of the cultures on LB-agar was observed in the presence of BDDA: BDTA at 50:25 mg L^{-1} spiked in wastewater before AOP (Fig 6.10b). The minimal growth observed in Fig 6.10b might be due to the fact that cationic charges of BACs interact with the negatively charged suspended particles in wastewater, thereby reducing the bactericidal effects of BACs to some extent (Araújo et al., 2013).

On the other hand, after 30 and 60 min of T-1 of wastewater with the same initial concentration of BACs, the mixed bacterial cultures grew as shown in Fig 6.10c and 6.10d, respectively. The growth of mixed bacterial cultures (Fig. 6.10c and 6.10d) was obviously greater than those seen in Fig 6.10a and 6.10b and was comparable to growth observed in LB-agar (without any BACs, Fig 6.10e). The results obtained after AOP treatment of wastewater are in agreement with the kinetic study discussed earlier, suggesting T-1 of AOP is capable of removing BACs so that mixed bacterial cultures could grow (Fig. 6.10c and 6.10d) as readily as in nutrient media (Fig. 6.10e). Biodegradability was also found to improve after 30 min of AOP for the same treatment conditions (Fig 6.9). No observable interferences in the efficiency of the O_3/H_2O_2 based AOP were found due to the turbidity of wastewater and similar results were seen by Huber et al. (2005) for the removal of pharmaceuticals from wastewater using ozonation. The results obtained after AOP of primary wastewater influent with BACs suggested that the selected AOP enhanced the biodegradability of BACs in wastewater indicating suitability of AOP as a viable pretreatment before biological treatment, as well as reducing the toxicity of BACs.

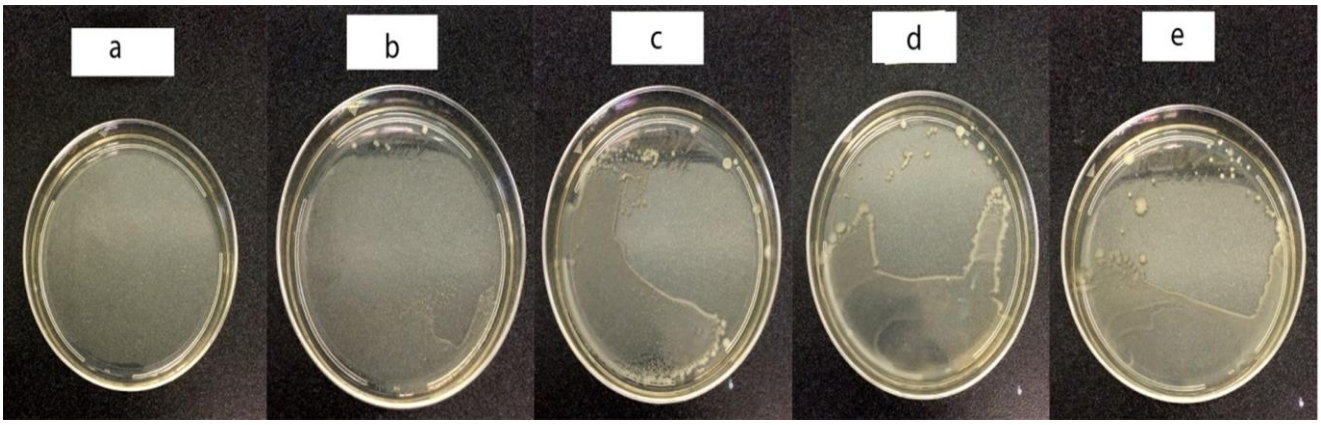

Fig.6.10 Growth of mixed bacterial cultures in presence of BDDA:BDTA at 50:25 mg L^{-1} with wastewater on LB-agar plates after 24 h incubation at 37°C. (a) BDDA:BDTA at 50:25 mg L^{-1} prepared in Milli-Q water; (b) BDDA:BDTA at 50:25 mg L^{-1} spiked in wastewater before AOP; (c) Wastewater after 30 min of AOP, (T-1); (d) Wastewater after 60 min of AOP (T-1) and (e) on LB-agar without BDDA and/or BDTA .

6.3.8 Cost estimation of AOP treatment for BACs containing solutions

The rate constants obtained from the kinetic study (Fig 6.4b and 6.4d) were used in Equation 6.9 to calculate the reaction time required for AOP for 90% removal of the target pollutants in the wastewater reactor. Higher rate constants for the removal of BACs were achieved by T-1 compared to T-2 and the values for BDDA and BDTA were k = 0.091 min^{-1} and k = 0.082 min^{-1}, respectively. The AOP reaction time was considered to be 30 min for the mixture of BACs (calculated times using Equation 6.9 for BDDA and BDTA were 25 and 28 min, respectively), for the purposes of the cost estimation.

With AOP T-1, the total cost was calculated to be $1.7 USD to treat 1000 US gal of BAC-contaminated wastewater in batch (or $0.44 USD per m^3 of WW) (see supplementary at the

end of this chapter). Of the total cost, highest cost (55%) is due to the chemicals, followed by labour and analytical costs (37.3%), and the remaining is capital investment and electrical cost (7.3%). The treatment of estrone with O_3/H_2O_2 was calculated to be less than $1.00 USD per 1000 gallons by Sarkar et al., (2014); however, it should be noted that the authors used 20 mg L^{-1} of H_2O_2 with O_3 to treat less than 5 mg L^{-1} of estrone. The cost of color removal from a polyester and acetate fibre dyeing effluent was calculated to be approximately $20 USD for 1000 US gal when ozone was used alone as an oxidant (Azbar et al., 2004). Other advanced oxidation techniques, such as ultrasound and/or ultraviolet, seem to be even more expensive; however, the cost dropped when these techniques were combined with O_3 and/or hydrogen peroxide (Mahamuni and Adewuyi, 2010).

6.4 Conclusions

Combined AOP pretreatment followed by biological treatment could be a cost-viable approach for future water treatment technologies, which will eventually reduce the concentration of recalcitrant organic pollutants (e.g., BACs) from various effluents. In this work, O_3/H_2O_2 oxidation was effective in removal of toxicity of two quaternary ammonium compounds and improved their biodegradability. To conduct AOP on IWW from various sources is essential to fully assess the technology as a pretreatment method. Fenton reagent or ferret might be an interesting alternative to O_3/H_2O_2 treatment process for future investigations. Addition of H_2O_2 doses during O_3/H_2O_2 treatment in instalment might be interesting to investigate for any further improvement of the process. Efficiency of O_3 generator (capable of producing high amount of O_3 with same flow rate) will reduce the process cost.

Supplementary for cost estimation

Cost estimation

The cost estimation of AOP was adopted from method described by Mahamuni and Adewuyi (2010) without further modifications. The annual cost of AOP was calculated based

on a total flow of wastewater of $5256*10^5$ L (or $1388.5*10^5$ US gallons) at a flow rate of 1000 L min^{-1} for 365 d.

Capital cost for O_3 generator

During the AOP, the O_3 dose was kept constant at 1.28 g h^{-1} and an ozone generator HC-30 (www.ozonesolutions.com), capable of producing ozone at a rate of 30 g h^{-1}, is sufficient for the system with an estimated cost of $ 7540 (displayed on the vendor's web-site). In Table 6.S1, symbol 'R' represents the cost of AOP reactor and the symbol 'T' represents the subtotal under each subsection to calculate the total capital cost per year.

Table 6.S1 General calculation of capital cost for a single AOP reactor (HC-30).

Item	Symbol	Cost in USD
AOP reactor (HC-30)	R	7540
Piping, valves, electrical (30%)	0.3 R	2262
Site work (10%)	0.1 R	754
Subtotal	1.4 R = T1	10556
Contractor O&P (15%)	0.15 T1	1583.4
Subtotal	1.15 T1 = T2	12139.4
Engineering (15%)	0.15 T2	1820.9
Subtotal	1.15 T2 = T3	13960
Contingency (20%)	0.2 T3	2792
Total capital cost per year	1.2 T3	16752

Since, the O_3 generator is replaced every year, no amortization cost will be considered.

Operation & Maintenance cost

Table 6.S2 Steps of O & M cost.

Item	Description	Cost in USD
Part replacement	1.5% of capital cost	251
Labour (reservoir connected with a pump can be used for H_2O_2 and pH adjustment using NaOH, so no additional labour cost was considered)	Ozone system O & M 48 (h) General O & M 312 (h) Annual sampling (4 samples per week and one h per sample) 208 (h) Total labour = 568 (h) Rate, \$80 h^{-1}	45440
Analytical costs	208 (h) at \$200 h^{-1}	41600
Chemical costs	Cost of H_2O_2: H_2O_2 50% (w/w); density = 1.197 g mL^{-1} (http://www.sigmaaldrich.com/catalog/product/sial/516813?lang=en&region=CA) Total H_2O_2 required at 200 mg L^{-1} = 157680 L. Commercial price = \$661 per 1000 kg = 104226\$ (http://www.alibaba.com) Cost of NaOH to raise pH of solution: Approximately 63072 kg NaOH is required per year to raise pH from 7 to 11 (pH 7 to 8 is the common pH of municipal wastewater) Commercial price = 410 \$ per 1000 kg = 25859 \$ (http://www.alibaba.com)	130085
Electrical costs	HC-30 (ozone generator) with energy consumption rate = 120 VAC * 5 amps = 600 watts or 0.6 kw per h.	473 USD

	For uninterrupted operation for 365 d, total energy consumption = 8760 h * 0.6 kW per h = 5256 kWh per year Unit price of London Hydro, Canada, 12.8 c kWh^{-1} = 0.09 USD (https://www.londonhydro.com/site/#!/) So, 5256 kWh * 0.09 USD/ kWh = 473 USD	
Total O & M	Part replacement cost + Labour cost + Analytical costs + Chemical costs + Electrical costs =	217849 USD

So, Total AOP investment and operating (including maintenance cost) cost = Total capital cost per year + Total O & M cost = (16752 + 217849) USD = 234601 USD

Total WW generated = $5256*10^5$ L yr^{-1}

AOP treatment cost = $\frac{234601\ USD}{5256*\ 10^5\ L}\ *\ \frac{3785.41\ L}{1000\ US\ gallon}$ = 1.68 USD per 1000 US gallon of WW

References

Adams C.D., Kuzhikannil J.J., 2000. Effects of UV/H_2O_2 peroxidation on the aerobic biodegradability of quaternary amine surfactants. Water Research 34, 668–672.

Alaton I.A., Dogruel S., Baykal E., Gerone G., 2004. Combined chemical and biological oxidation of penicillin formulation effluent. Journal of Environmental Management 73, 155–163.

Alsheyab M.A., Muñoz A.H., 2006. Reducing the formation of trihalomethanes (THMs) by ozone combined with hydrogen peroxide (H_2O_2/O_3). Desalination 194, 121–126.

Andreozzi R., Caprio V., Insola A., Marotta R., 1999. Advanced oxidation processes (AOP) for water purification and recovery. Catalysis Today 53, 51–59.

APHA, AWWA, WPCF, 2005. Standard methods for the examination of water and wastewater. American Public Health Association/American Water Works Association/Water Environment Federation, Washington DC, USA.

Araújo P.A., Lemos M., Mergulhão F., Melo L., Simões M., 2013**.** The influence of interfering substances on the antimicrobial activity of selected quaternary ammonium compounds. International Journal of Food Science 2013, 1–9. (https://www.hindawi.com/journals/ijfs/2013/237581/)

Azbar N., Yonar T., Kestioglu K., 2004. Comparison of various advanced oxidation processes and chemical treatment methods for COD and color removal from a polyester and acetate fiber dyeing effluent. Chemosphere 55, 35–43.

Bader H., Hoigné J., 1981. Determination of ozone in water by the indigo method. Water Research 15, 449–456.

Bassey D.E., Grigson S.J.W., 2011. Degradation of benzyldimethyl hexadecylammonium chloride by *Bacillus niabensis* and *Thalassospira* sp. isolated from marine sediments. Toxicological and Environmental Chemistry 93, 44-56.

Brycki B., Waligórska M., Szulc A., 2014. The biodegradation of monomeric and dimeric alkylammonium surfactants. Journal of Hazardous Materials 280, 797–815.

Cantwell R.E., Hofmann R., 2011. Ultraviolet absorption properties of suspended particulate matter in untreated surface waters. Water Research 45, 1322–1328.

Carbajo J.B., Petre A.L., Rosal R., Berná A., León P., García-Calvo E., Perdigón-Melón J.A., 2016. Ozonation as pretreatment of activated sludge process of a wastewater containing benzalkonium chloride and NiO nanoparticles. Chemical Engineering Journal 283, 740–749.

Chang S.H., Teng T.T., Ismail N., 2011. Optimization of Cu(II) extraction from aqueous solutions by soybean-oil-based organic solvent using response surface methodology. Water Air Soil Pollution 217, 567–576.

Cho I.H., Zoh K.D., 2007. Photocatalytic degradation of azo dye (Reactive Red 120) in TiO2/UV system: optimization and modeling using a response surface methodology (RSM) based on the central composite design. Dyes and Pigments 75, 533–543.

Clara M., Scharf S., Scheffknecht C., Gans O., 2007. Occurrence of selected surfactants in untreated and treated sewage. Water Research 41, 4339–4348.

Ferk F., Misık M., Hoelzl C., Uhl M., Fuerhacker M., Grillitsch B., Parzefall W., Nersesyan A., Micieta K., Grummt T., Ehrlich V., Knasmuller S., 2007. Benzalkonium chloride (BAC) and dimethyldioctadecyl-ammonium bromide (DDAB), two common quaternary ammonium compounds, cause genotoxic effects in mammalian and plant cells at environmentally relevant concentrations. Mutagenesis 22, 363–370.

Ferrer I., Furlong E.T., 2002. Accelerated solvent extraction followed by on-line solid-phase extraction coupled to ion trap LC/MS/MS for analysis of benzalkonium chlorides in sediment samples. Analytical Chemistry 74, 1275–1280.

Gardoni D., Vailati A., Canziani R., 2012. Decay of Ozone in Water: A Review. Ozone: Science & Engineering 34, 233–242.

Garner K.L., Keller A.A., 2014. Emerging patterns for engineered nanomaterials in the environment: a review of fate and toxicity studies. Journal of Nanoparticle Research 16, 2502–2530.

Geluwe S.V., Braeken L., Bruggen B.V., 2011. Ozone oxidation for the alleviation of membrane fouling by natural organic matter: A review. Water Research 45, 3551–3570.

Gerba C.P., 2015. Quaternary ammonium biocides: Efficacy in application. Applied and Environmental Microbiology 81, 464-469.

Hidaka H., Zhao J., Peiizzetti E., Serpone N., 1992. Photodegradation of surfactants. 8. Comparison of photocatalytic processes between anionic sodium dodecylbenzenesulfonate and cationic benzyldodecyldlmethylammonlum chloride on the TiO_2 surface. Journal of Physical Chemistry 96, 2226–2230.

Hoigné J., Bader H., 1976. The role of hydroxyl radical reactions in ozonation process in aqueous solutions. Water Research 10, 377–386.

Huber M.M., GÖbel A., Joss A., Hermann N., LÖffler D., Mcardell C.S., Ried A., Siegrist H., Ternes T.A., Gunten U.V., 2005. Oxidation of pharmaceuticals during ozonation of municipal wastewater effluents: a pilot study. Environmental Science and Technology 39, 4290–4299.

Hughey C.A., Hendrickson C.L., Rodgers R.P., Marshall A.G., Qian K., 2001. Kendrick mass defect spectrum: a compact visual analysis for ultrahigh-resolution broadband mass spectra. Analytical Chemistry 73, 4676-4681.

Hu C., Luo Q., Huang Q., 2014. Ecotoxicological effects of perfluorooctanoic acid on freshwater microalgae *chlamydomonas reinhardtii* and *scenedesmus obliquus*. Environmental Toxicology and Chemistry 33, 1129–1134.

Ismail Z.Z., Tezel U., Pavlostathis S.G., 2010. Sorption of quaternary ammonium compounds to municipal sludge. Water Research 44, 2303–2313.

Khadhraoui M., Trabelsi H., Ksibi M., Bouguerra S., Elleuch B., 2009. Discoloration and detoxicification of a Congo red dye solution by means of ozone treatment for a possible water reuse. Journal of Hazardous Materials 161, 974–981.

Khan A.H., Topp E., Scott A., Sumarah M., Macfie S.M., Ray M.B., 2015**.** Biodegradation of benzalkonium chlorides singly and in mixtures by a *Pseudomonas* sp. isolated from returned activated sludge. Journal of Hazardous Materials 299, 595–602.

Khan A.H., Shang J.Q., Alam R., 2014. Optimization of sample preparation method of total sulphur measurement in mine tailings. International Journal of Environmental Science and Technology 11, 1989–1998.

Kim M., Chowdhury M.M.I., Nakhla G., Keleman M., 2015. Characterization of typical household food wastes from disposers: Fractionation of constituents and implications for resource recovery at wastewater treatment. Bioresource Technology 183, 61–69.

Kümmerer K., Eitel A., Braun U., Hubner P., Daschner F., Mascart G., Milandri M., Reinthaler F., Verhoef J., 1997. Analysis of benzalkonium chloride in the effluent from European hospitals by solid-phase extraction and high-performance liquid chromatography with post-column ion-pairing and fluorescence detection. Journal of Chromatography A 774, 281–286.

Li X., Luo X., Mai B., Liu J., Chen L., Lin S., 2014. Occurrence of quaternary ammonium compounds (QACs) and their application as a tracer for sewage derived pollution in urban estuarine sediments. Environmental Pollution 185, 127-133.

Liu W., Andrews S.A., Stefan M.I., Bolton J.R., 2003. Optimal methods for quenching H_2O_2 residuals prior to UFC testing. Water Research 37, 3697–3703.

Loveira E.L., Fiol P.S., Senn A., Curutchet G., Candal R., Litter M.I., 2012. TiO_2-photocatalytic treatment coupled with biological systems for the elimination of benzalkonium chloride in water. Separation and Purification Technology 91, 108–116.

Lovern S.B., Klaper R., 2006. Daphnia magna mortality when exposed to titanium dioxide and fullerene (C_{60}) nanoparticles. Environmental Toxicology and Chemistry 25, 1132-1137.

Mahamuni N.N., Adewuyi Y.G., 2010. Advanced oxidation processes (AOPs) involving ultrasound for waste water treatment: A review with emphasis on cost estimation. Ultrasonics Sonochemistry 17, 990–1003.

Martínez-Carballo E., González-Barreiro C., Sitka A., Kreuzinger N., Scharf S., Gans O., 2007. Determination of selected quaternary ammonium compounds by liquid chromatography with mass spectrometry. Part II. Application to sediment and sludge samples in Austria. Environmental Pollution 146, 543-547.

Melero J.A., Martínez F., Botas J.A., Molina R., Pariente M.I., 2009. Heterogeneous catalytic wet peroxide oxidation systems for the treatment of an industrial pharmaceutical wastewater. Water Research 43, 4010–4018.

Merényi G., Lind J., Naumov S., Sonntag C.V., 2010. Reaction of ozone with hydrogen peroxide (peroxone process): a revision of current mechanistic concepts based on thermokinetic and quantum-chemical considerations. Environmental Science and Technology 44, 3505–3507.

Metcalf and Eddy., 2014. Wastewater engineering treatment and reuse, 4th Edition, McGraw Hill Eucation, pp- 1460 –1463.

Munter R., 2001. Advanced oxidation processes current status and prospects. Proceedings of the Estonian Academy of Sciences. 50, 59–80.

Myers R.H., Montgomery D.C., 2002. Response Surface Methodology, Process and Product Optimization Using Designed Experiments, 2nd edn. John Wiley & Sons, Canada

OECD-201, 1984. Algae growth inhibition test, guideline for testing chemicals. (http://www.oecd.org/chemicalsafety/risk-assessment/1948257.pdf; accessed September 2016)

Otero-González L., Field J.A., Sierra-Alvarez R., 2014. Inhibition of anaerobic wastewater treatment after long-term exposure to low levels of CuO nanoparticles. Water Research 58, 160–168.

Otero-González L., Field J.A., Sierra-Alvarez R., 2014**.** Fate and long-term inhibitory impact of ZnO nanoparticles during high-rate anaerobic wastewater treatment. Journal of Environmental Management 135, 110–117.

Paillard H., Brunet R., Dore M., 1988. Optimal conditions for applying an ozone-hydrogen peroxide oxidizing system. Water Research 22, 91–103.

Pérez P., Fernández E., Beiras R., 2009. Toxicity of benzalkonium chloride on monoalgal cultures and natural assemblages of marine phytoplankton. Water Air Soil Pollution 201, 319–330.

Poyatos J.M., Muñio M.M., Almecija M.C., Torres J.C., Hontoria E., Osorio F., 2010. Advanced oxidation processes for wastewater treatment: state of the art. Water Air Soil Pollution 205, 187–204.

Prakash O., Talat M., Hasan S.H., Pandey R.K., 2008. Factorial design for the optimization of enzymatic detection of cadmium in aqueous solution using immobilized urease from vegetable waste. Bioresource Technology 99, 7565–7572.

Preethi V., Parama Kalyani K.S., Iyappan K., Srinivasakannan C., Balasubramaniam N., Vedaraman N., 2009. Ozonation of tannery effluent for removal of cod and color. Journal of Hazardous Materials 166, 150–154.

Sarkar S., Ali S., Rehmann L., Nakhla G., Ray M.B., 2014. Degradation of estrone in water and wastewater by various advanced oxidation processes. Journal of Hazardous Materials 278, 16–24.

Silva J., Iannacone J., Cifuentes A., Troncoso L., Bay-Schmith E., Larrain A., 2001. Assessment of sensitivity to pentachlorophenol (PCP) in 18 aquatic species, using acute and chronic ecotoxicity bioassays. Ecotoxicology and Environmental Restoration 4, 10–17.

Staehelin J., Hoigné J., 1982. Decomposition of ozone in water: Rate of initiation by hydroxide ions and hydrogen peroxide. Environmental Science and Technology 16, 676–681.

Suchithra P.S., Carleer R., Ananthakumar S., Yperman J., 2015. A hybridization approach to efficient TiO_2 photodegradation of aqueous benzalkonium chloride. Journal of Hazardous Materials 293, 122–130.

Sueoka N., 1960. Mitotic replication of deoxyribonucleic acid in *Chlamydomonas reinhardi*. Proceedings of the National Academy of Sciences of the United States of America 46, 83–91.

Tezel U., Pavlostathis S.G., 2009. Transformation of benzalkonium chloride under nitrate reducing conditions. Environmental Science and Technology 43, 1342–1348.

Vandersmissen K., De Smedt F., Vinckier C., 2008. The impact of traces of hydrogen peroxide and phosphate on the ozone decomposition rate in ‘‘pure water’’. Ozone: Science and Engineering 30, 300–309.

Wang L., Min M., Li Y., Chen P., Chen Y., Liu Y., Wang Y., Ruan R., 2010. Cultivation of green algae *Chlorella* sp. in different wastewaters from municipal wastewater treatment plant. Applied Biochemistry and Biotechnology 162, 1174–1186.

Chapter 7

General Discussion and Recommendations

7.1 General discussion and recommendations for future work

This research generated important information about the fate of benzalkonium chlorides (BACs) in natural and engineered systems. In addition, a remedial treatment technology was developed, so that BACs can be removed before they are discharged to the natural environment.

Biodegradation is the major process of natural attenuation for any organic pollutant and the process dictates the fate of organic pollutants in both natural and engineered systems. It was a mystery that BACs, although readily biodegradable, are quite abundant in nature. The results of this work on the biodegradation of BACs, individually and in mixture using a pure strain of *Pseudomonas*, showed that longer alkyl chain BDTA inhibited the biodegradation of shorter alkyl chain BDDA, and BDTA was more toxic than BDDA (Chapter 3). BDDA at 100 mg L^{-1} degraded in 4 d but degradation of 50 mg L^{-1} of the BDDA took over 8 d when mixed with 25 mg L^{-1} of BDTA using the same density of *Pseudomonas* cells. This result suggests that co-contamination of various BACs is one of the reasons for their high abundance in nature. Furthermore, the kinetic data obtained in this study will support the scale-up process for engineered systems aimed at biodegradation of BACs in the natural environment. As anticipated, it would be beneficial to study other groups of cationic surfactants, such as monoalkonium and/or dialkonium halides at their various proportions of mixtures, so that a clear picture of their biodegradation can be seen. Additionally, the effect of a mixture of anionic and cationic surfactants could be an area to study, because of their opposite charges they might behave in a different way during the biodegradation process.

Sorption properties of organic contaminants determine their bioavailability, especially in the agricultural environment when contaminants are introduced due to soil amendment with biosolids or due to the use of reclaimed wastewater for irrigation. The adsorption and leaching characteristics of BDDA and BDTA were determined using three agricultural soils with varied proportions of silt, sand, clay, and organic matter (Chapter 4). The results

showed that the scope for BACs to enter the runoff water from agricultural land (if BACs are present due to soil amendment with biosolids or soil irrigated with reclaimed wastewater) is low especially for soils with a high clay and silt content. A soil-column experiment was performed and less than 1% of total BAC migrated through a 9 cm depth soil column and most of the BAC stayed inside the soil matrices. Due to their cationic characteristics, BACs are more likely to be adsorbed and less likely to be mobile in a soil environment; however, high organic content of solid matrices facilitates the leaching of BACs (60 to 90% of adsorbed BACs were leached from biosolids due to various flow rate of artificial rain water) in the soil column experiment. As a result, higher organic content soil materials, such as, landfill soils might facilitate BACs to leach into the landfill leachate. Additionally, the anaerobic condition in landfill is favourable for BACs persistence.

Findings from the biodegradation, adsorption and leaching experiments lead us to a very important question. What would be the half-life (DT_{50}; degradation time for 50% of the test substance) of BACs and other cationic surfactants in the natural environment, particularly in an agricultural soil environment? Higher persistence of BACs in the natural environment will increase the scope for bioavailability. Therefore, the chance of any eco-toxicological effects by BACs will be high. Many studies have demonstrated the toxic effect of cationic surfactants including BACs in varied organisms. To determine the DT_{50} of BACs in the soil environment, one has to develop and optimize a reliable extraction method for quantitative analysis of BACs from various agricultural soil matrices and biosolids, which is currently unavailable (except Kang et al., 2016). Another challenge for the determination of DT_{50} is that BACs are bactericidal compounds at higher doses and would have to be studied at lower doses for their natural attenuation in the soil environment. Quantification of very low concentrations of BACs (lower mg to µg level) requires either liquid chromatography coupled with mass spectrometry or a radiolabel technique, which are very specialized and not very common in many laboratories.

One of the major findings in this work was to confirm a possible route for BACs to reach into the highest level of the food chain. Major concern related to recalcitrant compounds is the possibility that they might enter into the food chain, including humans,

due to the use of biosolids as soil amendment materials or the use of reclaimed wastewater for irrigation. The outcome of this study (Chapter 5) is very important for hydroponic industries as well, identifying the need to regulate the use of reclaimed wastewater for irrigation. Crop plants were studied to determine if they were capable of taking up BACs into the roots and translocating them to the aboveground parts. Two common vegetables were grown in hydroponics: garden cress (*Lepidium sativum)* and lettuce *(Lactuca sativa)*. Both BACs were taken up by the roots of vegetable plants (lettuce and garden cress) and were translocated to the shoots. BACs were toxic to both plants at environmentally relevant concentration (0.25 mg L^{-1}). Since a hydroponic system does not resemble an agricultural soil environment, it is necessary to further investigate the toxic effect of such compounds in agricultural soil amended with biosolids. Nutrient analysis (micro and macro) in this study did not reveal a link between the toxic effect of BACs and elemental deficiency of plants; except for BAC-induced N and Mg deficiency in lettuce, as well as 50% higher Fe concentration in roots of both species in response to BACs. Different experiments, such as measurement of carbohydrate content, O_2 exchange rate, photosynthetic rate and chlorophyll production might provide some valuable information on the BAC-induced plant toxicity. Phytoremediation of BACs could be interesting as an alternative remedial approach to clean up BAC-contaminated sludge or soils.

Complete removal of recalcitrant compounds in the conventional biological wastewater treatment process is not possible. In the final part of this research, an advanced oxidation process (AOP) based on O_3/H_2O_2 was designed to treat influent wastewater before biological wastewater treatment, to reduce concentrations of BACs in the downstream processes, such as in activated sludge or wastewater effluent, and eventually in the natural environment (Chapter 6). A mixture of BACs was oxidised with O_3 and catalyzed with H_2O_2 at elevated pH in Milli-Q water and in wastewater influent collected from a municipal sewage treatment plant. Experimental conditions for AOP were optimized using a central composite design and were determined to be 1.28 g h^{-1} O_3 and 200 mg L^{-1} of H_2O_2 at pH 11, which degraded 90% of the initial BACs after 30 min. A comprehensive list of transformation products was identified and the products were shown to be nontoxic using a standard test

method. The outcome of this chapter can be used in the pilot scale AOP treatment process, which can further be implemented in the large scale AOP. The advanced oxidation treatment method can be used before biological wastewater treatment for various communities' effluents, such as, hospital effluents. Concentrations of recalcitrant compounds will vary among sources; for example, hospital effluents will contain more antibiotics or BACs than effluents produced from a shopping mall. The relatively high cost of AOP can be justified, if AOP treatment can improve the biodegradability of recalcitrant compounds and converting them to readily biodegradable products for further biological treatment. Additionally, implementing community-based AOP will be more appropriate rather than redesigning the existing biological treatment facilities for the removal of recalcitrant compounds. However, it is necessary to do more research for the removal of recalcitrant compounds based on various effluents, such as hospital effluents, and compare this technology to other chemical oxidation processes, such as using Ferrate (Fe VI).

The results obtained from this research and the proposed AOP treatment before biological treatment are presented in a simplified model (Schematic 7.1), which shows the distribution of BACs in the natural and engineered systems. Existing concentrations of BACs might not be a serious threat for humans or other large organisms but the toxicity profile of BACs still poses risk of many unforeseen toxicological effects, which might cause harm to the microorganisms. The scenario could be even worse for countries where wastewater remains untreated or undertreated. Furthermore, we still do not know if BACs have any relationship to the abundance of antibiotic resistance bacteria. If so, then BACs at existing environmental concentrations could pose a risk to humans, as shown in Schematic 7.1.

Overall, the value of this research lies in understanding the fate of BACs or similar cationic surfactants in the natural or engineered systems for better understanding of the environmental risks associated with these compounds. Studying the fate of BACs in various natural and engineered systems (biodegradation, adsorption, leaching, plant uptake and AOP) provides a whole picture of the contaminant's destination. A partial understanding would have emerged if the study was conducted in any one particular system. For example, studying the fate (adsorption, leaching, transport, dispersion and diffusion) in agricultural

soil will never provide the information about the translocation of BACs into plants. For this reason, this research is valuable to the policy makers who will be looking at recalcitrant compounds in nature and recommending necessary actions for their extenuation.

7.2 Conclusions

In conclusion, this research showed for the first time that BACs can harm vascular plants at environmentally relevant concentrations and might be consumed by animals through their food chain. It will be impractical to imagine that toxicity of BACs or any other personal care products or pharmaceuticals will be removed in nature in the near future. In that case, it will be impossible to take remedial actions without studying the fate of various groups of compounds in various natural components. The challenges to mitigate micropollutant-related contaminations are 1) they remain at a very low concentration in nature (water, soil or sediments) and 2) they are very difficult to remove once they are in natural environment. Therefore, pretreatment technologies might be a possible way to reduce their concentration before they get into the agricultural environment through the land application of sewage biosolids or application of reclaimed wastewater for irrigation. This research showed for the first time that AOP can remove BACs from influent municipal wastewater and remove their toxic effect with improved biodegradability.

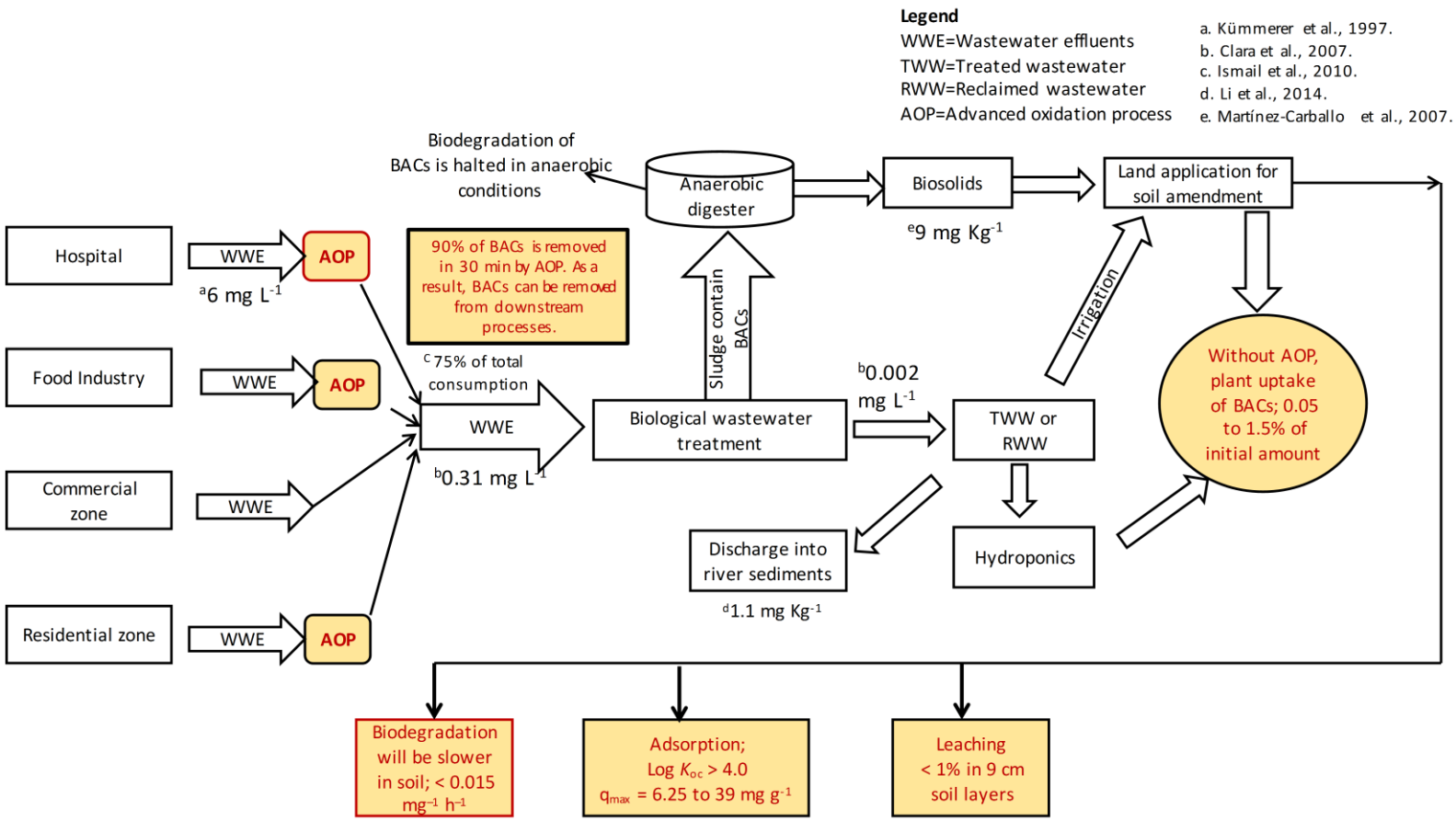

Schematic 7.1 Simplified model to present the fate of BACs in natural and engineered systems. AOP is proposed as pretreatment for the removal of BACs before biological wastewater treatment. Highlighted results were obtained from this research (Chapter 3 to 6). Other values (other than highlighted) were from published reports.

References

Clara M., Scharf S., Scheffknecht C., Gans O., 2007. Occurrence of selected surfactants in untreated and treated sewage. Water Research 41, 4339–4348.

Ismail Z.Z., Tezel U., Pavlostathis S.G., 2010. Sorption of quaternary ammonium compounds to municipal sludge. Water Research 44, 2303-2313.

Kang H.I., Shin H.S., 2016. Rapid and sensitive determination of benzalkonium chloride biocide residues in soil using liquid chromatography–tandem mass spectrometry after ultrasonically assisted extraction. Bulletin of the Korean Chemical Society 37, 1219–1227.

Kümmerer K., Eitel A., Braun U., Hubner P., Daschner F., Mascart G., Milandri M., Reinthaler F., Verhoef J., 1997. Analysis of benzalkonium chloride in the effluent from European hospitals by solid-phase extraction and high-performance liquid chromatography with post-column ion-pairing and fluorescence detection. Journal of Chromatography A 774, 281–286.

Li X., Luo X., Mai B., Liu J., Chen L., Lin S., 2014. Occurrence of quaternary ammonium compounds (QACs) and their application as a tracer for sewage derived pollution in urban estuarine sediments. Environmental Pollution 185, 127-133.

Martínez-Carballo E., González-Barreiro C., Sitka A., Kreuzinger N., Scharf S., Gans O., 2007. Determination of selected quaternary ammonium compounds by liquid chromatography with mass spectrometry. Part II. Application to sediment and sludge samples in Austria. Environmental Pollution 146, 543-547.

Resume

Adnan Hossain Khan

Academics

Graduate Education

2012 to 2016 Doctor of Philosophy
Department of Chemical and Biochemical Engineering,
(Specialized in Environmental and Green Process Engineering)
University of Western Ontario
Thesis title: *Fate of Benzalkonium Chlorides in Natural Environment and Treatment Processes*
Supervisors: Dr. Madhumita B. Ray and Dr. Sheila M. Macfie

2010 to 2012 Master of Engineering and Science (MESc)
Department of Civil and Environmental Engineering,
(Specialized in Environmental Engineering), University of Western Ontario
Thesis title: *Improvement of Total Sulphur Measurement Techniques for Management of Reactive Mine Tailings*
Supervisor: Dr. Julie Q. Shang

Master of Science (M.S.) in Applied Chemistry University of Dhaka

Publications

Journals (peer reviewed)

Adnan Hossain Khan, Edward Topp, Andrew Scott, Mark Sumarah, Sheila M. Macfie, Madhumita B. Ray, 2015. **Journal of Hazardous Materials** 299: 595–602.

Adnan Hossain Khan, Julie Q. Shang, Raquibul Alam, 2014. International **Journal of Environmental Science and Technology**, 11: 1989-1998.

Adnan Hossain Khan, Julie Q. Shang, Raquibul Alam, 2012. **Journal of Hazardous Materials**, 235-236: 376-383.

Adnan Hossain Khan, Mohammad Nurnabi, Parimal Bala, 2009. **Journal of Thermal analysis and Calorimetry**, 96 (3): 929-935.

Conferences

Adnan Hossain Khan, Jing Wan, Mark Sumarah, Sheila M. Macfie, Madhumita B. Ray, 2015. AIChE Annual Meeting, Salt Lake City, UT, USA (Proceedings and oral presentation).

Adnan Hossain Khan, Daniel Winnick, Mark Libby, Mark Sumarah, Sheila M. Macfie, Madhumita B. Ray. 2016. 66th Canadian Chemical Engineering Conference(Oral presentation, October 2016)

Book Chapter

Sreejon Das, Nillohit Mitra Ray, Jing Wan**, Adnan Khan**, Tulip Chakraborty and Madhumita Ray, 2016. Micropollutants in wastewater: fate and removal processes. INTECH open science (Accepted).

Journals (peer reviewed communicated)

Adnan Khan et al., 2016. Sorption and leaching of benzalkonium chlorides in agricultural soils. Journal of Environmental Management.

Adnan Khan et al., 2016. O_3/H_2O_2 pretreatment of benzalkonium chlorides for improved biodegradability before biological treatment. Journal of Hazardous Materials.

Adnan Khan et al., 2016. Uptake and phytotoxic effect of benzalkonium chlorides in *Lepidium sativum* and *Lactuca sativa* in a hydroponic system. Environmental Pollution.

Awards and Scholarships

2015	Ontario Graduate Scholarship
2013	Ross and Jean Clark Scholarships – for environmental research
2012	Ross and Jean Clark Scholarships – for environmental research
2015	GTA–Union research contribution scholarship at UWO
2012	GTA–Union research contribution scholarship at UWO
2015 & 2014	First Prize in Oral Presentation at the Annual Research Bridge; Sarnia, ON
1995 to 1999	Bangladesh Technical Education Board Scholarship (Govt. of Bangladesh)

Relevant Work Experiences

2014/2016	Worked part time as a lab manager for Dr. Madhumita Ray at UWO during my PhD research.
2013/2014	Internship at Agriculture and Agri-Food Canada as a part of my PhD research.
2008/2009	Chemical analyst at an ISO/IEC 17025 accredited laboratory (Ministry of Industry, Bangladesh).
2003/2010	Faculty (course instructor) (full time) at a constituent college of Dhaka University.

Volunteer and Extracurricular Activities

2012–2013	Elected and served duties as VP-external of the Graduate Engineering Society (GES) at Western University (http://www.eng.uwo.ca/ges/executives.html).
2012-till date	Member of Graduate Student Issues Committee; Bursary Committee and a councilor of the Society of Graduate Studies (SOGS) at Western University
2011-12-13	Photo exhibition in Pride London in London-Ontario, Verge photo contest in Toronto-Ontario; TVO Pick of the day photography month contest (Canada)